NASA/CR-1999-208989

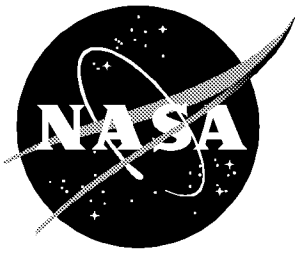

Benefit Estimates of Terminal Area Productivity Program Technologies

Robert Hemm, Gerald Shapiro, David Lee, Joana Gribko, and Bonnie Glaser
Logistics Management Institute, McLean, Virginia

January 1999

The NASA STI Program Office . . . in Profile

Since its founding, NASA has been dedicated to the advancement of aeronautics and space science. The NASA Scientific and Technical Information (STI) Program Office plays a key part in helping NASA maintain this important role.

The NASA STI Program Office is operated by Langley Research Center, the lead center for NASA's scientific and technical information. The NASA STI Program Office provides access to the NASA STI Database, the largest collection of aeronautical and space science STI in the world. The Program Office is also NASA's institutional mechanism for disseminating the results of its research and development activities. These results are published by NASA in the NASA STI Report Series, which includes the following report types:

- TECHNICAL PUBLICATION. Reports of completed research or a major significant phase of research that present the results of NASA programs and include extensive data or theoretical analysis. Includes compilations of significant scientific and technical data and information deemed to be of continuing reference value. NASA counterpart or peer-reviewed formal professional papers, but having less stringent limitations on manuscript length and extent of graphic presentations.

- TECHNICAL MEMORANDUM. Scientific and technical findings that are preliminary or of specialized interest, e.g., quick release reports, working papers, and bibliographies that contain minimal annotation. Does not contain extensive analysis.

- CONTRACTOR REPORT. Scientific and technical findings by NASA-sponsored contractors and grantees.

- CONFERENCE PUBLICATION. Collected papers from scientific and technical conferences, symposia, seminars, or other meetings sponsored or co-sponsored by NASA.

- SPECIAL PUBLICATION. Scientific, technical, or historical information from NASA programs, projects, and missions, often concerned with subjects having substantial public interest.

- TECHNICAL TRANSLATION. English-language translations of foreign scientific and technical material pertinent to NASA's mission.

Specialized services that complement the STI Program Office's diverse offerings include creating custom thesauri, building customized databases, organizing and publishing research results . . . even providing videos.

For more information about the NASA STI Program Office, see the following:

- Access the NASA STI Program Home Page at *http://www.sti.nasa.gov*

- Email your question via the Internet to help@sti.nasa.gov

- Fax your question to the NASA STI Help Desk at (301) 621-0134

- Telephone the NASA STI Help Desk at (301) 621-0390

- Write to:
  NASA STI Help Desk
  NASA Center for AeroSpace Information
  7121 Standard Drive
  Hanover, MD 21076-1320

NASA/CR-1999-208989

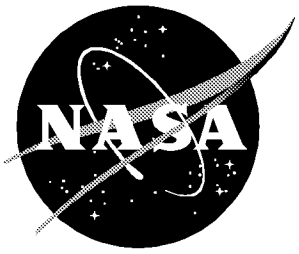

Benefit Estimates of Terminal Area Productivity Program Technologies

Robert Hemm, Gerald Shapiro, David Lee, Joana Gribko and Bonnie Glaser
Logistics Management Institute, McLean, Virginia

National Aeronautics and
Space Administration

Langley Research Center
Hampton, Virginia 23681-2199

Prepared for Langley Research Center
under Contract NAS2-14361

January 1999

Available from:

NASA Center for AeroSpace Information (CASI)
7121 Standard Drive
Hanover, MD 21076-1320
(301) 621-0390

National Technical Information Service (NTIS)
5285 Port Royal Road
Springfield, VA 22161-2171
(703) 605-6000

Executive Summary

The National Aeronautics and Space Administration's (NASAs) Terminal Area Productivity (TAP) program is pursuing technologies to enable airports to operate in bad weather at the rates they now only achieve in good weather. The TAP program includes three technology elements: reduced spacing operations (RSO), low visibility landing and surface operations (LVLASO), and air traffic management (ATM). Subelements of RSO include the Aircraft Vortex Spacing System (AVOSS) and airborne information for lateral spacing (AILS). Subelements of LVLASO include high-speed roll-out and turn-off (ROTO); taxi, navigation, and situation awareness (T-NASA); and dynamic runway occupancy measurement (DROM). The primary subelement of ATM is real-time interaction of the Center TRACON[1] Automation System (CTAS) with aircraft flight management systems (FMSs) (a.k.a. CTAS/FMS Integration). The NASA TAP technology program completes in 2000. Continued development and implementation will need to be conducted by the Federal Aviation Administration (FAA) and airlines.

- Our task has been to estimate the benefits and costs of implementing four of the TAP technologies.[2] Our purpose is to provide sound technical and economic information to support development decisions by NASA, the FAA, and the airlines. The current task is the latest in a series of tasks spanning the past 4 years. Previous efforts have produced preliminary benefit estimates for 3 TAP scenarios at first two and then at 10 TAP airports.[3] In the current effort we generated more refined benefit estimates for 19 scenarios at 10 airports. We also produced deliverable versions of the

[1] TRACON is Terminal Radar Approach Control.

[2] We analyzed AVOSS, DROM, ROTO, and ATM. NASA management elected not to include AILS in the current study. AILS could be estimated with straightforward modification to the current models. . NASA assigned T-NASA estimates to the MCA Research Corporation. We could indirectly estimate the impact of T-NASA by adding taxi queues to the current models.

[3] Boston Logan, Detroit Wayne County, New York Kennedy, New York LaGuardia, Newark, Atlanta Hartsfield, Dallas-Ft. Worth, Chicago O'Hare, Los Angeles International, and San Francisco are the airports addressed in this study.

Logistics Management Institute (LMI)-developed airport capacity and delay models for each of the 10 airports. [4]

Current results indicate that the TAP technologies will generate substantial benefits. The benefits are based on reduced airline direct operating costs resulting from reduced arrival delay. Additional benefits could accrue by the consideration of departure delays, passenger costs, increased airline revenue, and avoidance of new airport construction.

All potential benefits are based on the confirmation of the following key assumptions, which should be addressed by the research program:

- DROM will demonstrate average runway arrival times of <50 seconds in rain.
- Controllers will use 2.5 nautical mile minimum separations in IMC Category 1 conditions[5] based on DROM data.
- ROTO will enable average runway occupancy times of <50 seconds in low visibility IMC Category 2 and 3 conditions.
- AVOSS will reliably confirm the modeled wake vortex separation reductions for the wind criteria used.
- Controllers using the CTAS Active Final Approach Spacing Tool with a data link can exploit reduced uncertainties in aircraft speed and position to reduce separations.
- The flight plans produced by integrated CTAS and FMS computers can be safely accepted and executed by controllers and pilots.

[4] Cost estimates covering development, deployment in 2005, and operations and maintenance from 2006 through 2015 have been documented in previous work and are not addressed in this report.

[5] IMC is the acronym for instrument meteorological conditions. Categories 1, 2, and 3 correspond to decreasing levels of ceiling and visibility.

Contents

FIGURES

TABLES

Chapter 1
Background and Summary Results

OVERVIEW

This chapter describes the Terminal Area Productivity (TAP) technologies, the methods used to estimate their potential benefits, and a summary of the results. Subsequent chapters address individual airport results, and the computer program and data bases. Three appendixes address input parameter selection, model algorithms, and model structure. The last appendix is a user's guide for the models delivered to NASA.

The purpose of the TAP benefit and cost analysis is to provide accurate information to support internal NASA program decisions and also future decisions by the Federal Aviation Administration (FAA) and airlines to further develop and implement the TAP technologies. Our analysis of the benefits and costs of the TAP technologies has spanned the past 4 years. Previous reports have documented the development of the basic models discussed herein plus preliminary results of benefit and cost analyses. The best case would be for these analyses to be continuously updated and expanded through the year 2000 as improved TAP technology data becomes available. Because such a course may not be followed, this effort has focused on providing a complete set of results with models that could be used for in-house NASA analyses. This report covers benefit models. The preliminary cost models, which have previously been delivered to NASA, have not been updated.

The benefit analysis and airport capacity and delay models have evolved over the past 4 years. The structures of the models themselves have changed as we developed improved algorithms and programming techniques. Changes to the scenarios and parameters have changed as a result of feedback to the preliminary results. Those changes are referenced where necessary in the discussions that follow.

The overall goal of NASA's TAP program is to safely maintain good weather airport operating capacity during bad weather. The TAP program includes three technology elements: Reduced Spacing Operations (RSO), Low Visibility Landing and Surface Operations (LVLASO), and Air Traffic Management (ATM). Sub-elements of RSO include the Aircraft Vortex Spacing System (AVOSS) and Airborne Information for Lateral Spacing (AILS). Sub-elements of LVLASO include high-speed Roll-out and Turn-off (ROTO), Taxi, Navigation and Situational Awareness (T-NASA), and Dynamic Runway Occupancy Measurement (DROM). The ATM program addresses the technologies necessary for real time, two-way

interaction of the Center Terminal Radar Approach Control (TRACON) Automation System (CTAS) with aircraft flight management systems (FMSs) (a.k.a. CTAS/FMS integration).

We estimated the benefits accruing from deployment of AVOSS, DROM, ROTO, and CTAS/FMS Integration systems.[1] Benefits consist of the minutes of arrival delay saved by the TAP technologies at 10 major airports during a 10-year period from 2006 through 2015.[2] For benefit and cost estimating purposes, 2005 is assumed to be the deployment year for the technologies.

Figure 1-1 outlines the analysis approach. This basic approach has not changed over the past 4 years. Estimating arrival delay first requires calculating airport capacities as a function of runway configurations, weather-based air traffic control operating procedures, and the TAP technology levels. Second, future hourly demand is estimated by inflating current hourly demand by the growth predictions contained in the FAA Terminal Area Forecast (TAF). Next, capacity estimates, together with projected demand and historical weather data are used by an airport delay (queuing) model to generate arrival delay statistics as a function of TAP technology. The cost per minute of delay derived from historical airline data is used to estimate the dollar value of the delay reductions generated by the TAP technologies. Finally, the estimated savings are compared with the estimated life-cycle costs for the TAP systems to produce benefit-to-cost ratios.

Both the capacity and delay models use analytic (closed form) probabilistic algorithms.

Capacity results consist of arrival/departure tradeoff curves corresponding to each airport runway configuration and each meteorological operating condition. These curves often are called Pareto frontiers. For the 10 airports, the number of meteorological conditions ranges from 4 to 5 and the number of runway configurations ranges from 2 to 23. The number of curves calculated per airport for each technology case ranges from 8 (Atlanta) to 92 (Chicago). The capacity curves are calculated once for each technology case. The capacity curves, along with hourly weather data and airport hourly departure and arrival demand, are fed to the delay model.

[1] T-NASA benefit estimates, which require modeling of taxiway operations, have been addressed in a separate NASA study. NASA management elected not to include AILS in the current study. AILS could be estimated with straightforward modification to the current models. The impact of T-NASA can be estimated indirectly by adding taxi queues to the current models.

[2] The 10 airports include Boston Logan (BOS), New York John F. Kennedy (JFK), New York LaGuardia (LGA), Newark (EWR), Chicago O'Hare (ORD), Atlanta Hartsfield (ATL), Dallas-Fort Worth (DFW), Detroit Wayne County (DTW), Los Angeles International (LAX), and San Francisco (SFO).

Figure 1-1. Overview of Analysis Method

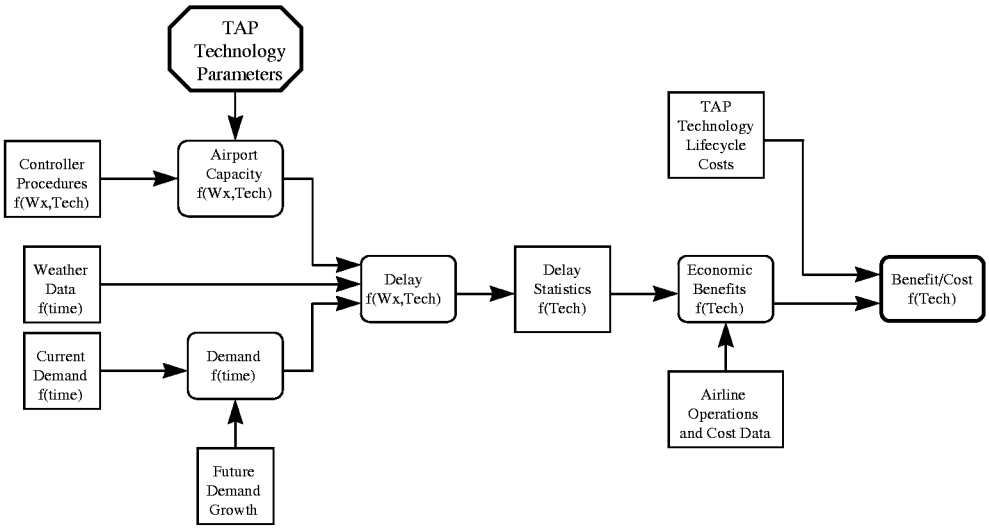

The delay model is run for each technology case and demand year. All demand years could be estimated, but our current practice is to estimate the delays for beginning and end years and to interpolate the interior years using a compound growth formula. For each airport operating hour, the delay model examines a weather data file to determine which runway configurations are legal (based on ceiling and visibility) and useable (based on cross- and tailwind) and then examines the capacity curves of the legal/usable runways to select the best configuration and determine that hour's airport capacity. Next, the model uses the capacity information along with the departure and arrival demand to feed a queuing algorithm that calculates delay. The delay time is accumulated as the process is repeated for subsequent hours. Three hours of zero demand are run after the airport closing time to work off the remaining queues. In order to produce reliable averages, we run the delay model with 35 years of hourly weather data for each technology case and demand (typically, about 260,000 hours).

The TAP program technologies impact capacity and delay through the capacity model input parameters. The parameters were selected to model the process used by controllers to establish aircraft spacing. The values used for the parameters are based on the information available to the controller. Typical parameters include, minimum allowed aircraft separations, runway occupancy times, uncertainties in approach speed, and uncertainties in position. A detailed discussion of the modeling parameters and the parameter values chosen for the TAP analysis is included in Appendix A. A sample of an input file is contained in Appendix D.

Nineteen technology scenarios were analyzed in the study. These include a current technology scenario and two 2005 baseline scenarios. One 2005 baseline represents the CTAS with the Passive Final Approach Spacing Tool (PFAST). The second 2005 baseline represents the CTAS with the Active Final Approach Spac-

ing Tool (AFAST). TAP technologies were added to these baselines. Table 1-1 lists the scenarios studied.

Table 1-1. 1998 Modeling Scenarios

Title	Baseline	Content	Technology Code
Current Technology	n/a	Current Technology	CT
2005 PFAST Baseline	CT	PFAST	BPF
PFAST DROM	PFAST	DROM	P1
PFAST ROTO DROM	PFAST	ROTO + DROM	P2
PFAST AVOSS	PFAST	AVOSS	P3
PFAST AVOSS DROM	PFAST	AVOSS + DROM	P4
PFAST ROTO DROM AVOSS	PFAST	AVOSS + DROM + ROTO	P5
2005 AFAST Baseline	CT	AFAST	BAF
AFAST DROM	AFAST	DROM	A1
AFAST ROTO DROM	AFAST	ROTO + DROM	A2
AFAST AVOSS	AFAST	AVOSS	A3
AFAST AVOSS DROM	AFAST	AVOSS + DROM	A4
AFAST ROTO DROM AVOSS	AFAST	AVOSS + DROM + ROTO	A5
ATM-1 CTAS/3DFMS	AFAST	AFAST + 3DFMS + data link	BAT
ATM-1 ROTO DROM	AFAST	ATM 1 + ROTO + DROM	C1
ATM-1 DROM AVOSS	AFAST	ATM-1 + DROM + AVOSS	C2
ATM-1 ROTO DROM AVOSS	AFAST	ATM 1 + ROTO + DROM + AVOSS	C3
ATM-2 CTAS/4DFMS	AFAST	AFAST + 4DFMS + data link	C4
ATM-2 ROTO DROM AVOSS	AFAST	ATM-2 + ROTO + DROM + AVOSS	C5

CT = Current Technology, BPF = Baseline Passive FAST, BAF = Baseline Active FAST, BAT = Baseline Active FAST plus ATM-1

TERMINAL AREA PRODUCTIVITY TECHNOLOGIES

Dynamic Runway Occupancy Measurement

The purpose of the DROM system is to provide accurate predictions of arrival runway occupancy times (ROTs) in all weather conditions. Several technical concepts have been considered for DROM. Under the TAP program, NASA Langley Research Center cooperated in a test of a Cardion® multilateration system at Atlanta. Multilateration correlates response times from aircraft transponder interrogations to establish aircraft position. Other schemes use position information from global positioning satellite (GPS)-equipped transponders. Using the identification and position information, DROM software tracks the aircraft and determines

where and when the aircraft leave the runways. The ROT data are used to continuously update ROT predictions.

Originally, DROM's benefit was considered to be only as an enabling technology that would enable use of the shorter miles-in-trail (MIT) separations expected from AVOSS. In our study, we postulate that DROM could have a larger and more immediate impact. Current operating rules limit minimum interarrival separation at the threshold to 3.0 nautical miles unless certain criteria are met. If the criteria are met, the separation can be reduced to 2.5 nautical miles. The most demanding criterion is a demonstrated average ROT of 50 seconds or less. Average ROTs under 50 seconds have been demonstrated for VMC (visual meteorological conditions) at all the TAP airports except San Francisco. No demonstrations for IMC (instrument meteorological conditions) have been made anywhere. It is controller practice to revert to 3.0 nautical mile separations whenever the runways are wet. Analysis of the meteorological data confirms that for all TAP airports, except LAX, the runways are usually wet in IMC-1 (standard IMC) and IMC-2 (low visibility, severe IMC). Significantly, the sparse available IMC ROT data and pilot anecdotes strongly support the case that wet runway ROTs are no longer and, in fact, may be shorter, than dry runway ROTs. Longer ROTs are expected only in icy or low visibility conditions. In our estimates, we assume that DROM data will confirm the <50 second average ROT in wet IMC-1 and allow use of 2.5 nautical mile minimum separations. Under this assumption, DROM provides significant benefits.

Roll-Out and Turn Off

The ROTO program consists of hardware and software that allows a physical reduction in ROT under severe, low-visibility, IMC-2. By itself, ROTO is expected to have little effect on arrival capacity because MIT separations rather than ROT historically determine minimum interarrival times in IMC-2. If used in conjunction with DROM, however, ROTO may be able to enable, and DROM confirm, average ROTs of <50 seconds in severe IMC-2 conditions, thus allowing 2.5 nautical mile minimum miles-in-trail separations for all levels of IMC. In our estimates, we assume that ROTO used with DROM will allow the use of 2.5 nautical mile minimum mile-in-trail separations in IMC-1 and IMC-2. Under this assumption, ROTO provides significant additional benefits.

Aircraft Vortex Spacing System

The threat of wake turbulence upset has caused the FAA to require conservative miles-in-trail separations well above the traffic management minimums for aircraft following heavy and B-757 aircraft. The wake vortex separations are applied by controllers in all cases even though it is known that under many wind and temperature conditions, the vortices dissipate quickly or are blown out of the flight path. The goal of the AVOSS is to reduce the excess distances by providing the

controller accurate knowledge of the wake vortex threat. The AVOSS consists of hardware and software capable of predicting the transport and decay of aircraft wake vortices as a function of meteorological conditions. AVOSS potentially allows significant reductions to the current miles-in-trail separations imposed to prevent wake vortex encounters. We currently use the Vortex Advisory System (VAS) wind criteria developed by the FAA in the 1970s to estimate when AVOSS will permit reduced separations. We estimate significant benefits from AVOSS despite the fact that the VAS criteria may be too conservative.

ATM (CTAS/FMS Integration)

We model two levels of CTAS/FMS integration (ATM-1 and ATM-2). The first is integration with a 3-D (position only) FMS. In this case, the aircraft can transmit to the CTAS its precise position, velocity, and intended path. Using those data, CTAS (when equipped with the active final approach spacing tool (AFAST)) can provide more accurate cues to the controller. The ATM-2 level of CTAS/FMS Integration invokes a 4-D (position plus time) FMS. In addition to the 3-D information, the 4-D FMS can provide CTAS with accurate estimates of threshold crossing time. ATM-2 expands beyond AFAST and assumes direct flight planning interaction between the CTAS computer and the aircraft FMS subject to human intervention. Such operation will require major adjustments to air traffic control practices. Both levels of ATM are modeled by reductions to position, speed, and wind uncertainties along the common path. Potential benefits from both levels of CTAS/FMS are quite substantial.

THE 2005 BASELINE

For cost- and benefit- estimating purposes, the TAP technologies are assumed to be in place at the 10 TAP airports by 2005. Estimates of TAP benefits should, therefore, be compared with the technology baseline expected to exist in 2005. In our initial work, we assumed that in 2005 GPS technology would be ubiquitous and would result in a reduction in position uncertainty from the current 0.25 nautical miles to 100 feet. We also assumed curved approach paths would enable an effective reduction in the common path of 1 nautical mile. During reviews of the preliminary results, it was pointed out that while GPS does increase aircraft position accuracy, the controller cannot take advantage of the increased accuracy unless the data are transmitted to the ground and presented to him or her in a useful fashion. It was decided that AFAST technology and an Automatic Dependent Surveillance (ADS) data link would be necessary and sufficient to make use of the increased accuracy. As noted above, AFAST is a necessary base for the ATM CTAS/FMS Integration technology.

Unfortunately, AFAST has neither been tested at an airport, nor is it yet planned for deployment. Consequently, a second baseline invoking the more limited passive FAST (PFAST) technology was also included in the current analysis. PFAST

has been tested at DFW. The impact of PFAST on model parameters is discussed in detail in Appendix A. As discussed in that appendix, the decision was made to add an inefficiency buffer in the model based on an exponential probability distribution. The buffer models the situation where a "following" aircraft would not be available to take advantage of the minimum safe spacing. The buffer is intended to simulate the impact of non-optimum runway balancing and sequencing. The mean of the distribution was set to 0.25 nautical miles for current technology and reduced to 0.1 and 0.05 nautical miles for PFAST and AFAST, respectively. The ATM technologies further reduce the buffer. As discussed in Appendix A, the 0.25 value is roughly based on DFW PFAST experience, but it is essentially speculative. Because of the uncertain nature of the buffer size, we ran all cases with the nominal buffer values and with the buffer set to zero. When the buffer is set to zero, the PFAST baseline is identical to current technology and provides no benefit. As will be shown below, the buffer assumption also has significant impact on the estimated benefits AFAST but only a minor impact on the benefits of TAP technologies relative to either baseline.

With respect to the buffer and gaps in the arrival stream, we should note that the queuing algorithm we use incorporates a Poisson-distributed arrival stream, so arrival gaps due to randomness of aircraft arrivals are modeled even when the efficiency buffer is set to zero. The inefficiency buffer models *avoidable errors* in maneuvering aircraft in the TRACON airspace. The buffer is expected to be highest for large, complex configurations, such as DFW, and lowest for simpler configurations, such as ATL.

RESULTS

Extracting useful insight from the mountain of results generated by many technology cases and airports is a key analytical challenge. The results have been summarized into the Tables 1-2 and 1-3. Those tables display the minutes of delay avoided by use of the TAP technologies and the 1997 constant-dollar value of those savings. The PFAST and AFAST baseline savings are relative to the current technology (CT). The TAP technology savings are relative to the PFAST and AFAST baselines. In the individual airport estimates discussed later, upper and lower bounds of benefits are estimated based on bounding definitions of direct operating costs. The values in the tables here are based on the average of those upper and lower bound costs. The individual airport results (discussed later) also include discounted dollar (using a 1997 base year and 7 percent discount rate) and the inflated then-year (using a 2.56 percent escalation rate) savings.

SUMMARY RESULTS WITH INEFFICIENCY BUFFER = 0

Table 1-2. 10-Year Cost Avoidance (1997 Constant Dollars in Millions)
(Costs Based on Average of Upper and Lower Direct Operating Cost Bounds)
Inefficiency Buffer = 0

Scenario	Compared to	Total	ATL	BOS	DTW	DFW	ORD	JFK	LGA	LAX	EWR	SFO
PFAST baseline	CT	0	0	0	0	0	0	0	0	0	0	0
PFAST DROM	PFAST	601	76	139	73	59	167	3	38	43	3	0
PFAST ROTO DROM	PFAST	1,359	136	165	87	190	447	45	88	146	16	39
PFAST AVOSS	PFAST	1,607	405	185	138	131	268	73	43	210	102	51
PFAST DROM AVOSS	PFAST	2,183	468	332	194	188	435	75	78	253	110	51
PFAST AVOSS ROTO DROM	PFAST	2,958	521	360	209	317	731	122	123	367	118	91
AFAST baseline	CT	3,088	604	225	167	358	490	84	117	783	179	81
AFAST DROM	AFAST	541	57	145	54	52	161	1	26	40	6	0
AFAST ROTO DROM	AFAST	1,171	89	174	68	140	430	36	62	124	10	38
AFAST AVOSS	AFAST	1,335	279	179	110	104	244	62	30	199	91	38
AFAST DROM AVOSS	AFAST	1,839	324	326	157	153	394	63	52	238	96	38
AFAST AVOSS ROTO DROM	AFAST	2,471	353	355	172	237	666	103	84	324	100	76
ATM-1 CTAS/3DFMS	AFAST	1,816	269	140	105	235	313	64	56	484	104	47
ATM-1 ROTO DROM	AFAST	2,766	343	306	164	324	693	96	103	539	112	84
ATM-1 DROM AVOSS	AFAST	3,368	532	444	263	345	606	126	89	677	207	79
ATM-1 AVOSS ROTO DROM	AFAST	4,056	579	525	281	405	915	163	126	735	211	116
ATM-2 CTAS/4DFMS	AFAST	3,596	529	297	210	426	634	133	106	951	220	91
ATM-2 AVOSS ROTO DROM	AFAST	5,488	750	791	349	529	1,086	218	153	1,146	312	154

SUMMARY RESULTS WITH NOMINAL INEFFICIENCY BUFFERS

Table 1-3. 10-Year Cost Avoidance (1997 Constant Dollars in Millions)
(Costs Based on Average of Upper and Lower Direct Operating Cost Bounds)
Includes Nominal Inefficiency Buffers

Scenario	Compared to	Total	ATL	BOS	DTW	DFW	ORD	JFK	LGA	LAX	EWR	SFO
PFAST Baseline	CT	3,666	647	267	234	609	375	110	171	769	228	255
PFAST DROM	PFAST	613	84	139	81	62	159	2	41	44	3	0
PFAST ROTO DROM	PFAST	1,385	147	165	95	197	441	40	95	147	17	41
PFAST AVOSS	PFAST	1,724	453	189	147	142	278	78	48	230	105	55
PFAST DROM AVOSS	PFAST	2,311	523	333	209	202	437	79	87	273	113	55
PFAST AVOSS ROTO DROM	PFAST	3,100	579	360	223	335	736	124	137	389	120	96
AFAST Baseline	CT	8,063	1,499	579	463	1,158	995	234	348	1,884	486	418
\AFAST DROM	AFAST	554	62	145	56	54	162	1	28	41	6	0
AFAST ROTO DROM	AFAST	1,190	96	173	70	144	430	34	67	126	10	40
AFAST AVOSS	AFAST	1,380	297	178	116	108	247	65	34	203	93	40
AFAST DROM AVOSS	AFAST	1,897	345	325	163	159	401	65	58	243	98	40
AFAST AVOSS ROTO DROM	AFAST	2,541	376	355	179	247	676	104	92	330	102	80
ATM-1 CTAS/3DFMS	AFAST	1,860	285	139	113	248	305	66	63	485	104	50
ATM-1 ROTO DROM	AFAST	2,855	362	310	176	342	707	99	114	543	113	89
ATM-1 DROM AVOSS	AFAST	3,492	567	450	276	364	609	131	100	702	210	83
ATM-1 AVOSS ROTO DROM	AFAST	4,217	615	533	295	428	941	168	140	762	214	121
ATM-2 CTAS/4DFMS	AFAST	4,598	667	372	275	589	728	163	150	1,209	289	155
ATM-2 AVOSS ROTO DROM	AFAST	6,490	888	866	414	693	1,180	249	197	1,404	381	218

DISCUSSION OF RESULTS

Several points of insight can be drawn from the summary results:

- The savings from ATM-2 AVOSS ROTO DROM "Ultimate TAP" are dramatic.
- The savings from the TAP technologies without ATM are significant.
- The benefits vary among the airports.
- The TAP savings without ATM are comparable to PFAST savings and less, but lower risk, than AFAST savings.
- The assumptions on the inefficiency buffer size and the selection of baselines have minor effects on the TAP technology benefit estimates.

Size of TAP Benefits

The benefits for the "Ultimate TAP" scenario, including ATM-2 and AFAST, are on the order of $550 to $650 million per year for the 10 airports. Since both ATM-2 and AFAST involve significant technical risk, lower risk scenarios were also modeled. The benefits for the lower risk technologies (DROM, ROTO, and AVOSS with PFAST) are on the orders of several millions of dollars per year. We note again that the benefits in the tables are based only on reductions in arrival delays. Additional benefits could be estimated and defended.

Limitation of benefits to the direct operating costs of *arrival delays* at individual airports was based on the desire to have solid, supportable results. The models also calculate *departure delay* benefits ranging from 20% to 80% of the arrival delays for corresponding airports and technologies. Up to now, we have not included departure delays because real world departure data tends to be strongly affected by multiple airport network behavior. The departure delays estimated by the models are, however, based on fundamental capacity limitations at each airport, and the estimated departure benefits result from better use of the existing runway capacity, independent of network behavior.

Inclusion of the value of passenger time would increase the current results, but estimates of the value of passenger time are varied and contentious.

One attractive alternative to estimating the benefits of delay reduction, would be to estimate the additional airline revenue (productivity) resulting from increased capacity at a fixed, acceptable level of delay. Since a profitable airline will have higher revenues per minute than costs, greater benefits should result from such a capacity analysis. Such analysis would be straightforward, though computation-

ally time-consuming, requiring many iterations of the delay models. We recommend this analysis for future work.

A second alternative analysis, also recommended for future work, would be to estimate how many years the employment of TAP technology would delay the need for major capital improvements or the construction of a whole new airport. This could also be done by straightforward iterative analysis using the current models. The savings here would be the capital costs of airport construction and airline relocation.

Variations Among Airports

The TAP savings vary significantly among the airports. Some of the differences are due to differences in volume at the different airports. The rest are due to differences in airport operating conditions. The differences indicate the value of accurately modeling airports and further confirm that there is no simple rule for projecting TAP benefits to airports in general. No single airport has the highest or lowest benefits for all technologies. Atlanta, for example, shows the highest benefits for AVOSS while Chicago shows the highest benefits for DROM. An examination of AVOSS utility at the airports illustrates some reasons for the differences.

AVOSS allows reduced minimum separations when the conditions exist for rapid wake vortex transport and/or dissipation. Since there is no plan for transmitting AVOSS information to pilots, the AVOSS benefits are only available during air traffic controller-managed approaches (i.e., in VMC-2, IMC-1, and IMC-2). In VMC-2 and IMC conditions, the delay model uses FAA Vortex Advisory System (VAS) wind criteria to determine when there is adequate wind to rapidly transport or dissipate the vortices. To gain additional insight, we extracted the frequency of AVOSS application at each airport. Table 1-4 contains three pieces of information we found. The first is the fraction of radar-controlled (i.e., VMC-2 and IMC) hours compared to total airport operating hours. The second is the fraction of radar-controlled hours meeting the VAS criteria compared with the total radar-controlled hours. The last is the fraction of radar-controlled hours meeting the VAS criteria compared with the total operating hours. Note that the last column is also the product of the first two.

The results show significant differences in both the potential for AVOSS use (based on the VMC-2 and IMC fractions) and the amount of that potential that can be exploited based on the VAS criteria. In comparing Tables 1-1 and 1-4, we find the maximum AVOSS benefits do not always correspond to the maximum AVOSS availability. The highest availability airport, DTW, has only the fifth highest AVOSS savings, while the lowest, LAX, has the third highest savings. We must look at demand and volume to understand the lack of correlation.

Table 1-4. AVOSS Statistics

Airport	Radar controlled fraction	VAS constraint reduction	AVOSS potential availability
	radar-controlled hours/total hours	Good VAS radar-controlled hours/ total radar-controlled hours	Good VAS radar-controlled hours/ total hours
DTW	0.38	0.57	0.22
ATL	0.43	0.39	0.17
ORD	0.38	0.38	0.14
BOS	0.22	0.58	0.13
JFK	0.32	0.40	0.13
EWR	0.35	0.36	0.13
DFW	0.18	0.34	0.06
SFO	0.19	0.39	0.07
LGA	0.25	0.19	0.05
LAX	0.33	0.15	0.05

When average delays are equal, differences in volume of demand produce proportional differences in savings. Under such conditions, busier airports will produce more total savings than less used airports just because more aircraft are saving time. In most cases, however, airports do not operate at equal fractions of capacity, some are operating near capacity while others have excess capacity. Increases in capacity or demand at airports near capacity will produce much larger changes in average delay than similar changes at underused airports. Among the TAP airports, DFW and DTW have significant excess capacity while others, ATL, ORD, LGA, EWR, and LAX are currently operating near maximum capacity. Consequently, we are not surprised to see larger savings for capacity changes at LAX versus those seen at lower volume, less heavily loaded DTW.

In addition to the average volume, the timing of demand causes differences in delay among airports. Demand varies periodically during the day, particularly at hub airports. If reduced capacity IMC conditions correlate with the arrival peaks, there will be a large buildup of delay. Different patterns of both demand and weather exist for the different airports and help produce differences in benefits.

Airspace operating conditions also affect the impact of the technologies. The differences in meteorological operating minimums, common path lengths, distances to departure turns, and other parameters generate relative differences in the impact of the TAP technologies on the airports.

The fact that the delay model performs hour-by-hour analysis with hourly weather and demand data allows detailed investigation of very specific questions. For example, we could examine the specific weather conditions under which VAS criteria are met for a specific runway, or we could examine the impact of changing demand patterns or meteorological operating minimums. Such analyses are options for future work.

TAP Savings Compared to PFAST and AFAST

The 10-year savings due to PFAST range from zero (when the inefficiency buffer is zero) to $3.7 billion (when buffers are applied to all airports). The maximum PFAST savings are on the order of the combined total savings for DROM, ROTO, and AVOSS. The PFAST benefits are entirely based on the buffer assumptions. Uncertainty regarding those assumptions was discussed earlier.

The 10-year savings due to AFAST range from $3.1 billion to $8.2 billion depending on the buffer assumption. The benefits of AFAST are dependent both on the buffer assumption and on AFAST's estimated reduction of speed, position, and wind uncertainty. We describe the selection of uncertainty parameter reductions in Appendix A. The analysis discussed in Appendix A tested the reasonableness of the reductions by comparing the resulting interarrival time uncertainty with those derived from data and simulations. Both the parameters we chose and the single runway results they produced are in keeping with results from other sources. Consequently, we have reasonable confidence in the predicted results for the TAP airports. We note here again that there are no plans for AFAST deployment, and we must consider AFAST benefits to be high risk.

Impact of Inefficiency Buffer Assumptions on TAP Benefits

The tables show that the TAP technology benefits are relatively unaffected by the differences in buffer values of the choice of baselines. The TAP technology results differ by less than 10 percent for the two inefficiency buffer assumptions and not more than 20 percent for the different baselines. The insensitivity indicates that TAP benefits are not seriously dependent on future baseline technologies.

SAFETY CONSIDERATIONS

All the TAP technologies (plus PFAST and AFAST) generate their benefits by reducing spacing between aircraft. As described in Appendix A, the capacity model algorithms include confidence factors of 95 percent for miles-in-trail separation and 97 percent for single-aircraft runway occupancy. These are standard values used in airport analysis and are applied for all technologies.

A more conservative approach would be to increase the confidence factors as separations are reduced below current threshold minimums and/or reductions are made in speed, wind, and position uncertainties. The threshold minimum reduction would apply to ATM cases where minimums are reduced to 2.3 nautical miles, and the uncertainty reductions would apply to AFAST and ATM.

DROM, ROTO, and AVOSS do not by themselves reduce the interarrival spacing below the minimum 2.5 and 3.0 nautical mile interarrival separations used today, and they do not reduce the speed, position, or wind uncertainties. Consequently, the current confidence factors are adequate for those technologies.

SUMMARY

This chapter outlined the NASA technologies, our analysis, and the key results. The remainder of the report includes more detail and background information. At this stage of the analysis, we can conclude that the TAP technologies have attractive potential benefits based on arrival delay reduction alone. We note that all potential benefits are based on the confirmation of the following key assumptions that should be addressed by the research program:

- DROM will demonstrate average runway arrival times <50 seconds in rain.
- Controllers will use 2.5 nautical mile minimum separations in IMC-1 conditions based on DROM data.
- ROTO will enable average runway occupancy times <50 seconds in low-visibility IMC-2 conditions.
- AVOSS will reliably confirm the modeled wake vortex separation reductions for the wind criteria used.
- Controllers using the CTAS Active Final Approach Spacing Tool with a data link can exploit reduced uncertainties in aircraft speed and position to reduce separations.
- The flight plans produced by integrated CTAS and FMS computers can be safely accepted and executed by controllers and pilots.

Chapter 2
Individual Airport Results

OVERVIEW

This chapter briefly addresses the characteristics and results for each of the 10 TAP airports. The airport results reported in this chapter include the inefficiency buffer values discussed in Appendix A. The benefit results reported in Chapter 1 that include the inefficiency buffer are the average of the high and low values contained in this chapter. The high and low values in *this* chapter are based on different definitions of direct operating costs. The lower values do not include fuel or aircraft amortization. The lower values correspond to ground holds such as those produced by the FAA Ground Delay Program. The higher values more closely model airborne delays. The values used are shown in Table 2-1.

Table 2-1. Direct Operating Costs

Airport	Low DOC	High DOC
ATL	$18.17	$32.04
BOS	$15.36	$27.59
DTW	$18.00	$31.70
ORD	$21.01	$37.61
JFK	$23.26	$43.08
LGA	$17.71	$31.05
EWR	$18.29	$32.74
DFW	$18.89	$33.66
LAX	$20.13	$36.70
SFO	$22.88	$41.90

General Modeling Assumptions

The benefit estimates in this report are subject to several modeling assumptions. Appendix A documents the assumptions and logic used to select the input parameters for modeling AFAST, PFAST, and the TAP technologies. We discuss here three other assumptions that apply to the current analyses.

VMC-1 SPEED UNCERTAINTY AND POSITION UNCERTAINTY

In VMC-1 conditions, when the pilot can see the airport and/or the traffic in front of him, the pilot can request a visual approach. In a visual approach, the pilot is responsible for separation. The basic separations used for modeling VMC-1 operations are discussed in Appendix A. We assume for the current technology that

the position, speed, and wind uncertainties are the same for the pilot as they are for the controller. In the preliminary analyses, we also assumed that the reductions in speed, position, and wind uncertainties generated by AFAST and ATM technologies would apply to VMC-1 conditions. On reflection, it is more logical to assume that pilot uncertainties will not be improved by AFAST and ATM technologies and, therefore, uncertainty reductions should only apply to VMC-2 and IMC conditions. The results contained in this report reflect that new thinking.

Departure Wind Speed Uncertainty

The input parameter tables include a single value for wind speed uncertainty. The wind uncertainty represents the difference in wind speed experienced by the leader and follower aircraft. The process for selecting the values used for the parameter are described in Appendix A. The ATM CTAS/FMS Integration technologies produce reductions in wind speed uncertainty. In the preliminary analyses we erroneously applied the ATM reductions to departures as well as arrivals. In the models used for the current results the wind speed uncertainty for departures is fixed at 7.5 knots.

Practical Limitations on Estimated Demand

The delay models require hourly arrival and departure demand data for each airport. Chapter 2 includes a discussion of how those data are produced. The basic data are multiplied by factors derived from the FAA *Terminal Area Forecast* (TAF) to produce the demands appropriate for future years.

In the first year of our study, we noted that uncritical use of the TAF factors could result in unfeasible delays. In order to identify an appropriate maximum demand level to allow for the TAP airports, we calculated the average delay per arrival for the PFAST baseline technology for all the airports for the years 1997 through 2015. We found that for some airports (i.e., LAX, ATL, and EWR) the TAF projections clearly result in unfeasible delays. We limited the demand growth when the average delay for the PFAST baseline technology case reaches subjectively determined "unacceptable levels." Table 2-2 shows the demand years used for the 10 airports.

Other, more sophisticated, approaches have been examined, such as limiting growth to the point where, in VMC-1, the delay from an arrival push is not worked off before the next arrival push. Also, we have anecdotal information that at least one airline considers developing a new hub when the VMC arrival delay exceeds 10 minutes. Time did not allow us to apply these techniques for the current analysis.

Table 2-2. Delay Analysis Demand Years

Airport	Airport Code	Demand years
Atlanta	ATL	*2000 only*
Boston	BOS	2005 – 2015
New York Kennedy	JFK	2005 – 2015
New York LaGuardia	LGA	2005 – 2015
Newark	EWR	*2005 only*
Detroit	DTW	2005 – 2015
Dallas-Fort Worth	DFW	2005 – 2015
Chicago O'Hare	ORD	2005 – 2015
Los Angeles	LAX	*2005 – 2010*
San Francisco	SFO	2005 – 2015

RECOMMENDATION

Since both the volume and hourly distribution of assumed demand has a large impact on benefits, we recommend that future work include updating the demand information with the most current demand data and projections.

AIRPORT RESULTS

Boston Logan (BOS)

OPERATIONAL ISSUES

Boston has a complex set of runways and relatively small total area. None of the parallel runways can operate independently in instrument meteorological conditions (IMC). In IMC, the dual approach streams to the parallel runways collapse to a single stream. The very short 33R/15L runway is only useful for small/turboprop aircraft in visual meteorological conditions (VMC). Noise and other political considerations have resulted in legal limits on BOS capacity. Consequently, TAP benefits only can be based on reductions in delay, not increases in capacity.

MODELING ISSUES

Boston was the first airport modeled. In the Boston model, based on BOS controller practice, fixed arrival/departure ratios are used for each runway configuration as a function of meteorological conditions. For example, when using the 4R/4L/9 configuration in VMC, the controllers operate the parallel 4s in the mixed arrival/departure mode with 25 percent departures and 75 percent arrivals. The model for this case interpolates to find the 25/75 departure-to-arrival (D/A) operating point on the appropriate arrival/departure curve. In the other airport models, the D/A point is changed to match the current hour's D/A demand ratio.

The capacity model for BOS produces the maximum departure (D), equal arrival/departure (E), maximum arrival (A), and maximum arrival plus free departures (F) capacities for both standard and AVOSS separations for all meteorological conditions. The capacities for the runway configurations are constructed in the delay model. Due to the repeated calculation of the fixed ratio capacities and the configuration capacities, the BOS model takes twice as long to run as the other delay models.

Figure 2-1 shows the layout of BOS. Table 2-3 identifies the runway configurations used at BOS. Table 2-4 contains the BOS benefit estimates.

Figure 2-1. General Edward Lawrence Logan International Airport, Boston, Massachusetts

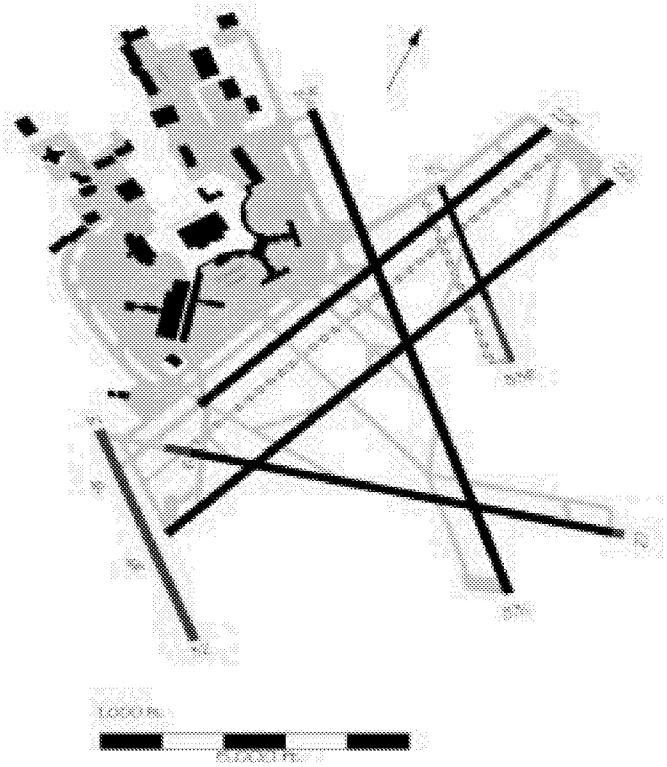

Table 2-3. Boston Logan Configurations

		Runway									
Configuration	MC	4L	4R	22L	22R	9	27	15R	15L	33R	33L
22L/22R/27	MC 1-2			AD	D		A				
22L/22R/27	MC 3-4			A	D		A				
4L/4R/9	MC 1-2	AD	AD			D					
4L/4R/9	MC 3-4	D	A			D					
33L/33R/27	MC 1-2						AD			A	AD
33L/33R/27	MC 3-4						AD				AD
15L/15R/9	MC 1-2					D		A	A		
15L/15R/9	MC 3-4					AD		AD			
22L/22R	MC 1-2			AD	AD						
22L/22R	MC 3-4			AD	D						
4R/4L	MC 1-2	AD	AD								
4R/4L	MC 3-4	D	AD								
33L/33R	All MC									AD	AD
15L/15R	All MC							AD	AD		
27	All MC						AD				
9	All MC						AD				

MC = Visual or Instrument Meteorological Conditions (VMC and IMC)
MC 1 = VMC-1, MC 2 = VMC-2, MC 3 = IMC-1, MC 4 = IMC-2 and higher
A = arrival, D = departure, AD = mixed arrival/departure

Table 2-4. Boston 10-Year Arrival Delay Benefits

Scenario	Cost avoidance compared to	Minutes (millions)	1997 Constant (millions)		Present Value (millions)		Then-year (millions)	
			Lower Bound	Upper Bound	Lower Bound	Upper Bound	Lower Bound	Upper Bound
PFAST Baseline	CT	12.5	191	344	77	138	273	490
PFAST DROM	PFAST	6.5	99	179	40	73	141	254
PFAST ROTO DROM	PFAST	7.7	118	212	48	86	168	302
PFAST AVOSS	PFAST	8.8	135	243	55	98	192	346
PFAST DROM AVOSS	PFAST	15.5	238	427	96	173	338	608
PFAST AVOSS ROTO DROM	PFAST	16.8	258	463	104	188	366	658
AFAST Baseline	CT	27.0	414	744	167	300	590	1,060
AFAST DROM	AFAST	6.7	103	186	42	75	147	264
AFAST ROTO DROM	AFAST	8.0	124	222	50	90	176	316
AFAST AVOSS	AFAST	8.3	127	229	52	93	181	325
AFAST DROM AVOSS	AFAST	15.1	233	418	94	169	331	594
AFAST AVOSS ROTO DROM	AFAST	16.5	254	456	103	185	361	648
ATM-1 CTAS/3DFMS	AFAST	6.5	100	179	40	72	142	255
ATM-1 ROTO DROM	AFAST	14.4	222	399	90	161	316	567
ATM-1 DROM AVOSS	AFAST	21.0	322	578	130	234	458	823
ATM-1 AVOSS ROTO DROM	AFAST	24.8	381	685	154	277	542	974
ATM-2 CTAS/4DFMS	AFAST	17.3	266	478	107	193	379	680
ATM-2 AVOSS ROTO DROM	AFAST	40.3	619	1,113	249	448	883	1,586

Atlanta Hartsfield (ATL)

OPERATIONAL ISSUES

Atlanta is well-designed with two widely-spaced pairs of parallel runways. There are some ground congestion problems and there are occasional departure delays due to congestion in the crowded eastern enroute sectors. Most of the delay at Atlanta, however, is due to the fact that the two arrival runways are running at near capacity.

MODELING ISSUES

Atlanta was the first airport modeled with the closely spaced parallel runway algorithms. As with Boston, the capacity model for Atlanta produces D, E, A, and F points, and the configuration capacities are generated in the delay model.

Figure 2-2 shows the layout of ATL. Table 2-5 identifies the runway configurations used at ATL. Table 2-6 contains the ATL benefit estimates.

Figure 2-2. The William B. Hartsfield Atlanta International Airport, Atlanta, Georgia

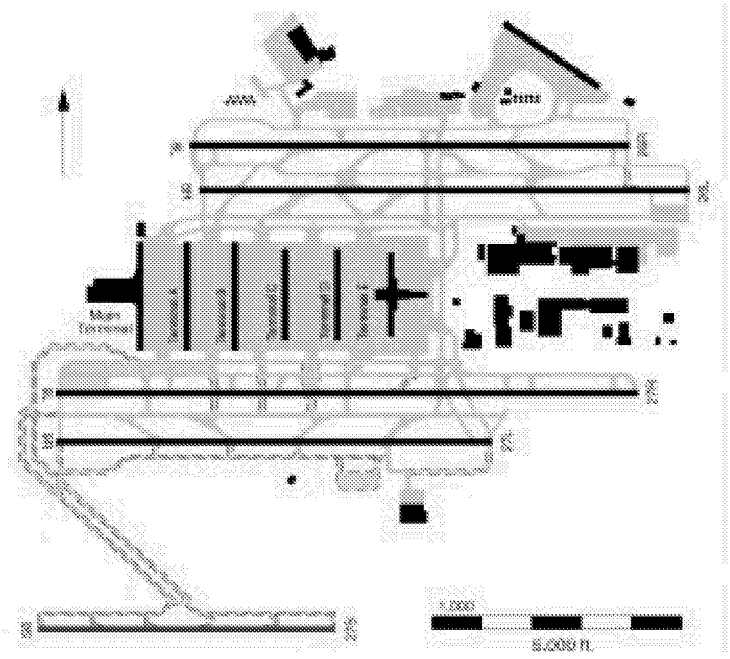

Table 2-5. Atlanta Configurations

Configuration	MC	Runway							
		8L	8R	9L	9R	27L	27R	26L	26R
East Flow	MC 1-2	A*	D	D	A*				
	MC 3-4	A*	D	D	A*				
	MC 4 Cat 2	A*	D	D	A*				
	MC 4 Cat 3	A	D						
West Flow	MC 1-2					A*	D	D	A*
	MC 3-4					A*	D	D	A*

* One of these runways will run departures during departure pushes

Table 2-6. Atlanta 10-Year Arrival Delay Benefits

Scenario	Cost avoidance compared to	Minutes (millions)	1997 Constant (millions)		Present Value (millions)		Then-year (millions)	
			Lower bound	Upper bound	Lower bound	Upper bound	Lower bound	Upper bound
PFAST Baseline	CT	25.8	469	826	192	338	664	1,172
PFAST DROM	PFAST	3.3	61	107	25	44	86	152
PFAST ROTO DROM	PFAST	5.9	107	188	44	77	151	267
PFAST AVOSS	PFAST	18.0	328	578	134	236	465	819
PFAST DROM AVOSS	PFAST	20.8	378	667	155	273	536	946
PFAST AVOSS ROTO DROM	PFAST	23.1	419	738	171	302	594	1,047
AFAST Baseline	CT	59.7	1,085	1,913	444	782	1,539	2,713
AFAST DROM	AFAST	2.5	45	79	18	32	63	112
AFAST ROTO DROM	AFAST	3.8	70	123	29	50	99	174
AFAST AVOSS	AFAST	11.8	215	379	88	155	305	537
AFAST DROM AVOSS	AFAST	13.7	250	440	102	180	354	624
AFAST AVOSS ROTO DROM	AFAST	15.0	272	480	111	196	386	681
ATM-1 CTAS/3DFMS	AFAST	11.4	207	364	84	149	293	517
ATM-1 ROTO DROM	AFAST	14.4	262	462	107	189	372	656
ATM-1 DROM AVOSS	AFAST	22.6	410	723	168	296	582	1,026
ATM-1 AVOSS ROTO DROM	AFAST	24.5	445	785	182	321	631	1,113
ATM-2 CTAS/4DFMS	AFAST	26.6	483	851	197	348	685	1,207
ATM-2 AVOSS ROTO DROM	AFAST	35.4	643	1,134	263	463	912	1,608

New York LaGuardia (LGA)

OPERATIONAL ISSUES

LaGuardia has only two intersecting runways. The ability of arrivals to hold short at the intersection has a large impact on the capacities of the 4/13 and 31/4 configurations. If the arrivals can hold short, then the two runways operate as an independent arrival and departure pair. If the arrivals do not hold short, then the runways operate like a single runway operating in an alternating arrival/departure mode. Historically, about 60 percent of the large aircraft and 40 percent of the heavy aircraft can hold short. When conditions are wet, no one can be expected to hold short.

In the 22/31 configuration, extra spacing is added to the average interarrival time to account for the required 2-minute delay of the next arrival after a heavy or B-757 departure.

MODELING ISSUES

The LaGuardia capacity model includes adjustments to the aircraft mix to accommodate the fractions of arrivals that hold short of the intersection. The model also includes separate "wet" and "dry" IMC configurations. The delay model uses the "wet" and "dry" data in the weather file to select the correct configuration.

Figure 2-3 shows the layout of LGA. Table 2-7 identifies the runway configurations used at LGA. Table 2-8 contains the LGA benefit estimates.

Figure 2-3. La Guardia Airport, New York, New York

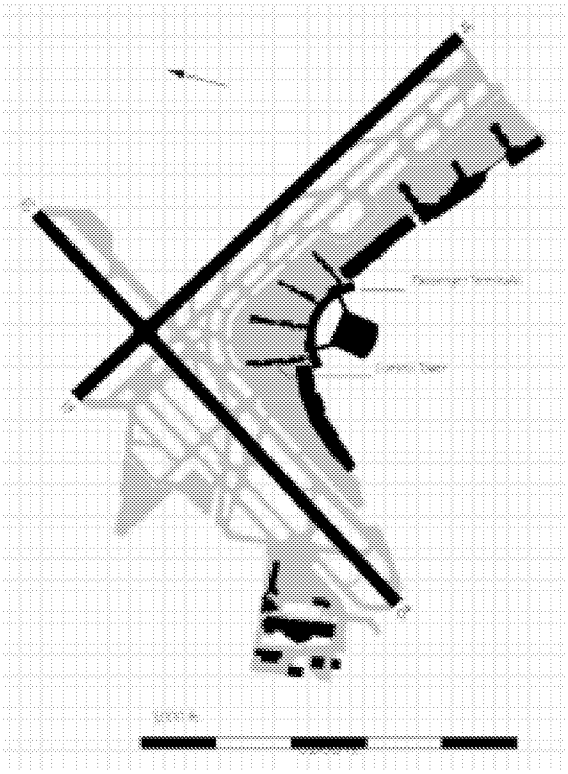

Table 2-7. LaGuardia Configurations

Configuration	MC	Runway			
		4	13	22	31
Single	MC 1-2	AD*	AD*	AD*	AD*
4/13 Dry	MC 3-4	A	D		
22/13	MC 1-2		D	A	
22/31	MC 3-4			A	D
31/4 Dry	MC 1-2	D			A
Wet	MC 3-4	AD**	AD**	AD**	AD**

* One runway only

** One pair of runways: arrive on one, depart on the other

Table 2-8. LaGuardia 10-Year Arrival Delay Benefits

Scenario	Cost avoidance compared to	Minutes (millions)	1997 Constant (millions)		Present Value (millions)		Then-year (millions)	
			Lower bound	Upper bound	Lower bound	Upper bound	Lower bound	Upper bound
PFAST Baseline	CT	7.0	124	217	50	88	176	309
PFAST DROM	PFAST	1.7	30	52	12	21	42	74
PFAST ROTO DROM	PFAST	3.9	69	121	28	49	98	173
PFAST AVOSS	PFAST	2.0	35	61	14	25	50	87
PFAST DROM AVOSS	PFAST	3.6	64	111	26	45	90	158
PFAST AVOSS ROTO DROM	PFAST	5.6	100	175	40	71	142	249
AFAST Baseline	CT	14.3	253	443	102	179	359	630
AFAST DROM	AFAST	1.1	20	36	8	14	29	51
AFAST ROTO DROM	AFAST	2.7	49	85	20	34	69	121
AFAST AVOSS	AFAST	1.4	24	43	10	17	35	61
AFAST DROM AVOSS	AFAST	2.4	42	73	17	30	60	104
AFAST AVOSS ROTO DROM	AFAST	3.8	67	117	27	48	95	167
ATM-1 CTAS/3DFMS	AFAST	2.6	46	80	19	33	65	114
ATM-1 ROTO DROM	AFAST	4.7	83	146	34	59	118	207
ATM-1 DROM AVOSS	AFAST	4.1	72	127	29	51	103	180
ATM-1 AVOSS ROTO DROM	AFAST	5.7	101	178	41	72	144	253
ATM-2 CTAS/4DFMS	AFAST	6.1	109	191	44	78	155	271
ATM-2 AVOSS ROTO DROM	AFAST	8.1	143	251	58	102	204	357

New York John F. Kennedy International (JFK)

OPERATIONAL ISSUES

Kennedy Airport has a lot of concrete, moderate demand, and very congested airspace. Approach and departure routes conflict with those of Laguardia and Newark. The relatively narrow range of IMC-1 (700 to 1,000 feet ceiling and 1 to 2 miles visibility) limit the potential impact of DROM. The high percentage of heavy class aircraft (42 percent) at JFK enhances the impact of AVOSS.

MODELING ISSUES

The congestion results in common path lengths of 12 nautical miles for runways 22L and 22R, and 8 nautical miles for the rest. When using the parallel 31s, runway 31R is used for turboprop departures only. The model will assign some turboprops to the 31L departure mix if needed to balance the turboprop and jet departure rates.

Figure 2-4 shows the layout of JFK. Table 2-9 identifies the runway configurations used at JFK. Table 2-10 contains the JFK benefit estimates.

Figure 2-4. John F. Kennedy International Airport, New York City

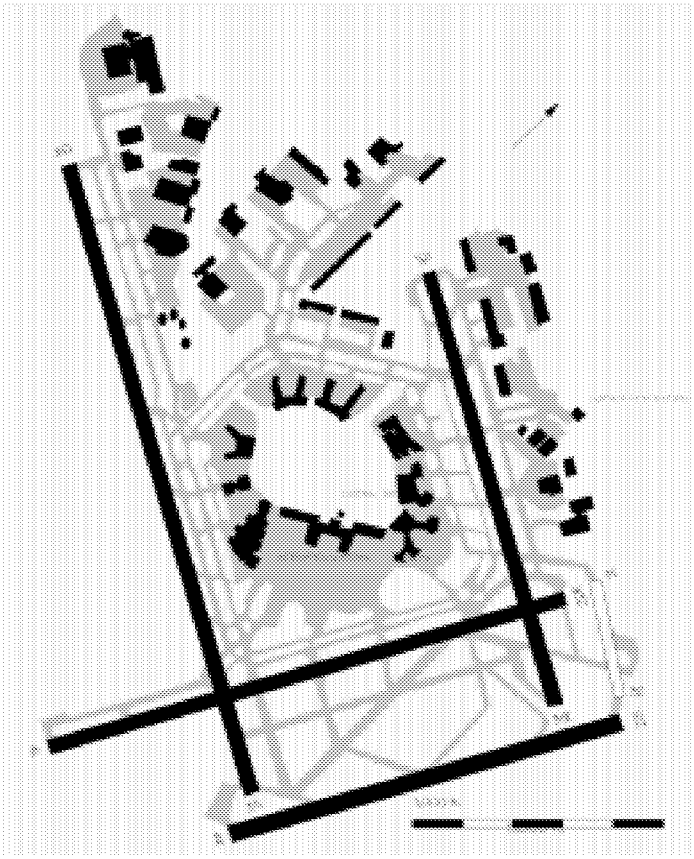

Table 2-9. New York Kennedy Configurations

Configuration	MC	Runway							
		4L	4R	22L	22R	31L	31R	13L	13R
Departures only	MC 2	D	D	D	D	D	D	D	D
13s overflow 22	MC 1-2			A				D	AD
Depart 31L 22R	all MC			A	D	D			
Arrive 13R 22L	MC 1-2			A	D				A
Arrive 4R 13 L	MC 1-2	D	A					A	
Depart 4L 31L	all MC	D	A			D			
Parallel 31	all MC					AD/A	AD/A		
Parallel 4	all MC	AD/A	AD/A						
Parallel 22				AD/A	A/D				
Parallel 13								D	A
Parallel 31 low vis	all MC					D	AD/A		
Parallel 4 low vis	all MC	D	AD/A						
Parallel 22 low vis	all MC			AD/A	D				

Table 2-10. New York Kennedy 10-Year Arrival Delay Benefits

Scenario	Cost avoidance compared to	Minutes (millions)	1997 Constant (millions)		Present Value (millions)		Then-year (millions)	
			Lower bound	Upper bound	Lower bound	Upper bound	Lower bound	Upper bound
PFAST Baseline	CT	3.3	77	142	31	57	109	203
PFAST DROM	PFAST	0.0	1	2	0	1	2	3
PFAST ROTO DROM	PFAST	1.2	28	52	11	21	40	74
PFAST AVOSS	PFAST	2.3	54	101	22	40	78	144
PFAST DROM AVOSS	PFAST	2.4	56	103	22	41	80	148
PFAST AVOSS ROTO DROM	PFAST	3.7	87	161	35	65	124	230
AFAST Baseline	CT	7.1	164	305	66	122	235	435
AFAST DROM	AFAST	0.0	0	1	0	0	1	1
AFAST ROTO DROM	AFAST	1.0	24	45	10	18	34	63
AFAST AVOSS	AFAST	1.9	45	84	18	33	65	120
AFAST DROM AVOSS	AFAST	2.0	46	84	18	34	65	121
AFAST AVOSS ROTO DROM	AFAST	3.1	73	135	29	54	104	193
ATM-1 CTAS/3DFMS	AFAST	2.0	46	86	19	34	66	123
ATM-1 ROTO DROM	AFAST	3.0	69	128	28	51	99	183
ATM-1 DROM AVOSS	AFAST	3.9	92	170	37	68	131	243
ATM-1 AVOSS ROTO DROM	AFAST	5.1	118	219	47	87	169	313
ATM-2 CTAS/4DFMS	AFAST	4.9	114	212	46	85	164	303
ATM-2 AVOSS ROTO DROM	AFAST	7.5	174	323	69	129	250	462

Newark International (EWR)

Operational Issues

The ability to use circling approaches to Runway 11 has a large impact on capacity at Newark. To accurately model that ability, we had to include a separate IMC_CM circling minimum meteorological condition. In the Normal 22s or Normal 11s configurations, Runway 11/29 can be used for arrivals or departures but not for both at the same time.

Modeling Issues

To account for airspace structure, a 5-nautical mile common path for arrivals and departures is used for the 22s configurations; a 6 nautical mile common path is used for the 4s configurations.

Figure 2-5 shows the layout of EWR. Table 2-11 identifies the runway configurations used at EWR. Table 2-12 contains the EWR benefit estimates.

Figure 2-5. Newark International Airport, Newark, New Jersey

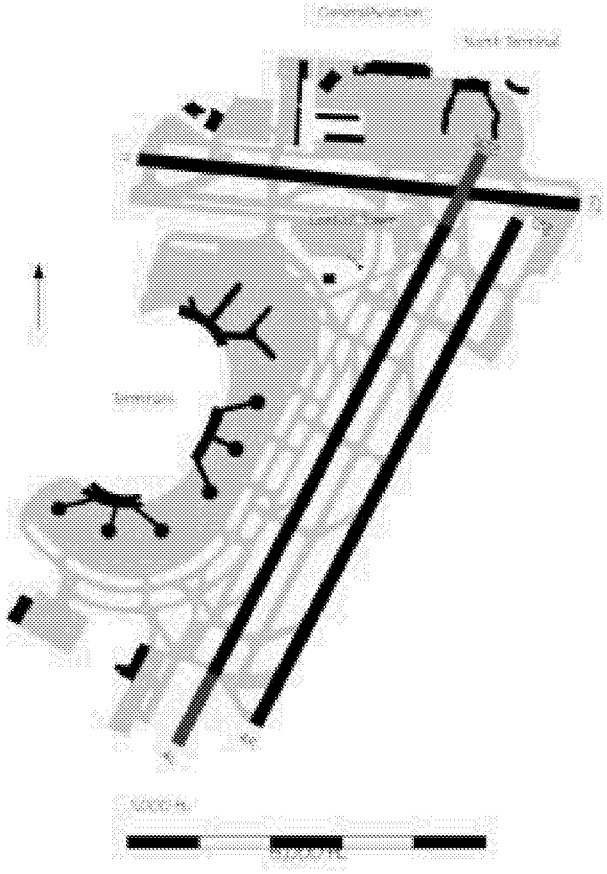

Table 2-11. Newark Configurations

Configuration	MC	Runway					
		4L	4R	22R	22L	29	11
Normal 22s	MC 1-2/IMC1_CM			D	A	D*	A*
Normal 4s	MC 1-2/IMC1_CM	D	A			D*	A*
22s only	MC 2-3			D	A		
4s only	MC 2-3	D	A				
4/11	MC 1-2/IMC1_CM	D	A				A
4/29	MC 1-2/IMC1_CM	D	A			D	
22/11	MC 1-2/IMC1_CM			D	A		
22/29	MC 1-2/IMC1_CM			D	A	D	
11/29 only	MC 1-2/IMC1_CM					A/D	A/D

* Simultaneous operations not allowed.
IMC1_CM = IMC1 circling minimum

Table 2-12. Newark 10-Year Arrival Delay Benefits

Scenario	Cost avoidance compared to	Minutes (millions)	1997 Constant (millions)		Present Value (millions)		Then-year (millions)	
			Lower Bound	Upper Bound	Lower Bound	Upper Bound	Lower Bound	Upper Bound
PFAST Baseline	CT	9.1	165	291	67	119	234	412
PFAST DROM	PFAST	0.1	2	4	1	2	3	5
PFAST ROTO DROM	PFAST	0.7	12	21	5	9	17	30
PFAST AVOSS	PFAST	4.2	76	134	31	55	108	190
PFAST DROM AVOSS	PFAST	4.5	82	144	33	59	116	205
PFAST AVOSS ROTO DROM	PFAST	4.8	87	154	36	63	124	218
AFAST Baseline	CT	19.3	351	620	144	253	498	879
AFAST DROM	AFAST	0.2	5	8	2	3	6	11
AFAST ROTO DROM	AFAST	0.4	7	13	3	5	10	18
AFAST AVOSS	AFAST	3.7	67	118	27	48	95	168
AFAST DROM AVOSS	AFAST	3.9	71	125	29	51	101	178
AFAST AVOSS ROTO DROM	AFAST	4.1	74	130	30	53	105	184
ATM-1 CTAS/3DFMS	AFAST	4.2	75	133	31	54	107	189
ATM-1 ROTO DROM	AFAST	4.5	82	145	34	59	116	205
ATM-1 DROM AVOSS	AFAST	8.4	152	268	62	110	216	380
ATM-1 AVOSS ROTO DROM	AFAST	8.5	155	273	63	112	220	387
ATM-2 CTAS/4DFMS	AFAST	11.5	209	368	85	151	296	522
ATM-2 AVOSS ROTO DROM	AFAST	15.2	276	486	113	199	391	689

Detroit Metropolitan Wayne County (DTW)

OPERATIONAL ISSUES

Detroit has a high capacity runway configuration with widely spaced independent runways. Capacity can be limited by ground congestion, but a new terminal is planned that will improve the ground situation. The capacity on the 27 runways is artificially restricted by law for noise reasons.

Detroit's widely spaced parallel runways enable it to continue independent operations in IMC conditions. The benefits for AVOSS at DTW are helped by the fact that there are twice as many radar-controlled (i.e., VMC-2 and IMC) hours that meet the VAS wind conditions at DTW than at BOS.

MODELING ISSUES

Detroit was the second airport analyzed. The DTW capacity model produces D, E, A, and F values for each meteorological condition and the configuration curves are produced in the delay model. Versions of the DTW models can be run on-line from the NASA Aviation System Analysis Capability (ASAC) Website (www.asac.lmi.org).

Figure 2-6 shows the layout of DTW. Table 2-13 identifies the runway configurations used at DTW. Table 2-14 contains the DTW benefit estimates.

Figure 2-6. Detroit Metropolitan Wayne County Airport, Detroit, Michigan

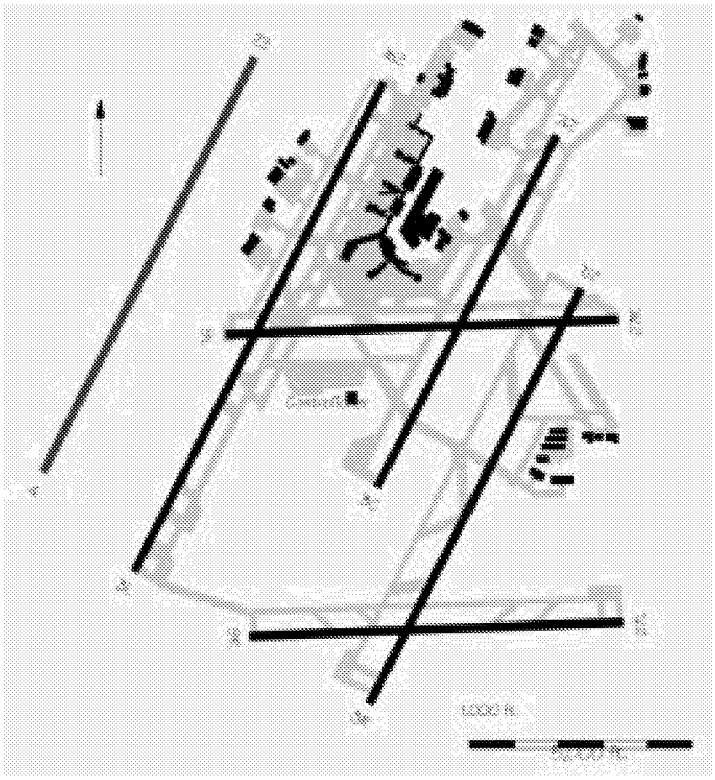

Table 2-13. Detroit Wayne County Configurations

Configuration	MC	Runway									
		21R	21C	21L	3R	3C	3L	27R	27L	9R	9L
21L/21C/21R	All MC	AD	D	A							
3L/3C/3R	MC 1-3				A	D	AD				
3L/3C/3R	MC 2				A	D	AD				
27L/27R	All MC							A	AD		
27L/27R/21R	All MC	D						A	A		

Table 2-14. Detroit Wayne County 10-Year Arrival Delay Benefits

Scenario	Cost avoidance compared to	Minutes (millions)	1997 Constant (millions)		Present Value (millions)		Then-year (millions)	
			Lower Bound	Upper Bound	Lower Bound	Upper Bound	Lower Bound	Upper Bound
PFAST Baseline	CT	9.4	170	299	64	112	248	437
PFAST DROM	PFAST	3.3	59	103	22	39	85	150
PFAST ROTO DROM	PFAST	3.8	69	122	26	47	100	177
PFAST AVOSS	PFAST	5.9	106	187	40	70	155	273
PFAST DROM AVOSS	PFAST	8.4	151	266	57	100	221	389
PFAST AVOSS ROTO DROM	PFAST	9.0	162	285	61	108	236	416
AFAST Baseline	CT	18.6	335	591	126	222	491	864
AFAST DROM	AFAST	2.3	41	71	15	27	59	104
AFAST ROTO DROM	AFAST	2.8	51	89	19	34	74	130
AFAST AVOSS	AFAST	4.7	84	149	32	56	123	217
AFAST DROM AVOSS	AFAST	6.6	118	208	45	79	173	304
AFAST AVOSS ROTO DROM	AFAST	7.2	129	228	49	87	189	332
ATM-1 CTAS/3DFMS	AFAST	4.6	82	144	31	55	120	211
ATM-1 ROTO DROM	AFAST	7.1	127	224	48	85	185	326
ATM-1 DROM AVOSS	AFAST	11.1	200	353	76	133	292	515
ATM-1 AVOSS ROTO DROM	AFAST	11.9	213	376	81	143	311	548
ATM-2 CTAS/4DFMS	AFAST	11.1	199	351	75	133	291	513
ATM-2 AVOSS ROTO DROM	AFAST	16.7	300	528	114	200	437	769

Chicago O'Hare International (ORD)

OPERATIONAL ISSUES

Chicago O'Hare capacity is strongly affected by the ability to use three independent arrival runways ("triples" or "trips"). In IMC, one of the parallel runway configurations (9s, 14s, 22s, 27s, or 32s) must be used.

MODELING ISSUES

The salient modeling feature of ORD is the many configurations. Initial runs showed that, based on weather only, the configurations often would switch every hour, which never happens in real life. Special criteria had to be established to limit configuration changes based on controller logic. Similar logic is used in the DFW, SFO, and EWR models.

In some of the triple configurations, heavy jets are prohibited from landing on one of the long runways. In others, only turboprops may use one of the runways. The model computes the arrival mix on the non-restricted runways that balances arrival rates for all aircraft classes. ORD also uses a mixed arrival/departure mode where arrival spacing allows two departures between each arriving pair. Special code in the ORD model computes the runway capacity in this mode.

Figure 2-7 shows the layout of ORD. Table 2-15 identifies the runway configurations used at ORD. Table 2-16 contains the ORD benefit estimates.

Figure 2-7. Chicago O Hare International Airport, Chicago, Illinois

Table 2-15. ORD Runway Configurations

Configuration	Runway											
	4L	4R	9L	9R	14L	14R	22L	22R	27L	27R	32L	32R
Depart Only	Not modeled, assume two in use											
Plan B Trip 22					AT	A	M	A	D			
Plan B Trip 27					AT	A	D	A	D	AX		
Parallel 27 Trip 32L							D		A	A	M	D
Plan X	D	A	M	A							D	D
Plan Weird Trip 27							D	A	A	AX	D	
Plan B						A	D	A	D			
Plan Weird							D	A	A		D	
P27s							D		A	A	D	D
Mod Plan X	D	A	A	D								D
P9s depart 4L 22L	D		A	M			D					
P9s depart 32R 22L			A	M			D					D
P9s depart 22L			A	M			D					
P9s depart 4L	D		A	M								
P9s depart 32R			A	M								D
P14s			D		A	A	D		D			
P14s no depart 27			D		A	A	D					
P14s no depart 9	D				A	A	D		D			
P14s no depart 9 or 4					A	A	D		D			
P14s no depart 22			D		A	A			D			
P14s depart 9s			D	D	A	A						
P32s									D		M	M
P22s							M	M	D	D		

A: arrival only for any type of aircraft, AT: turboprop arrivals, AX: any arrivals except heavy jets, D: departures only, M: mixed operations - arrival and departures

Table 2-16. Chicago O'Hare 10-Year Arrival Delay Benefits

Scenario	Cost avoidance compared to:	Minutes (millions)	1997 Constant (millions)		Present Value (millions)		Then-year (millions)	
			Lower Bound	Upper Bound	Lower Bound	Upper Bound	Lower Bound	Upper Bound
PFAST Baseline	CT	12.8	269	482	107	192	385	689
PFAST DROM	PFAST	5.4	114	204	46	82	162	291
PFAST ROTO DROM	PFAST	15.0	316	566	128	229	450	805
PFAST AVOSS	PFAST	9.5	199	357	80	143	285	510
PFAST DROM AVOSS	PFAST	14.9	313	561	126	225	447	801
PFAST AVOSS ROTO DROM	PFAST	25.1	528	945	213	381	752	1,347
AFAST Baseline	CT	33.9	713	1,277	285	511	1,020	1,825
AFAST DROM	AFAST	5.5	116	208	47	84	166	297
AFAST ROTO DROM	AFAST	14.7	308	552	124	223	439	786
AFAST AVOSS	AFAST	8.4	177	317	71	127	253	453
AFAST DROM AVOSS	AFAST	13.7	287	515	115	206	411	735
AFAST AVOSS ROTO DROM	AFAST	23.1	485	868	195	349	692	1,239
ATM-1 CTAS/3DFMS	AFAST	10.4	218	391	88	157	312	558
ATM-1 ROTO DROM	AFAST	24.1	507	907	203	364	723	1,295
ATM-1 DROM AVOSS	AFAST	20.8	437	782	175	313	624	1,118
ATM-1 AVOSS ROTO DROM	AFAST	32.1	674	1,207	270	483	963	1,725
ATM-2 CTAS/4DFMS	AFAST	24.9	522	935	209	374	746	1,336
ATM-2 AVOSS ROTO DROM	AFAST	40.3	846	1,514	338	605	1,210	2,166

Dallas-Fort Worth International (DFW)

OPERATIONAL ISSUES

Dallas has tremendous runway capacity and wide open airspace. The runways are widely dispersed, which allows independent operation, but wide dispersion also makes runway balancing more difficult. Most of the terminals are situated on the east side of the airport, which can lead to either imbalance between east and west runways or long taxi times from the west runways. Optimized runway balancing was an important feature of PFAST at DFW. The TAP technology savings for DFW are significant but fundamentally limited because of the high fraction of VMC operations and the huge capacity of the airport relative to the projected demand.

MODELING ISSUES

At DFW, some runways permit only turboprop departures. The model adjusts the departure mix on the other runways to reflect this.

Figure 2-8 shows the layout of DFW. Table 2-17 and 2-18 identify the runway configurations used at DFW. Table 2-19 contains the DFW benefit estimates.

Figure 2-8. Dallas-Fort Worth International Airport, Dallas/Fort Worth, Texas

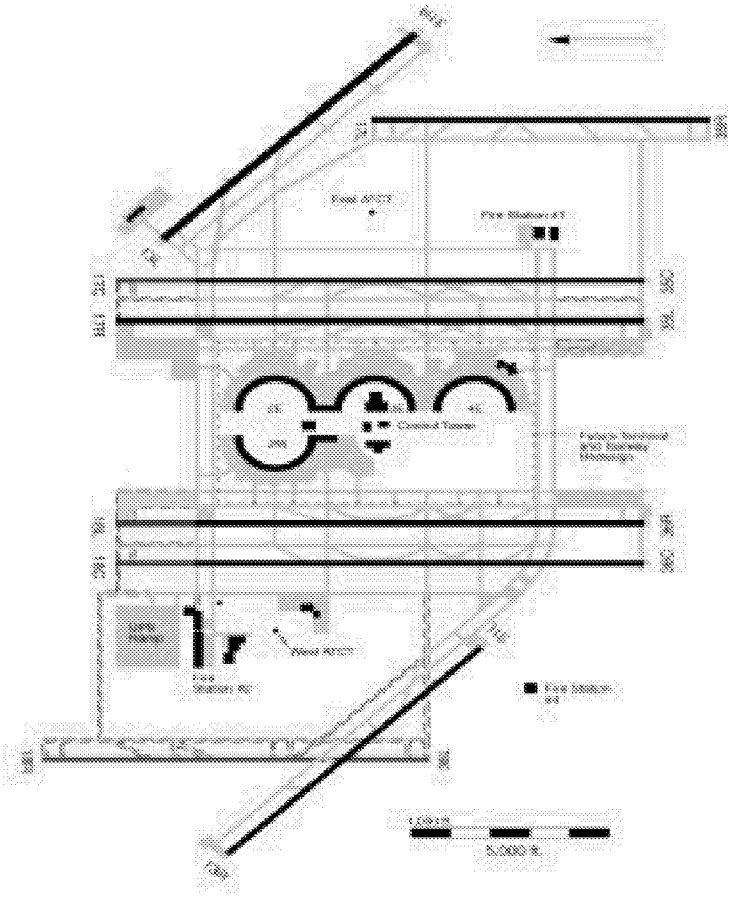

Table 2-17. Dallas-Fort Worth International Configurations (North Flow)

	Runway							
Configuration	MC	36L	36R	35L	35C	35R	31L	31R
Northflow	MC 1-2	A	D	D	A	A	DT	A
Northflow	MC 3-4	A	D	D	A	AD	DT	
Only 31	MC 1-4						AD	AD
No 31	MC 1-4	A	D	D	A	AD		

DT = Turboprop departures

Table 2-18. Dallas-Fort Worth International Configurations (South Flow)

	Runway							
Configuration	MC	17L	17C	17R	18L	18R	13L	13R
Southflow	MC 1-2	A	A	D	D	A	DT	A
Southflow	MC 3-4	A	A	D	D	A	DT	
Only 13	MC 1-4						AD	AD
No 13	MC 1-4	AD	A	D	D	A		

Table 2-19. Dallas-Fort Worth 10-year Arrival Delay Benefits

Scenario	Cost avoidance compared to	Minutes (millions)	1997 Constant (millions)		Present Value (millions)		Then-year (millions)	
			Lower Bound	Upper Bound	Lower Bound	Upper Bound	Lower Bound	Upper Bound
PFAST Baseline	CT	23.2	438	781	160	284	648	1,154
PFAST DROM	PFAST	2.4	45	79	17	30	65	116
PFAST ROTO DROM	PFAST	7.5	141	252	55	98	204	363
PFAST AVOSS	PFAST	5.4	102	181	39	69	149	265
PFAST DROM AVOSS	PFAST	7.7	145	258	55	98	211	376
PFAST AVOSS ROTO DROM	PFAST	12.7	241	429	93	165	349	622
AFAST Baseline	CT	44.1	833	1,483	306	546	1,227	2,186
AFAST DROM	AFAST	2.0	39	69	15	26	56	101
AFAST ROTO DROM	AFAST	5.5	104	185	40	71	150	268
AFAST AVOSS	AFAST	4.1	78	139	29	52	114	203
AFAST DROM AVOSS	AFAST	6.1	114	204	43	77	167	298
AFAST AVOSS ROTO DROM	AFAST	9.4	178	316	68	120	259	461
ATM-1 CTAS/3DFMS	AFAST	9.4	178	318	66	118	262	466
ATM-1 ROTO DROM	AFAST	13.0	246	438	92	164	360	641
ATM-1 DROM AVOSS	AFAST	13.9	262	467	98	174	384	685
ATM-1 AVOSS ROTO DROM	AFAST	16.3	308	548	115	205	451	803
ATM-2 CTAS/4DFMS	AFAST	22.4	424	755	156	278	624	1,112
ATM-2 AVOSS ROTO DROM	AFAST	26.4	498	887	183	327	733	1,307

Los Angeles International (LAX)

OPERATIONAL ISSUES

Los Angeles can operate its two pairs of parallel runways independently in IMC conditions. The airspace is crowded in the Los Angeles area and the lineup for LAX starts many miles to the east. Aircraft are fed into the line from the north and south (and even from directly below for flights from Ontario Airport).

Airport capacity suffers when east flow approaches are required. Part of the reason is increased ROTs for the runways in east flow and part is due to the fact that east flow is infrequent and the patterns less practiced.

Unlike the other nine TAP airports, LAX experiences a high proportion of dry IMC-1 conditions during which the airport operates with 2.5 nautical mile minimum separations. Under wet IMC-1 conditions, the airport reverts to 3.0 nautical mile minimum separations.

MODELING ISSUES

Two sets of IMC-1 input files are required for LAX to cover the dry and wet conditions. A second set of ROTs also is added for the east flow runways.

Figure 2-9 shows the layout of LAX. Table 2-20 identifies the runway configurations used at LAX. Table 2-21 contains the LAX benefit estimates.

Figure 2-9. Los Angeles International Airport, Los Angeles, California

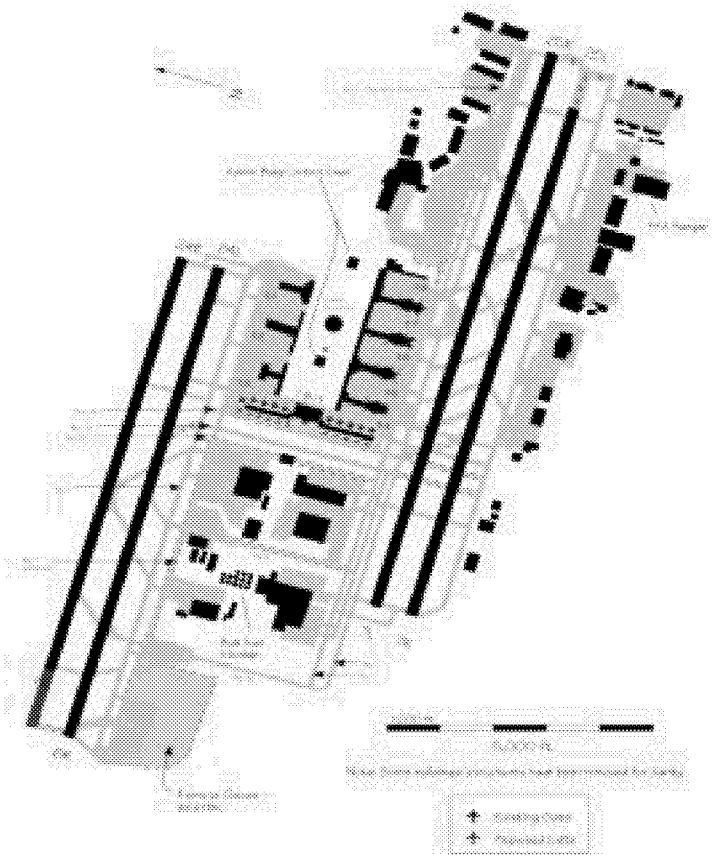

Table 2-20. Los Angeles International Configurations

Configuration	MC	Runway							
		6L	6R	7L	7R	25L	25R	24L	24R
West Flow	MC 1-2					AD	AD	AD	AD
West Flow	MC 3-4					A	D	D	A
East Flow	MC 1-2	AD	AD	AD	AD				
East Flow	MC 3-5	A	D	D	A				

Table 2-21. Los Angeles 10-Year Arrival Delay Benefits

Scenario	Cost avoidance compared to	Minutes (millions)	1997 Constant (millions)		Present Value (millions)		Then-year (millions)	
			Lower Bound	Upper Bound	Lower Bound	Upper Bound	Lower Bound	Upper Bound
PFAST Baseline	CT	27.1	545	993	216	395	780	1,422
PFAST DROM	PFAST	1.5	31	56	12	23	44	80
PFAST ROTO DROM	PFAST	5.2	104	190	42	77	148	270
PFAST AVOSS	PFAST	8.1	163	297	65	119	233	424
PFAST DROM AVOSS	PFAST	9.6	194	353	78	141	277	504
PFAST AVOSS ROTO DROM	PFAST	13.7	276	503	111	202	393	717
AFAST Baseline	CT	66.3	1,335	2,433	532	969	1,910	3,482
AFAST DROM	AFAST	1.5	29	53	12	21	42	76
AFAST ROTO DROM	AFAST	4.4	89	163	36	65	128	232
AFAST AVOSS	AFAST	7.1	144	262	57	104	206	375
AFAST DROM AVOSS	AFAST	8.5	172	314	68	125	247	449
AFAST AVOSS ROTO DROM	AFAST	11.6	234	426	93	170	335	610
ATM-1 CTAS/3DFMS	AFAST	17.1	344	627	137	249	492	897
ATM-1 ROTO DROM	AFAST	19.1	384	701	153	279	550	1,003
ATM-1 DROM AVOSS	AFAST	24.7	497	907	197	360	713	1,300
ATM-1 AVOSS ROTO DROM	AFAST	26.8	540	985	214	391	774	1,411
ATM-2 CTAS/4DFMS	AFAST	42.6	857	1,562	339	618	1,229	2,240
ATM-2 AVOSS ROTO DROM	AFAST	49.4	995	1,814	394	718	1,427	2,602

San Francisco International (SFO)

OPERATIONAL ISSUES

The two primary operational issues with San Francisco (SFO) are the close spacing of the parallel runways (750 feet) and the mid-runway location of the runway intersection. The close spacing of the parallel runway precludes independent operation in IMC conditions. Because the runway exits for efficient ground operations are beyond the intersection, SFO has not been able to demonstrate ROTs under 50 seconds in VMC.

MODELING ISSUES

In VMC, the SFO runways operate with the capacity of two independent runways, each in the arrival/departure mode. Two aircraft are landed side-by-side. Once they exit or pass the intersection, two departures are launched on the cross runways. In IMC, capacity is reduced to that of a single runway operated in the arrival/departure mode. If the crossing runways are not available due to wind, the active pair operates in the close-spaced parallel pair mode.

The SFO capacity model does not have the same level of sophistication and verification as the other TAP models. For SFO, the capacities of the specific configurations are factored to match the existing capacity data (e.g., the capacity of the close-spaced parallel pair model is scaled to match the measured capacities for each of the four parallel configurations). The same scaling factors are used for all technologies.

Figure 2-10 shows the layout of SFO. Table 2-22 identifies the runway configurations used at SFO. Table 2-23 contains the SFO benefit estimates.

Figure 2-10. San Francisco International Airport, San Francisco, California

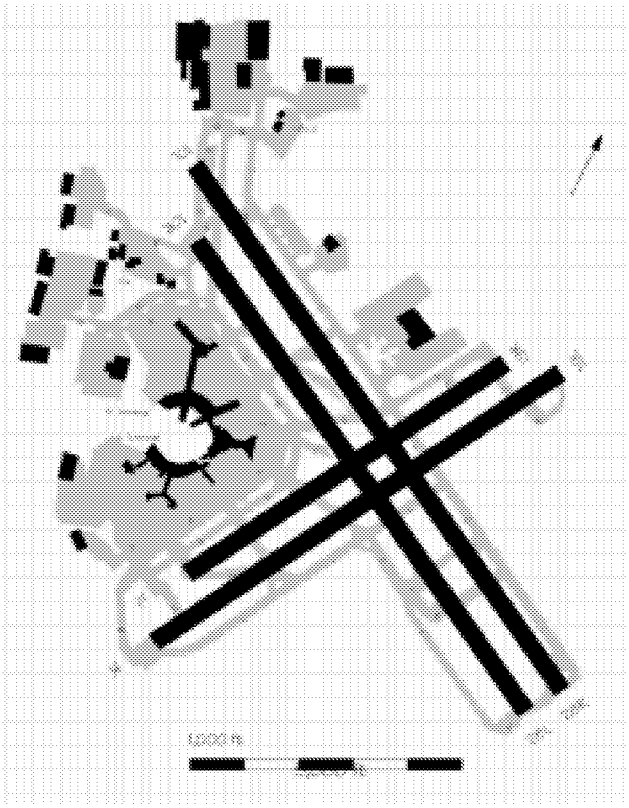

Table 2-22. San Francisco 10-Year Arrival Delay Benefits

Scenario	Cost avoidance compared to	Minutes (millions)	1997 Constant (millions)		Present Value (millions)		Then-year (millions)	
			Lower Bound	Upper Bound	Lower Bound	Upper Bound	Lower Bound	Upper Bound
PFAST Baseline	CT	9.7	184	327	70	125	267	476
PFAST DROM	PFAST	0.0	0	0	0	0	0	0
PFAST ROTO DROM	PFAST	1.5	29	52	12	21	42	75
PFAST AVOSS	PFAST	2.1	40	71	15	28	58	103
PFAST DROM AVOSS	PFAST	2.1	40	71	15	28	58	103
PFAST AVOSS ROTO DROM	PFAST	3.6	69	123	27	48	99	177
AFAST Baseline	CT	15.9	300	535	115	204	437	778
AFAST DROM	AFAST	0.0	0	0	0	0	0	0
AFAST ROTO DROM	AFAST	1.5	29	51	11	20	41	74
AFAST AVOSS	AFAST	1.5	29	52	11	20	42	75
AFAST DROM AVOSS	AFAST	1.5	29	52	11	20	42	75
AFAST AVOSS ROTO DROM	AFAST	3.0	57	102	22	40	83	147
ATM-1 CTAS/3DFMS	AFAST	1.9	36	65	14	25	52	94
ATM-1 ROTO DROM	AFAST	3.4	64	114	25	45	93	165
ATM-1 DROM AVOSS	AFAST	3.2	60	106	23	41	87	154
ATM-1 AVOSS ROTO DROM	AFAST	4.6	87	156	34	60	126	225
ATM-2 CTAS/4DFMS	AFAST	5.9	112	199	43	76	162	289
ATM-2 AVOSS ROTO DROM	AFAST	8.3	157	279	60	107	227	405

Table 2-23. San Francisco Configurations

Configuration	MC	Runway							
		28L	28R	1L	1R	19L	19R	10L	10R
Preferred	All MC	A	A	D	D				
SEPlan	All MC					A	A	D	D
Parallel 28s	All MC	A	D						
Parallel 10s	All MC							A	D
Parallel 1s	All MC			A	D				
Parallel 19s	All MC					A	D		

Chapter 3
Computer Programs and Databases

OVERVIEW

Estimating TAP benefits has required development of computer programs and input databases. The programs include both analytical models and utility programs. The databases include essential input data for the analyses. An understanding of the models and the data is helpful in assessing the validity of the estimated benefits, the potential for improvements, and potential for analysis of other technologies. This chapter briefly discusses the following computer programs and data sources:

- Shell and batch airport capacity and delay models
- Benefit workbook
- Weather database
- Demand database
- TAF factor data

All of the programs and data bases contained in the list are being delivered to NASA for their use.

SHELL AND BATCH AIRPORT CAPACITY AND DELAY MODELS

Analysis of many airports and technologies required automation of the modeling tools. Consequently, for this year's effort, we pursued development of a Windows-based run-time shell that automates operation of the airport capacity and delay models. Besides facilitating model operation, the run-time shell development provided other important benefits. The conversion of the models for shell operation required review of all the models and data sources, resulting in improved model structure and correction of previous errors. Also, the consolidation of the models and data for the shell has established a formal configuration control process. Finally, the shell versions of the models provide NASA with powerful user-friendly airport capacity and delay models.

The shell models are being provided to NASA on a compact disk. The disk includes the capacity and delay models, the demand data, the weather data, the TAF factor tables, and a full set of input data. The shell allows analysts to use either standard or custom inputs. The installation and use of the shell models are described in Appendix D. Figure 3-1 shows the standard analysis screen for the shell model.

Figure 3-1. Capacity Delay Standard Analysis Screen

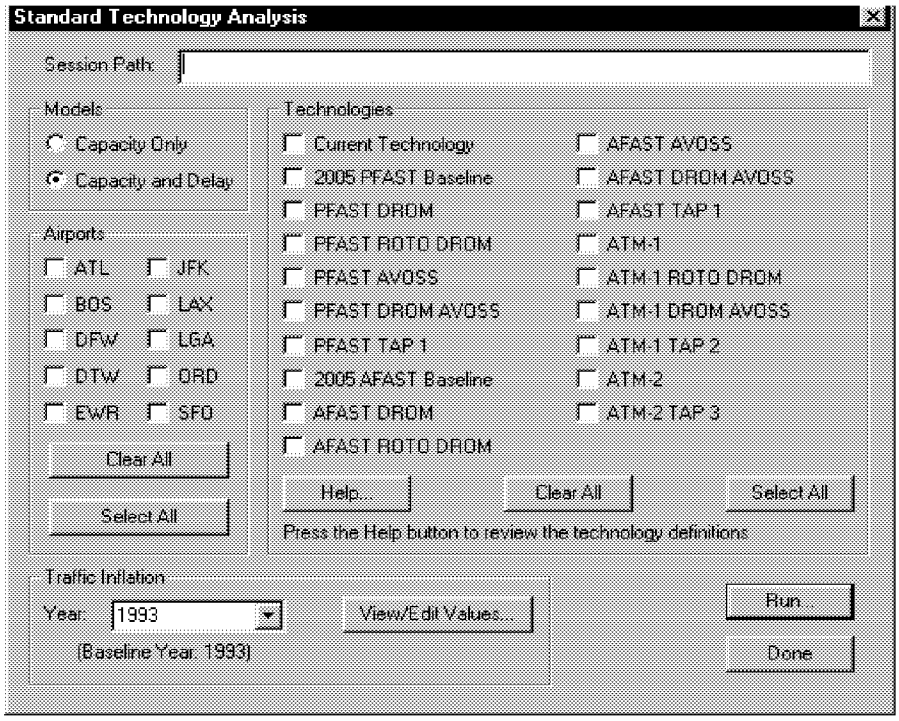

Because completion of the capacity and delay models required priority attention from the programmers, the final programming of the run-time shell was postponed until late in the task. Automation of the analyses was accomplished with DOS-based batch-mode versions of the capacity and delay models. The batch-mode versions are Pascal models using the same structure and algorithms as those used in the shell. The batch models can be rapidly modified to perform analyses and generate diagnostic outputs not included in the shell model. Automated runs of the batch-mode models are controlled by DOS batch files. The batch-mode models are not, however, particularly user-friendly. Moreover, the modification ability that makes them valuable requires installation of a Pascal compiler.

BENEFIT WORKBOOK

From the capacity and delay models we get values for the minutes of arrival delay per year as a function of demand year and TAP technology. These numbers need further economic analysis to produce useful benefit information. The benefit

workbook was designed to automate and document the economic analysis. The benefit workbook is an Microsoft Excel workbook containing several spreadsheets.

The workbook contains two primary spreadsheets for each airport. The delay data is input to the first of these. Typically, data for the 2005 and 2015 demand years for each technology are entered into the top table on first spreadsheet. The compound growth rate between the two dates is calculated and used to fill in the delays for the intervening years. Linked tables automatically calculate the savings in minutes, constant dollars, discounted present value dollars, and inflated then-year dollars. As noted in Chapter 2, the projected demand for some airports must be limited to years before 2015. The growth formulas for those airports are adjusted to allow use of a shorter span or, in some cases, just 1 year. The second spreadsheet contains the summary results for each airport that were displayed in Chapter 2.

Other spreadsheets in the workbook contain the benefit summary for all the airports displayed in Chapter 1 and the table of direct operating costs displayed in Chapter 2.

Separate workbooks are produced for each analysis (e.g., there is one workbook for the zero buffer case and one for the nominal buffer case).

WEATHER DATA

The weather data include hourly weather reports from the National Climatic Data Center (NCDC) for the 10 TAP airports for the years 1961 to 1995. The data have been processed for TAP modeling use. For some years at certain airports weather data were collected only every 3 hours. In those cases, the missing hours were filled in with the weather from adjacent hours. An error flag was added to the data whenever this was done so the data could be removed or ignored if necessary. Error flags also are appended for missing or erroneous data. Table 3-1 shows the content of the data file. The weather codes in the NCDC data have been used to identify and annotate wet and dry conditions for each hour. Each 35-year weather data file is about 14 Megabytes.

Table 3-1. Weather Data Parameters

Variable Name	Definitions	Type	Values
DOT_AC	DOT Airport Code	Alpha(3)	ATL, etc.
Date	Year(4) Month(2) Day(2)	Num(8)	19610101 - 19951231
Hour	Hour	Num(2)	1 - 24
Temp_f	Fahrenheit temp.	Num	-8 - 112, 9999=missing
Wind_dir	Wind direction in degrees	Num(3)	0,360=N; 90=E; 180=S; 270=W; 999=missing
Wind_spd	Wind speed in knots	Num	0 - 91; 9999=missing
Vis	Horizontal visibility in miles	Num	0 - 100; 777=unlimited; 99999=missing
Ceiling	Ceiling height in feet	Num	0 - 50000; 77777=unlimited; 88888=cirroform; 999999=missing
Met_cond	Meteorological conditions	Alpha	VFR1, VFR2, IFR1, IFR2, XXXX=missing
Wet	Wet or dry runway conditions	Num	1=Wet, 0=Dry or undeterminable
Mis_data	Missing data	Num	1 = Missing or replaced with previous 1 or 2 hour's data 0 = Not missing

DEMAND DATABASE

The arrival and departure demand profiles for the airports are based on *1993 Official Airlines Guide (OAG)* data. The NASA Aviation System Analysis Capability (ASAC) contains OAG data processed to show hourly demand for average days of the week and months of the year. In our analyses, we download these tables and examine plots of the data to identify daily and seasonal differences. We usually found two distinct seasonal periods (roughly winter and summer) and three distinct daily periods (Saturday, Sunday, and weekdays). Typically, the seasonal demand was factored by the daily differences to generate the base set of demand profiles for the model (e.g., Saturday-Winter and Saturday-Summer).

TERMINAL AREA FORECAST FACTOR DATA

The ASAC also contains the FAA Terminal Area Forecast (TAF) demand growth projections for the TAP airports. The TAF projections extend through 2010. We derived the compound growth factors for the TAF projections and used them to extrapolate growth through 2015. The TAF projections generally project nearly constant rates of growth so the mathematical error of extrapolation is small. Factors for each year indicating the demand relative to the 1993 demand are tabulated for each airport. Those factors are used to scale the 1993 base demand data for the demand year being analyzed.

SUMMARY

In this chapter, we briefly reviewed the principal models and databases used in the current analysis. Deeper discussions of the capacity and delay models are in the appendices. A compact disk containing the run-time shell, capacity and delay models, weather data, demand data, and baseline input files is being delivered to NASA for their use and distribution. All Pascal models are written in Borland Turbo Pascal 7.0 for DOS. The workbook is written in Microsoft Excel 7.0 for Windows 95.

Appendix A
Capacity/Delay Modeling Parameters for TAP Technologies

INTRODUCTION AND OVERVIEW

During 1998, we estimated the benefits for the set of 19 scenarios representing different implementations of TAP technologies. This appendix describes the modeling approach, documents the input parameters selected, displays basic results obtained in the selection process, and compares the results with other estimates and data.

Three sections of this appendix follow the introduction. Section 1 describes our modeling approach. Section 2 discusses our capacity modeling algorithms including a new modification to address maneuvering inefficiencies. Section 3 describes the results of a spreadsheet version of the runway capacity model used to investigate the impact of input parameters on key performance measures. Section 3 also recommends input parameters and displays the spreadsheet analysis results for the baselines and ATM technologies.

The scenarios identified for analysis in 1998 are identified and defined in Table A-1.

Table A-1. 1998 Modeling Scenarios

Title	Baseline	Content
Current Technology (CT)	N/A	
2005 PFAST Baseline	CT	PFAST
PFAST DROM	PFAST	DROM
PFAST ROTO DROM	PFAST	ROTO + DROM
PFAST AVOSS	PFAST	AVOSS
PFAST DROM AVOSS	PFAST	DROM and AVOSS
PFAST AVOSS DROM ROTO	PFAST	AVOSS + DROM + ROTO
2005 AFAST ADS-B Baseline	CT	AFAST
AFAST DROM	AFAST	DROM
AFAST ROTO DROM	AFAST	ROTO + DROM
AFAST AVOSS	AFAST	AVOSS
AFAST DROM AVOSS	AFAST	DROM + AVOSS
AFAST AVOSS DROM ROTO	AFAST	AVOSS + DROM + ROTO
ATM 1 CTAS/3DFMS Integration	AFAST	AFAST + 3DFMS + Data Link
ATM 1 DROM ROTO	AFAST	ATM 1 + ROTO + DROM

Table A-1. 1998 Modeling Scenarios (Continued)

Title	Baseline	Content
ATM 1 DROM AVOSS	AFAST	ATM 1 + DROM + AVOSS
ATM 1 DROM AVOSS ROTO	AFAST	ATM 1 + ROTO + DROM + AVOSS
ATM 2 CTAS/4DFMS Integration	AFAST	AFAST + 4DFMS + Data Link
ATM 2 Ultimate TAP	AFAST	AFAST + 4DFMS + Data Link + ROTO + DROM + AVOSS

SECTION 1. METHOD OF ANALYSIS

As described in Reference [A1], we estimate the benefits of TAP technologies by determining how much the technologies reduce arrival delays at particular airports. The estimate is made using a coupled pair of analytic models. First, our capacity model estimates airport capacity as a function of technology level and meteorological conditions for each airport operating configuration. The capacity results are then used by our delay (queuing) model to estimate annual delay as a function of hourly weather and hourly demand. Since the CTAS and TAP technologies directly impact the parameters and results of the capacity model, our discussion focuses on that model.

Our capacity model is based on the controller's decision process for maintaining safe separations during final approach. Safe separations are determined by the single occupancy requirement for runways, wake vortex hazards, and controller equipment accuracy. Current practice is to ensure separation by issuing speed and direction advisories up to a point where the aircraft turns onto the final approach. The separation existing at that point must be such that differences in speed and wind will not result in unsafe separations for the remainder of the flight. The final "uncontrolled" or "open loop" distance is called the common path, and it varies from 5 to 12 nautical miles depending on the operating conditions and the airport. The controller establishes the separation at the beginning of the common path based on the minimum allowed separation, the relative speeds of the aircraft, the accuracy of the aircraft position data, and uncertainties produced by variations in wind and aircraft velocity.

It is common to divide the applied separation into two parts: a base requirement that includes the allowed minimum separation and the speed differential, plus a buffer that covers the uncertainties. Using the methods described in Reference [A1] and discussed later, we calculate the separation the controller applies at the beginning of the common path for each aircraft pair in the mix to guarantee satisfaction of minimum separations (a.k.a., the miles-in-trail or MIT constraint). We also calculate the minimum separation required to satisfy the runway single occupancy constraint (a.k.a., the runway occupancy time or ROT constraint).

Applying the more restrictive of the two constraints at the beginning of the common path, we calculate the means and standard deviations of the interarrival times that result at the threshold after the aircraft fly the common path. The average of the interarrival times, weighted by the aircraft mix, is used to determine runway capacity.

For analysis, and in practice, the FAA minimum separations for IFR conditions are universally used as the target separations for IMC conditions and for VMC conditions under radar control. In the absence of mandated minimums, the reportedly empirical VMC separations contained in Reference [A3] (FAA EM-78-8A) are typically used for VMC operations that are not under radar control. Controllers whom we interviewed at the 10 TAP airports generally have agreed that the EM-78-8A separations are reasonable. We must point out, however, that the lack of reliable VMC separation data as a function of aircraft type and meteorological condition is *a*, if not *the*, major source of error in capacity modeling.

The buffers discussed so far include only the time (or distance) that is intentionally inserted by the controller to ensure the target separation. In addition to this intentional separation buffer, there is additional time (or distance) separation that can be described as an inefficiency buffer resulting from inefficient delivery or maneuvering of aircraft within the TRACON airspace. While the controller has some ability to reduce the inefficiency buffer by speed and vectoring commands in the TRACON airspace, once at the beginning of the common path, he is stuck with whatever "inefficiency buffer" he was not able to remove.

Non-optimum aircraft sequencing is a source of inefficiency addressed by CTAS that does not show up in the buffer. Due to wake vortex hazard criteria and aircraft speed differentials, certain aircraft sequences generate large interarrival times. Specifically, small aircraft following heavy aircraft require large separations due to wake vortex hazards. In addition, because smaller aircraft generally are slower than larger aircraft, the minimum separation must be applied at the beginning of the common path, and the separation grows larger as the aircraft fly to the threshold. Some airports mitigate this inefficiency by designating specific runways for jets and turboprops. In most cases, those assignments only apply in VMC conditions. In IMC conditions, all aircraft use the limited number of IMC runways.

Unbalanced runways are a source of inefficiency that occurs at airports with multiple runways fed by multiple arrival gates. Improvements in runway balancing have been cited as a source of the CTAS benefits observed at DFW. As with sequencing, the imbalance effects are not included in the inefficiency buffer.

CTAS and ATM technologies can potentially improve capacity by improving the arrival sequence, balancing multiple runways, reducing the inefficiency buffer, reducing the required separation buffer, and/or reducing the minimum required (target) separations. Table A-2 categorizes the potential impacts.

Table A-2. Potential Technology Impacts

Technology	Impact
PFAST	Improve arrival sequence Balance runways Reduce inefficiency buffer
AFAST + data link	Reduce separation buffer
ATM (CTAS/FMS Integration)	Further reduce separation buffer Reduce minimum separations

SECTION 2: DETAILED DESCRIPTION OF LMI RUNWAY CAPACITY MODEL ALGORITHMS

In this section, we describe the algorithms used in our model for estimating arrival capacity. The parameters that we will use are identified in Table A-3.

Table A-3. Key Airport Modeling Parameters

Symbol	Definition
D	Length of common approach path
p_i	Fraction of operating aircraft that are type i
Ra_i	Arrival runway occupancy time of *ith* aircraft
δRa_i	Variation in Ra_i
S	Miles-in-trail separation minimum
V_i	Approach speed of aircraft i
δV_i	Variation in approach speed of aircraft i
δW_i	Wind variation experienced by aircraft i
δX_i	Position uncertainty of aircraft i
μ	Time increment imposed by controller

We will assume that each of the δRa_i, δVi, δWi, and δXi are independent normal random variables with mean zero and standard deviation σ_{RAi}, σ_{Vi}, σ_{Wi}, or σ_{Xi} as appropriate.

In the following, we take a "controller-based view" of operations. That is, we assume that a person controls the aircraft, introducing time (or, equivalently, space) increments in operations streams to meet all applicable rules (e.g., miles-in-trail requirements) with specified levels of confidence. For example, consider the arrival-arrival sequence of Figure A-1.

Figure A-1. Time Phase for Arrivals When Follower Velocity > Leader Velocity

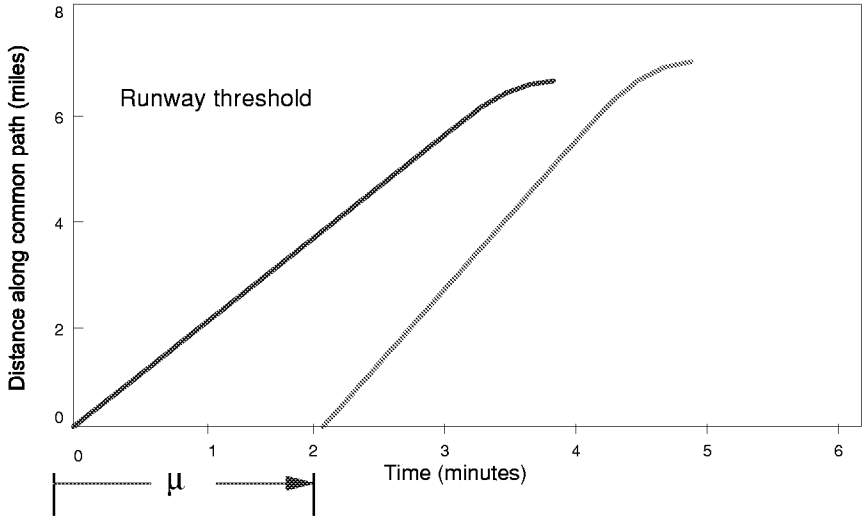

Figure A-1 shows the space-time trajectories of two arrivals. Zero distance is the beginning of the common approach path. In this model, the controller maneuvers the following aircraft so that it enters the common approach path a time μ after the lead aircraft enters it. (The controller actually may achieve this by bringing the following aircraft onto the common path when the lead aircraft has advanced a specified distance along the path.) The controller chooses the time interval μ in light of his/her knowledge of typical approach speeds for the two aircraft, as well as knowledge of disturbances—winds, position uncertainties, variations in pilot technique— affecting their relative positions in order to ensure that miles-in-trail requirements and runway occupancy rules are met with assigned levels of confidence. As we will see soon, this action of the controller, together with information on statistics about aircraft operating parameters and the disturbances to arrival operations, such as winds and position uncertainties, leads directly to statistics of operations and of runway capacity.

Arrivals Only

While Reference [A1] discusses the combinations of arrivals and departures, in this paper, we are concerned with arrival-arrival cases only. Two cases are important. The first, illustrated by Figure A-1, occurs when the mean approach speed of the following aircraft exceeds that of the leader.

Follower Velocity ≥ Leader Velocity

MILES-IN-TRAIL CONSTRAINT

For this case, the miles-in-trail constraint (distance) applies as the leader crosses the runway threshold. At that time, the leader's position is *D* (position *0* being the beginning of the common path). We will derive a condition on the controller's interval, μ, to guarantee that the miles-in-trail requirement is met (i.e., that at the time the leader crosses the threshold, the follower is at least distance *S* away from the threshold, with a probability of 95 percent).

The position of the lead aircraft is given by

$$X_L = \delta X_L + (V_L + \delta V_L + \delta W_L)t\,, \qquad \text{[Eq. A-1]}$$

and the position of the following aircraft by

$$X_F = \delta X_F + (V_F + \delta F_F + \delta W_F)(t - \mu)\,. \qquad \text{[Eq. A-2]}$$

The leader crosses the runway threshold at time t_{LO}, given by

$$t_{LO} = \frac{D - \delta X_L}{V_L + \delta V_L + \delta W_L}\,. \qquad \text{[Eq. A-3]}$$

At time t_{LO}, the follower is at $X_F\,(t_{LO})$, given by

$$X_F(t_{LO}) = \delta X_F + (V_F + \delta V_F + \delta W_F)\left(\frac{D - \delta X_L}{V_L + \delta V_L + \delta W_L} - \mu\right). \qquad \text{[Eq. A-4]}$$

We wish to derive a condition on μ, which makes $D - X_F\,(t_{LO}) \geq S$ with probability at least 95 percent. To keep the problem tractable, we will assume that all disturbances are of first order and linearize Equation A-4. When linearized, the equation becomes

$$X_F(t_{LO}) = \delta X_F + \frac{DV_F}{V_L}\left(1 + \frac{\delta V_F + \delta W_F}{V_F} - \frac{\delta X_L}{D} - \frac{\delta V_L + \delta W_L}{V_L}\right) - \mu V_F\left(1 + \frac{\delta V_F + \delta W_F}{V_F}\right). \qquad \text{[Eq. A-5]}$$

In this linear approximation, $X_F\,(t_{LO})$ is a normal random variable of mean

$$\frac{DV_F}{V_L} - \mu V_F\,, \qquad \text{[Eq. A-6]}$$

and variance

$$\sigma_1^2 = \frac{D^2 V_F^2}{V_L^2}\left(\frac{\sigma_{VF}^2 + \sigma_{WF}^2}{V_F^2} + \frac{\sigma_{XL}^2}{D^2} + \frac{\sigma_{VL}^2 + \sigma_{WL}^2}{V_L^2}\right) + \mu^2 V_F^2 \frac{\sigma_{VF}^2 + \sigma_{WF}^2}{V_F^2} + \sigma_{XF}^2 \text{ .[Eq. A-7]}$$

The condition that $D - X_F(t_{LO}) \geq S$, with probability at least 95 percent, may then be stated as

$$\frac{DV_F}{V_L} - \mu V_F + 1.65\,\sigma_1 \leq D - S \qquad \text{[Eq. A-8]}$$

or

$$\mu \geq \frac{D}{V_L} - \frac{D-S}{V_F} + \frac{1.65\sigma_1}{V_F}. \qquad \text{[Eq. A-9]}$$

Equation A-9 gives, in essence, the desired condition. Since σ_1 is a function of μ, we find μ appearing on both sides of the inequality. Straightforward manipulations lead to an explicit condition on μ, which may be written

$$\mu \geq \frac{A + \sqrt{A^2 B^2 + C^2(1 - B^2)}}{1 - B^2}, \qquad \text{[Eq. A-10]}$$

where

$$A \equiv \frac{D}{V_L} - \frac{D-S}{V_F} \qquad \text{[Eq. A-11]}$$

$$B^2 \equiv 1.65^2 \left\{\frac{\sigma_{VF}^2 + \sigma_{WF}^2}{V_F^2}\right\}, \qquad \text{[Eq. A-12]}$$

and

$$C^2 \equiv \frac{1.65^2}{V_F^2}\left\{\frac{D^2 V_F^2}{V_L^2}\left(\frac{\sigma_{VF}^2 + \sigma_{WF}^2}{V_F^2} + \frac{\sigma_{XL}^2}{D^2} + \frac{\sigma_{VL}^2 + \sigma_{WL}^2}{V_L^2}\right) + \sigma_{XF}^2\right\}. \qquad \text{[Eq. A-13]}$$

The closed form solution above is used in the spreadsheet analysis described later in the paper. For the capacity model, it is more computationally convenient to solve for the smallest satisfactory μ by iteration using the following equation:

$$\mu_{n+1} = \frac{D}{V_L} - \frac{D-S}{V_F} + \frac{1.65\sigma_1(\mu_n)}{V_F}, \qquad \text{[Eq. A-14]}$$

where $\sigma_1(\mu)$ is defined by Equation A-7.

RSO CONSTRAINT

Having determined the minimum μ that satisfies the miles-in-trail constraint, we must now develop a condition on μ that will guarantee that the follower aircraft does not cross the runway threshold until the leader has left the runway, with probability 98.7 percent. The leader will exit the runway at time $t_{LO} + RA_L$, and the follower will cross the threshold at time t_{FO}, given by

$$t_{FO} = \frac{D - \delta X_F}{V_F + \delta V_F + \delta W_F} + \mu \, . \qquad \text{[Eq. A-15]}$$

Linearizing as above, we find that in the linear approximation, t_{FO} - t_{LX} is a normal random variable with mean $\frac{D}{V_F} + \mu - \frac{D}{V_L} - \overline{RA}_L$, where $\overline{RA}_L$ denotes the mean of RA_L and variance

$$\sigma_2^2 = \frac{D^2}{V_F^2}\left(\frac{\sigma_{XF}^2}{D^2} + \frac{\sigma_{VF}^2 + \sigma_{WF}^2}{V_F^2}\right) + \frac{D^2}{V_L^2}\left(\frac{\sigma_{XL}^2}{D^2} + \frac{\sigma_{VL}^2 + \sigma_{WL}^2}{V_L^2}\right) + \sigma_{RAL}^2 \, . \qquad \text{[Eq. A-16]}$$

It follows that the condition on μ for the follower to not cross the threshold until the leader has exited the runway, that is, t_{FO} - $t_{LX} > 0$ with probability 98.7 percent, is

$$\mu \geq \frac{D}{V_L} - \frac{D}{V_F} + \overline{RA}_L + 2.215\sigma_2 \, . \qquad \text{[Eq. A-17]}$$

The controller will impose, at the beginning of the common path, that value of time interval μ that is the smallest μ satisfying both Eq. A-14 and Eq. A-17.

Given μ at the beginning of the common path, the interarrival time (IAT) between threshold crossings of successive arrivals of individual pairs is, in our approximation, a normal random variable of mean

$$< IAT_{FL} > = \frac{D}{V_F} - \frac{D}{V_L} + \mu \qquad \text{[Eq. A-18]}$$

and variance

$$SDiat_{FL}{}^2 = \sigma_3^2 = \frac{D^2}{V_F^2}\left(\frac{\sigma_{XF}^2}{D^2} + \frac{\sigma_{VF}^2 + \sigma_{WF}^2}{V_F^2}\right) + \frac{D^2}{V_L^2}\left(\frac{\sigma_{XL}^2}{D^2} + \frac{\sigma_{VL}^2 + \sigma_{WL}^2}{V_L^2}\right). \qquad \text{[Eq. A-19]}$$

Follower Velocity < Leader Velocity

MILES-IN-TRAIL CONSTRAINT

When the follower's approach speed is slower than the leader's, the controller will bring the follower onto the common path after the leader has advanced a distance *S* along it, as illustrated in Figure A-2.

Figure A-2. Time Phase of Arrivals When Follower Velocity < Leader Velocity

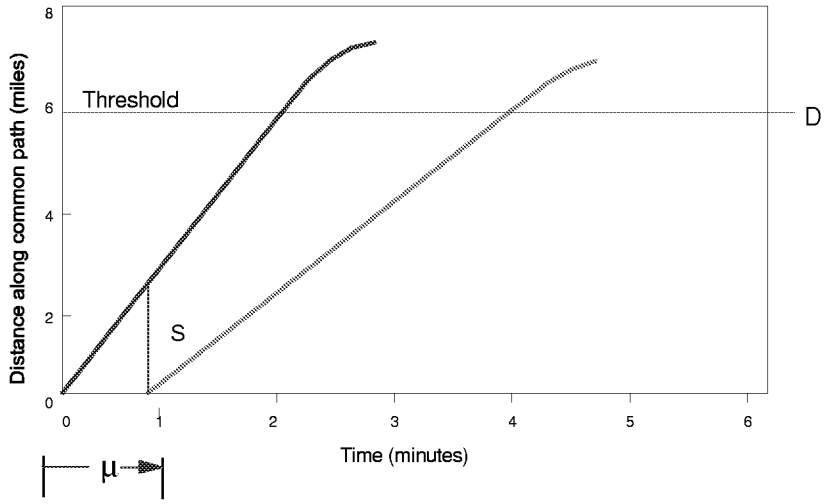

In this case, the positions of the two aircraft as functions of time are again given by Equation A-1 and Equation A-2. The miles-in-trail requirement is now, $X_L(\mu) - X_F(\mu) \geq S$, with probability at least 95 percent. Because

$$X_L(\mu) - X_F(\mu) = \delta X_L + (V_L + \delta V_L + \delta W_L)\mu - \delta X_F \qquad \text{[Eq. A-20]}$$

is a normal random variable of mean $V_L\mu$ and variance

$$\sigma_4^2 = \mu^2(\sigma_{VL}^2 + \sigma_{WL}^2) + \sigma_{XF}^2 + \sigma_{XL}^2, \qquad \text{[Eq. A-21]}$$

it follows that the condition that the miles-in-trail requirement is met, with 95 percent confidence, is

$$\mu \geq \frac{S}{V_L} + 1.65\frac{\sigma_4}{V_L}. \qquad \text{[Eq. A-22]}$$

Equation A-22 may be written as a single condition on μ using Equation A-10 by replacing Equations A-11, A-12, and A-13 with the new definitions

$$A \equiv \frac{S}{V_L}, \qquad \text{[Eq. A-23]}$$

$$B^2 \equiv 1.65^2 \frac{\sigma_{VL}^2 + \sigma_{WL}^2}{V_L^2}, \text{ and} \qquad \text{[Eq. A-24]}$$

$$C^2 \equiv 1.65^2 \frac{\sigma_{XL}^2 + \sigma_{XF}^2}{V_L^2}. \qquad \text{[Eq. A-25]}$$

Again, the capacity model uses iteration rather than the direct method to solve for the MIT-constrained μ.

RSO CONSTRAINT

The condition that the single-occupant rule (ROT constraint) is met with 98.7 percent confidence is derived exactly as is that condition for $V_F \geq V_L$ In the present case, too, the result is given by Equation A-17. The controller imposes, at the beginning of the common path, the smallest μ that satisfies both the miles-in-trail and single occupant constraints.

As before, the equations for the mean and standard deviation of IAT, given μ, are given by Equations A-18 and A-19. Substituting the miles-in-trail equations for μ into the equation for IAT, we get the two equations for IAT shown below.

$$<IAT_{F>L}> = \frac{S_{ij}}{V_F} + \frac{1.65(\sigma_1 or \sigma_2)}{V_F} \text{ and} \qquad \text{[Eq. A-26]}$$

$$<IAT_{F<L}> = \left(\frac{D}{V_F} - \frac{D}{V_L}\right) + \frac{S_{ij}}{V_L} + \frac{1.65(\sigma_4 or \sigma_2)}{V_L}, \qquad \text{[Eq. A-27]}$$

where the subscripts *i* and *j* refer to the minimum separation requirement for the specific follower-leader pair.

These can be compared with the commonly referenced "standard" FAA IAT equations developed in Reference [A11] and used in Reference [A5] and elsewhere:

$$<FAAIAT_{F>L}> = \frac{S_{ij}}{V_F} + 1.65\sigma_{IAT} \text{ and} \qquad \text{[Eq. A-28]}$$

$$<FAAIAT_{F<L}> = \left(\frac{D}{V_F} - \frac{D}{V_L}\right) + \frac{S_{ij}}{V_F} + 1.65\sigma_{IAT}. \qquad \text{[Eq. A-29]}$$

Two differences exist between our algorithm and the FAA model. The first is that we use individual σ_{ij}'s for each pair rather than a single σ_{IAT}. The second difference occurs in the case where the follower is slower than the leader. In our algorithm, the spacing for this case is controlled by the leader speed, not the follower speed. Based on the logic described above, we believe our algorithm is more accurate. The impact of the difference is not large for typical airspeeds.

Statistics of Multiple Operations

At this point, we have expressions for the means and variances of normal random variables representing interarrival times for two cases: (1) when the runway is used for arrivals only and (2) when it is used for alternating arrivals and departures. Now, we wish to use these to generate statistics of multiple arrivals, or multiple arrivals and departures, to capacity curves for single runways.

First, we consider the statistics of sequences of arrivals only. Statistics of the overall interarrival time will be determined by the mix of aircraft using the runway, with their individual values of the aircraft parameters of Table A-1. Suppose n aircraft types use the runway and the fraction of the aircraft of type i in the mix is p_i. Then, the results of the preceding sections give interarrival time for each leader-follower pair as a normal random variable. Let t_{AAij} denote the random variable that is the interarrival time for aircraft of type i following an aircraft of type j. As shown in our model, t_{AAij} is a normal random variable; let its mean and standard deviation be μ_{ij} and σ_{ij}, respectively. (The subscripted variable μ_{ij} should not be confused with symbol μ that denotes the time separation imposed by the controller.)

Now, to determine the distribution of the overall interarrival time, t_{AA}, we consider a classical "urn" problem: we have a population of interarrival times, from which we draw one member, and we wish to know the distribution function of the result. The probability of drawing t_{AAij} is $p_i p_i$, and the distribution function of the result is the weighted sum of the distribution functions for the individual t_{AAij}. That is, the distribution function for the overall interarrival time $t_{AA}(1)$ is

$$t_{AA}(1) \sim \sum_i \sum_j p_i p_j N(t; \mu_{ij}, \sigma_{ij}), \qquad \text{[Eq. A-30]}$$

where $N(t; \mu, \sigma)$ denotes the normal probability distribution function. Obviously, the distribution of interarrival times is not necessarily normal. An example of an interarrival time distribution of the type defined in Equation A-30 is shown in Figure A-3.

Figure A-3. Example Probability Distribution of Interarrival Time

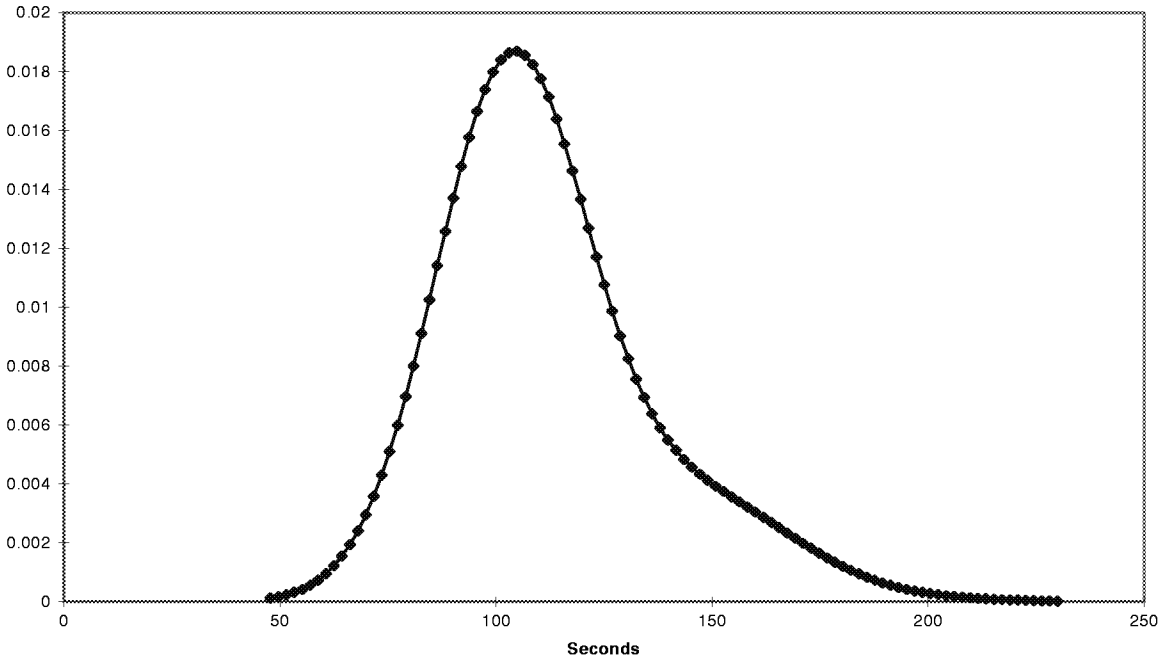

As suggested in Figure A-3, the interarrival time distribution is not necessarily monomodal.

One can compute the mean and variance of the interarrival time distribution given in Equation A-30 straightforwardly: the results are

$$< t_{AA}(1) > = \sum_i \sum_j p_i p_j \mu_{ij} \qquad \text{[Eq. A-31]}$$

and

$$\text{var}(t_{AA}(1)) = \sum_i \sum_j p_i p_j (\sigma_{ij}^2 + \mu_{ij}^2) - < t_{AA}(1) >^2 . \qquad \text{[Eq. A-32]}$$

To find the number of arrivals that the runway can accommodate in a given period of time with a specified confidence, we need the distribution of the time required for a sequence of M arrivals. We determine that distribution as follows: Consider first the case of two arrivals. With probability $p_i p_j p_k$, the observed total time for a sequence of two arrivals will be $t_{AAij} + t_{AAjk}$. For given i, j, and k, that total time is distributed normally, with

$$t_{AAij} + t_{AAjk} \sim N\left(\mu_{ij} + \mu_{jk}, \sqrt{\sigma_{ij}^2 + \sigma_{jk}^2}\right). \qquad \text{[Eq. A-33]}$$

Thus, the time $t_{AA}(2)$ for a sequence of two arrivals will have the distribution

$$t_{AA}(2) \sim \sum\sum\sum p_i p_j p_k N\left(\mu_{ij} + \mu_{jk}, \sqrt{\sigma_{ij}^2 + \sigma_{jk}^2}\right), \qquad \text{[Eq. A-34]}$$

where the sums range over the number of aircraft in the mix.

Continuing in this way to reckon the distributions of the time required for 3, 4, …, *M* arrivals, we conclude that $t_{AA}(M)$ has the distribution

$$\sum\sum\ldots\sum p_i p_j \ldots p_y p_z N\left(\mu_{ij} + \mu_{jk} + \ldots + \mu_{yz}, \sqrt{\sigma_{ij}^2 + \sigma_{jk}^2 + \ldots + \sigma_{yz}^2}\right). \quad \text{[Eq. A-35]}$$

In Equation A-35, the sums range over the set of aircraft using the runway. There are $M + 1$ summations, and $M + 1$ terms in $p_i p_j \ldots p_y p_z$. There are *M* terms in both the sums $\mu_{ij} + \mu_{jk} + \ldots + \mu_{yz}$ and $\sigma_{ij}^2 + \sigma_{jk}^2 + \ldots + \sigma_{yz}^2$.

Evaluating the expected value $<t_{AA}(M)>$ is straightforward. We find

$$< t_{AA}(M) > = \sum\sum\ldots\sum p_i p_j \ldots p_y p_z \left(\mu_{ij} + \mu_{jk} + \ldots + \mu_{yz}\right), \qquad \text{[Eq. A-36]}$$

which leads directly to

$$< t_{AA}(M) > = M \sum\sum p_i p_j \mu_{ij}\ , \qquad \text{[Eq. A-37]}$$

since the p_i sum to 1.0.

Evaluating the variance of $t_{AA}(M)$ is more involved. After considerable manipulation, we find

$$\text{var}\left(t_{AA}(M)\right) = M \sum\sum p_i p_j \left(\sigma_{ij}^2 + \mu_{ij}^2\right) + 2(M-1) \sum\sum\sum p_i p_j p_k \mu_{ij} \mu_{jk}\ , \quad \text{[Eq. A-38]}$$

$$- (3M - 2)\left(\sum\sum p_i p_j \mu_{ij}\right)^2 . \qquad \text{[Eq. A-39]}$$

In Equation A-38, the sums again range over the set of aircraft types that use the runway.

Evaluating the number of arrivals that a runway can accommodate in 1 hour, with assigned confidence, is conceptually straightforward: one finds the largest *M* for which the cumulative distribution corresponding to the probability distribution of Equation A-35, evaluated at 3,600 seconds, is not less than the desired confidence. It is tempting to approximate the distribution defined by Equation 35 with a normal distribution for this purpose, since direct evaluation of the CDF corresponding to Equation 35 involves lengthy sums when *M* takes values near typical hourly arrival numbers, usually around 30.

If the individual interarrival times in a sequence of arrivals were statistically independent, an appeal to the central limit theorem would justify that approximation. Of course, they are not independent, because the follower in a given pair is the leader for the next pair of the sequence.

Nevertheless, numerical experiments suggest that members of the family of distributions (Equation A-35) are well-approximated by normal distributions, even for fairly small M, even when the distribution of a single interarrival time departs considerably from a normal distribution. Figures A-4 and A-5 illustrate this, with the distribution functions for the time of two and of four arrivals, respectively. The single-arrival distribution is the same as that of Figure A-3.

Figure A-4. Distribution Function Of The Time For Two Arrivals

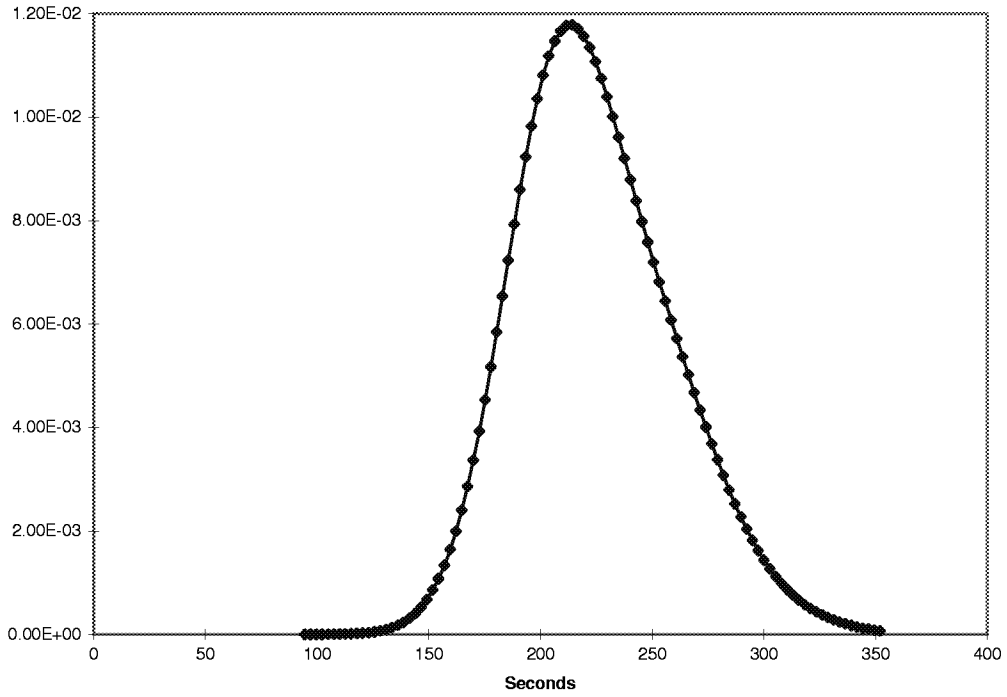

Figure A-5. Distribution of the Time for Four Arrivals

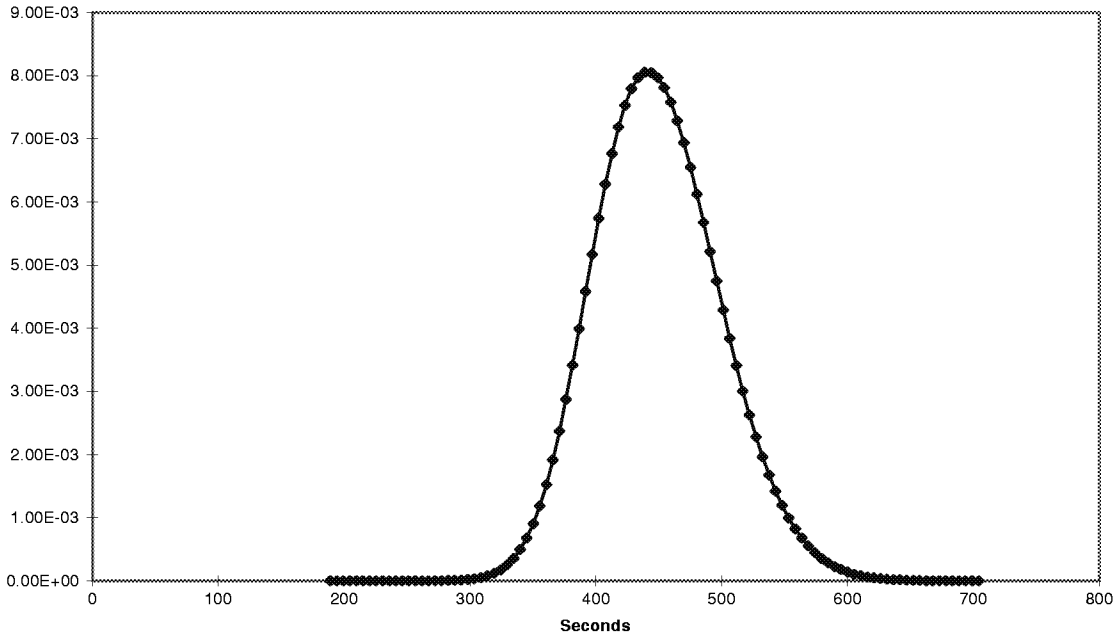

In view of results like those of Figures A-4 and A-5, we approximate the distribution of the time required for M arrivals as a normal distribution whose parameters are the mean and variance given by Equations A-37 and A-38, respectively. Then, the largest number of arrivals that the runway can accommodate in one hour, with 95 percent confidence, is the largest value of M for which

$$<t_{AA}(M)>+1.65\sqrt{\text{var}(t_{AA}(M)} \leq 3600 \qquad \text{[Eq. A-40]}$$

where $t_{AA}(M)$ and $var(t_{AA}(M))$ are evaluated by Equations A-37 and A-38, respectively. For the case illustrated by Figures A-4 and A-5, this leads to a capacity of 30 arrivals per hour.

An alternative definition of runway capacity is the largest number of arrivals for which the expected[1] total time is not larger than 3,600 seconds. With this definition, the capacity of the runway for the case illustrated in the figures is 32 arrivals per hour. In this report, we will use this definition for capacity. Because our capacity is actually a rate, we are willing to consider non-integer capacity values. Accordingly, we take as our working definition of capacity

$$C \equiv \frac{60}{<t_{AA}(1)>} \text{ arrivals/hour,} \qquad \text{[Eq. A-41]}$$

where $<t_{AA}(1)>$, defined by Equation A-31, is in minutes.

[1] "Expected' here indicates the mean. Because the distribution for a large number of arrivals is very nearly normal, the mean very nearly represents the 50 percent confidence point.

Input-Stream Effects

So far, we have developed our model as though the controller could always impose the desired time separation μ, whatever the nature of the stream of arriving aircraft reaching him or her. Because of maneuvering or feeder errors, this may not in fact always be the case. We extend our model to address input-stream effects in this way: We suppose that the controller, wishing to impose separation μ, actually can impose the separation $\mu + \nu$, where ν is a random variable, independent of all others in the analysis, characterizing input-stream effects. We take ν to have the exponential distribution with parameter λ, that is,

$$\nu \sim \begin{cases} \lambda e^{-\lambda \nu}, \nu \geq 0 \\ 0, \text{else} \end{cases} \qquad \text{[Eq. A-42]}$$

We chose the exponential distribution because it assigns zero probability to negative values, and because its shape resembles patterns of observed data. The mean and standard deviation of ν are both equal to $1/\lambda$.

With the addition of the random variable ν, the interarrival time for specified leader and follower is the sum of a normal random variable and an exponential random variable. The normal random variable has, in every case, precisely the same mean and variance as in the cases where input stream effects are not considered. It follows straightforwardly that in the present, augmented cases, the mean, variance, and standard deviation of interarrival times for leader *j* and follower *i* are

$$mean = \mu_{ij} + \frac{1}{\lambda} \qquad \text{[Eq. A-43]}$$

$$variance = \sigma_{ij}^2 + \frac{1}{\lambda^2} \qquad \text{[Eq. A-44]}$$

$$standard\ deviation = \sqrt{\sigma_{ij}^2 + \frac{1}{\lambda^2}}. \qquad \text{[Eq. A-45]}$$

The distribution function of interarrival time for fixed leader and follower is no longer normal, but, rather, it is the convolution of a normal random variable and an exponential random variable. Specifically, the distribution is

$$H(t;\mu,\sigma,\lambda) \equiv \frac{\lambda}{\sqrt{2\pi}\sigma} \int_0^\infty e^{-\frac{(t-\tau-\mu)^2}{2\sigma^2} - \lambda\tau} d\tau. \qquad \text{[Eq. A-46]}$$

This distribution function may be evaluated conveniently using the expression

$$H(t;\mu,\sigma,\lambda) = \lambda e^{-\lambda(t-\mu)+\frac{\lambda^2\sigma^2}{2}}\left[1 - C(\mu, t-\lambda\sigma^2, \sigma)\right] \qquad \text{[Eq. A-47]}$$

where $C(x,\mu,\sigma)$ denotes the cumulative normal distribution for mean μ and standard deviation σ, evaluated at x.

Figure A-6 illustrates this class of distribution, together with the normal distribution that would have been seen absent input-stream effects. The example of Figure A-6 is somewhat extreme – for the sake of illustration. Typically, input-stream effects would introduce a mean error of 10 seconds or less.

Figure A-6. Example InterarrivalDistribution with Input-Stream Effects

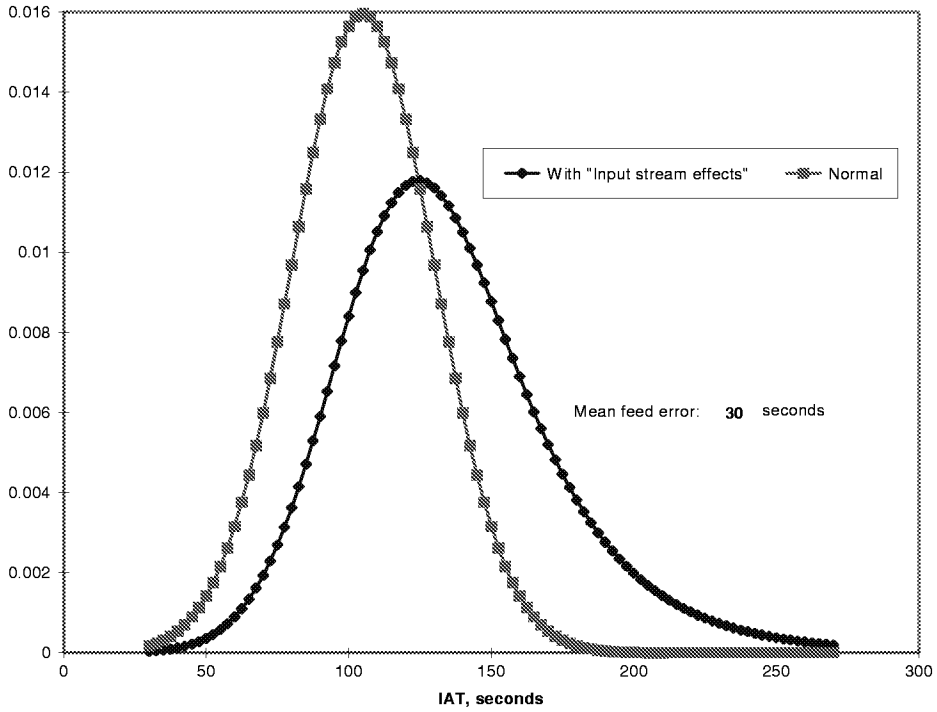

With the addition of our model of input-stream effects, the distribution of interarrival times changes from that of Equation A-30 to

$$t_{AA}(1) \sim \sum_i \sum_j p_i p_j H(t;\mu_{ij},\sigma_{ij},\lambda)\,, \qquad \text{[Eq. A-48]}$$

and the distribution function of $t_{AA}(M)$ changes from that of Equation A-35 to

$$\sum\sum\ldots\sum p_i p_j \ldots p_y p_z \hat{H}\left(t;\mu_{ij}+\mu_{jk}+\ldots+\mu_{yz}, \sqrt{\sigma_{ij}^2+\sigma_{jk}^2+\ldots+\sigma_{yz}^2}, \lambda, M\right) \text{[Eq. A-49]}$$

where

$$\hat{H}(t;\mu,\sigma,\lambda,K) \equiv \frac{\lambda^K}{\sqrt{2\pi}\sigma(K-1)!}\int_0^\infty \tau^{K-1} e^{-\frac{(t-\tau-\mu)^2}{2\sigma^2}-\lambda\tau}\, d\tau \qquad \text{[Eq. A-50]}$$

It is not difficult to show that the mean and variance of $t_{AA}(M)$ may be obtained from the values in Equations A-37 and A-38, simply by adding M/λ to $<t_{AA}(M)>$, and $M/(\lambda^2)$ to $var(t_{AA}(M))$. With these results, and the assumption that the distribution of $t_{AA}(M)$ may be adequately approximated by a normal distribution for sufficiently large M, we may compute runway capacities with our augmented model of input-stream effects.

For example, taking the value $1/\lambda = 6.3$ seconds, which certain data for operations at DFW suggest, reduces the 95 percent confidence capacity to 28 arrivals/hour, and the "expected-total-arrival-time" capacity to 30.

We close this section by noting again that we do not have a parameter that addresses runway imbalance. Our model inherently assumes balanced runways. This shortcoming may reduce estimates of PFAST benefits relative to the Current Reference for those airports with complex approach paths and many runways. At DFW, runway imbalances tend to occur when high demand from one direction does not get distributed to all runways.

SECTION 3: SPREADSHEET CAPACITY MODEL, MODELING PARAMETERS, AND ANALYSIS

In order to examine the relationship among input parameters, buffers, and capacity, we developed a spreadsheet model for a single arrival runway. The spreadsheet layout allows the display and comparison of both final results and intermediate values. The model contains multiple replications of a basic 4×4 matrix consisting of small, large, B-757, and heavy aircraft. Separate matrices are included for each of the equations in the closed form solution (e.g., A's, $B^{2'}$s, C'^2s, and μ's) for both faster leader and faster follower cases. Matrices also are included for outputs of interest, such as the various σ's and the interarrival time. Both the best possible capacity (based on the target separation matrix, aircraft speeds, and common path length) and the expected capacity (including distance, speed, and wind uncertainties plus the inefficiency buffer) are calculated. Excess spacing buffers for the weighted average and individual pairs are estimated based on the difference in those capacities.

The FAA capacity model algorithm also is included in the spreadsheet so that the capacity and interarrival time estimated by that model can be compared with ours.

Table A-16, located at the end of the report, displays the input and results summary for the spreadsheet model. The inputs correspond to our current technology case for DFW airport.

Table A-14 shows a sample matrix. The sample corresponds to the input/output data in Table A-16. The matrix shown is for the nonweighted values of the standard deviations of the interarrival time, $\sqrt{\sigma_3^2}$. The table values correspond to the interarrival uncertainties that would exist if each pair in the matrix was the only combination flying. The square root of the sum of the corresponding weighted variances provides the standard deviation interarrival of the uncertainty at the threshold for the specific aircraft mix, 19.0 seconds for this case.

Table A-4. Non-Weighted Standard Deviations of Interarrival Time, $Sd_{iat}s$ (in Seconds)

						Leader				
						D	7	7	7	7
						V	135	140	140	145
Non-weighted SD of individual pairs						SD V	5	5	5	5
in seconds						SD X	0.25	0.25	0.25	0.25
						SD W	7.5	7.5	7.5	7.5
Follower						A/C	0.14	0.71	0.075	0.075
D	V	SD V	SD X	SD W	A/C		Small	Large	757	Heavy
7	135	5	0.25	7.5	0.14	Small	21.1	12.0	13.3	13.8
7	140	5	0.25	7.5	0.71	Large	20.8	19.8	20.7	12.6
7	140	5	0.25	7.5	0.075	757	20.8	19.8	20.7	12.6
7	145	5	0.25	7.5	0.075	Heavy	20.5	19.9	20.4	19.4

With the spreadsheet model, we can test proposed inputs for modeling TAP technologies and compare the results with data and other analyses, but, before examining numerical results, it is useful to review the model parameters. For clarity of discussion, we begin with the output parameters.

Output Parameters

Expected Arrival Capacity The expected hourly capacity is the bottom line product of the model. It represents the expected arrival capacity for a single runway operating in the all-arrival mode. It is defined as 60 divided by the Mean Interarrival Time.

Perfect Arrival Capacity The perfect capacity is the hourly capacity that would be possible if all uncertainties and the inefficiency buffer were zero. It is defined as 60 divided by the Perfect Interarrival Time.

Mean Interarrival Time (IAT) This is the weighted sum of the interarrival times for the individual leader-follower pairs plus the mean of the inefficiency buffer. The Mean IAT is influenced by the common path length, aircraft speeds, aircraft mix, and the uncertainties in position, speed, and wind.

Perfect Interarrival Time The Perfect IAT is the weighted sum of the interarrival pairs that occurs when the inefficiency buffer, and the uncertainties are zero.

Excess Spacing Buffer The excess spacing buffer contained in the spreadsheet is the difference between the Mean IAT and the Perfect IAT. Both the weighted average value and a matrix of the non-weighted individual pair buffers are displayed. The distance equivalent of the averaged buffer is generated using the average speed of the aircraft ensemble.

Standard Deviations of the Interarrival Time The spreadsheet model calculates three different standard deviations developed from our algorithms. The first, SD_{IAT}, is the combination of standard deviation corresponding to a normal approximation of the distribution of interarrival times. It is calculated from the weighted variances of the individual threshold interarrival times, i.e., the σ_3 s and $1/\lambda$s defined in the previous section. The second, SDt_{AA}, is the standard deviation derived from the variance, $var(t_{AA})$, of the actual, non-normal H-distribution. The third standard deviation, SD_{IND}, is generated from the variances in the controller's uncertainties (σ_1, σ_2, and σ_4) that appear in the calculation of the controller's separation buffer times (μs). SD_{IND} represents the composite interarrival uncertainty at the beginning of the common path, and, while not directly used, does reflect the composite of the individual σs that *are* used in our model to calculate capacity.

As mentioned previously, SD_{IAT} is the most appropriate for use in the FAA capacity algorithm. When the inefficiency buffer ($1/\lambda$) is zero and all speeds and separation minimums are equal, SD_{IAT} equals SDt_{AA}. When separation differences, speed differences, and/or an inefficiency buffer exist, the interarrival time distribution is skewed to the right with SDt_{AA} greater than SD_{IAT}.

FAA Algorithm Capacity and IAT For comparison with our approach, we calculate the capacity and the *IAT* using the FAA capacity algorithm and the SD_{IAT} defined above.

Average Speed The average speed is the weighted average of individual aircraft speeds. It is used for the conversion of times to distance.

MIT/ROT Information For each leader-follower pair, we check whether the miles-in-trail (MIT), or runway occupancy time (ROT) spacing was controlling and display the results in a matrix. The percent of ROT-constrained flights is also reported.

Input Parameters

This subsection identifies the input parameters and discusses how their nominal values were chosen.

Common Path Length We normally use a 6-nautical-mile common path length based on the recommended value in Reference [A3]. We have lengthened the common path to 7 nautical miles for DFW. While Ballin & Ertzberger in Reference [A6] estimated common path lengths of 6 nautical miles for VFR and 9 nautical miles for IFR at DFW based on radar tracks, our selection of 7 nautical miles is based on identification by DFW controllers of the last point where they typically issue speed or direction advisories.

Position Uncertainty The position uncertainty of 0.25 nautical miles is based on discussions with controllers. An aircraft traveling at 170 knots will travel approximately a quarter nautical mile between hits by a radar turning at 1/5 Hertz.

Aircraft Mix The aircraft mix is based on OAG data for DFW. Based on controller input, we assume that the small aircraft are business jets or commercial turboprops rather than small piston-engine private aircraft.

Average Approach Speeds and Uncertainties In previous analyses, we used average approach speeds of 145, 145, 145, and 155 knots for small, large, B-757 and heavy aircraft, respectively. Those speeds are substantially higher than final touchdown speeds, and reflect the average speed over the common path. Based on the data and analysis discussed below, we have reduced the average speeds somewhat for the current baseline. We also reviewed our values of 5 knots and 7.5 knots for the standard deviations of aircraft and wind speeds based on the data below. Those values have not changed.

Reference [A6] (Ballin and Ertzberger) documents a thorough and innovative collection and analysis of data from the Dallas/Fort Worth airport (DFW). The authors extracted meaningful information from data containing mixes of aircraft classes, variations in trajectories, and other real world artifacts. Speed estimates in the report are derived from aircraft pair time and distance data. Those data include the location of the following aircraft when the leader crossed the threshold and the time subsequently taken by the follower to cross the threshold. An average speed for the follower can be derived from the quotient of distance over time. The data are widely scattered with large class aircraft speeds ranging from 99 to 180 knots in VMC and 92 to 185 knots in IMC. Table A-3 in Reference [A6] contains linear fits of the speed data for several aircraft classes in IMC and VMC conditions. Table A-6 of Reference [A6] shows the standard deviations of the times of flight from the final approach fix (FAF) to the threshold for the same aircraft classes. Using data and the spreadsheet model, we can derive the standard deviation of speed by setting the common path length

equal to the FAF-to-Threshold distance, σ_W and σ_X to zero, and iterating to find σ_V. The results are contained in Table A-5.

Table A-5. Deviation in Time of Flight and Speed From Final Approach Fix to the Threshold (DFW 35R)

Aircraft class	Average speed (knots)*	Standard deviation of flight time from FAF** (sec.)***	Standard deviation of speed (knots)****
IMC cases:			
Heavy	136	9	6.4
Large Jet	133	20	13.6
Large Turboprop	121	18	10.1
Small Turboprop	116	13	6.7
B 757	128	12	12.0
Combined IMC data	129	19	12.1
VMC cases:			
Heavy	134	22	15.2
Large Jet	127	20	12.4
Large Turboprop	123	21	12.2
Small Turboprop	Insufficient data	Insufficient data	Insufficient data
B 757	Insufficient data	Insufficient data	Insufficient data
Combined IMC data	126	22	13.4

* Data from Table 3 of Ref. A6

** FAF to threshold distances for Runways 35 and 36, left and right are all 5.1 nautical miles from Figure 2 of Ref. A6

*** Data from Table 6 of Ref. A6

**** Derived using the SD_{IAT} algorithm with distance and wind uncertainties set to zero

The authors note that the VMC Heavy, Small Turboprop, and B-757 uncertainties are small enough to be explained by the 15-knot wind variations in the data (total variation, not standard deviation). They also note that the large aircraft class includes a wide range of aircraft weights and types. They offer no explanation for the other large uncertainties.

In addition to the Reference [A6] DFW data, Seagull, Inc., in Reference [A9], documents approach speed data collected at Memphis using the precision runway monitor (PRM) radar. The data were collected to develop a three-step approach model. The three steps of that model are (1) initial flight at the pattern speed, V_1, for a period of time, T_1, (2) deceleration to approach speed at rate, a, and (3) final flight at approach speed, V_3. The researchers used a nonlinear, least-squares technique to derive values for V_1, T_1, a, and V_3 from the data. Five sets of data were collected for large- and small-class aircraft. Parameters were estimated for approaches from the outer marker (OM) and from a 6 nautical mile final spacing point (FSP). Using the parameters from the report it is possible to derive the average speeds for each class of aircraft. The results are contained in Table A-6.

Table A-6. Average Speed Estimates Derived from Memphis Data

Aircraft class	Entry point	Entry speed (knots)	Threshold speed (knots)	Average speed (knots)
Large	FSP	173	138	147
Small	FSP	166	130	139
Large	OM	164	138	142
Small	OM	154	130	133

In References [A7] and [A10], the Seagull analysts use their three-step approach model for estimating the benefits of CTAS and CTAS improvements. In those reports, they equate the OM to the FSP and set the distance at 5 nautical miles. They use threshold speeds of 120, 125, and 135 knots for small, large, and heavy aircraft that are nominally taken from Reference [A6]. Table A-7 contains the report values and the average approach speeds we derive from them. Table A-7 also contains results for two variations on the Seagull data. The first variation is use of a 7-nautical mile FSP with the additional 2 miles flown at the 170-knot pattern speed. The second variation is a 130-knot threshold speed for large aircraft that seems more in accordance with the results of Reference [A6].

Table A-7. Average Speed Estimates Derived from Memphis Data

Aircraft class	Entry point	Entry speed (knots)	Threshold speed (knots)	Average speed (knots)
Heavy	OM (5 nmi.)	170	135	141
Large	OM (5 nmi.)	170	125	133
Large	OM (5 nmi.)	170	130	137
Small	OM (5 nmi.)	170	120	129
Heavy	FSP (7 nmi.)	170	135	147
Large	FSP (7 nmi.)	170	125	141
Large	FSP (7 nmi.)	170	130	144
Small	FSP (7 nmi.)	170	120	137

The results from the references cited indicate that the speeds we previously used were too high. Based on our analysis of the data, average speeds of 135, 140, 140, and 145 knots for small, large, B-757, and heavy aircraft are more appropriate.

Speed and Wind Uncertainties Our baseline values for aircraft speed and wind uncertainty are 5 knots and 7.5 knots. These are based on discussions with controllers held early in our modeling program. In our calculations, the speed and wind uncertainties always appear as a root sum squared (RSSd) result.

Speed Uncertainty Credeur and Capron in Reference [A4] (p. 14) report that approach speeds for the same models of aircraft vary on the order of 25 to 30 knots due to weight differences. A 30-knot speed range supports a 5-knot 1σ

speed uncertainty. Seagull, Inc. in Reference [A10] (p. 25) postulates a 3-knot speed uncertainty at the outer marker and 7-knot speed uncertainty at the threshhold. Our 5- knot average speed uncertainty for the final approach is, thus, in fundamental agreement with both Credeur and Capron's and Seagull's estimates.

Wind Uncertainty: Our wind uncertainty represents the difference in winds experienced by the leader and follower aircraft traversing the common path, not just the uncertainty in wind measurement. The root sum squared (RSS) of the 5-knot speed uncertainty and the 7.5-knot wind uncertainty is 9 knots. That value is appropriate to compare with the undifferentiated standard deviations of speed for DFW, reported above in Table A-2. Nine knots falls nicely in the range of the DFW data. Seagull, Inc., in Reference [A10] (p. 25), postulates a wind forecast error of only 3.7 knots. We believe that estimate may be too low, based on the DFW data.

Mean of the Inefficiency Buffer ($1/\lambda$) The inefficiency buffer includes maneuvering errors that result in imperfect delivery of the aircraft to the head of the common path. As discussed previously we model the inefficiency buffer using an exponential distribution with a mean of $1/\lambda$. The existence of the inefficiency buffer is not in doubt, since the implementation of PFAST at DFW clearly demonstrated its reduction. Quantifying the current size and potential reduction of the buffer is, however, problematic.

Ballin and Ertzberger in Reference [A6] (Tables A-19, A-21, and A-23) estimate the excess spacing buffers at DFW for three rush periods:

- IMC, 57 minutes for 29 aircraft,
- VMC, 34 minutes for 19 aircraft, and
- IMC, 80 minutes for 46 aircraft.

For their analysis, they assume a separation buffer of 0.25 nautical miles which is not included in the excess buffer. The excess buffers they estimate are 1.66 nmi., 0.72 nmi., and 0.28 nmi. for the three cases. The 0.25 nmi. separation uncertainty appears too small. Achieving the 0.25 nmi. value using the reported common path length and aircraft velocities required model inputs for velocity and wind uncertainties (RSSd standard deviations) of only 1.4, 2.1, and 1.4 seconds for the three cases (with position uncertainty of zero nautical miles). These values are remarkably low. We are reluctant to reduce our velocity and wind uncertainty values because they fall in the middle of the DFW velocity data. Reducing the distance uncertainty is similarly not supported by data. Our model would assign more of the buffer to the separation requirement and less to inefficiency. We also find that the maximum capacities estimated in the report cannot be achieved with the average aircraft velocities reported, even with the

small required separations. More work with the data in this report will be necessary to determine a reliable inefficiency buffer value.

The simulation program reported in Reference [A5] is another potential source of buffer data. The simulation produced mean and standard deviation statistics for the *interarrival errors* generated by the test controllers. In the manual case, the error was defined by the difference between the FAA minimum IFR separations and the actual separations. There was considerable variation in performance among the 12 test subjects. The lumped distribution of the errors was approximately normal with a mean of 6.37 seconds and a standard deviation of 19.49 seconds. The normal distribution is not unreasonable because only the errors and not the actual interarrival times are measured, thus removing the effect of multiple separation distance requirements. The authors of the study were primarily interested in the standard deviation of the error, but we are also interested in the mean. The mean should represent the average buffer applied by the controller for separation plus his maneuvering inefficiencies. The value of 6.37 seconds, or approximately 0.25 nmi. is very small. Indeed, the histogram in Figure A-16 of Reference [A5] shows a significant number of separation violations. Again, more information about the basic data will be required to determine a good $1/\lambda$ value.

In the absence of a value directly based on data, our approach is to choose a value that, along with the other inputs, results in reasonable outputs. The primary outputs for comparison are the arrival capacity, excess buffer size, and the standard deviation of the interarrival time.

Separation Matrices The separation matrices used in our analyses are shown in Tables A-8 to A-13. We have added one new separation matrix to the five used in previous analyses. The new matrix, LaRC 2.3, applies to AVOSS when used with ATM.

Table A-8. FAA 3.0 Separation Matrix

	Leader			
Follower	Small	Large	B-757	Heavy
Small	3	4	5	6
Large	3	3	4	5
B-757	3	3	4	5
Heavy	3	3	4	4

Table A-9. FAA 2.5 Separation Matrix

Follower	Leader			
	Small	Large	B-757	Heavy
Small	2.5	4	5	6
Large	2.5	2.5	4	5
B-757	2.5	2.5	4	5
Heavy	2.5	2.5	4	4

Table A-10. LaRC 3.0 Separation Matrix

Follower	Leader			
	Small	Large	B-757	Heavy
Small	3	3	3.5	3.5
Large	3	3	3	3
B-757	3	3	3	3
Heavy	3	3	3	3

Table A-11. LaRC 2.5 Separation Matrix

Follower	Leader			
	Small	Large	B-757	Heavy
Small	2.5	3.5	3.5	3.5
Large	2.5	2.5	3	3
B-757	2.5	2.5	3	3
Heavy	2.5	2.5	2.5	2.5

Table A-12. LaRC 2.3 Separation Matrix

Follower	Leader			
	Small	Large	B-757	Heavy
Small	2.3	3	3.5	3.5
Large	2.3	2.3	3	3
B-757	2.3	2.3	3	3
Heavy	2.3	2.3	2.3	2.3

Table A-13. FAA EM-78-8A VMC-1 Separation Matrix

	Leader			
Follower	Small	Large	B-757	Heavy
Small	1.9	2.7	3.5	4.5
Large	1.9	1.9	3.0	3.6
B-757	1.9	1.9	3.0	3.6
Heavy	1.9	1.9	2.7	2.7

The separations in the LaRC matrices are based on results of the AVOSS deployment at DFW. At DFW, AVOSS frequently predicted conditions where safe wake vortex separations were less than the ATC minimum separation of 2.5 nautical miles. Analyses that correlate those conditions to the ground meteorological data (wind speed and direction) have been proposed but have not been done. In lieu of such analyses we rely on the criteria developed for the FAA Vortex Advisory System (VAS) to identify when any of the AVOSS separations can be used. When the spreadsheet model analyses were performed AVOSS was only credited with being able to reduce the separations above the ATC minimums by 0.5 nautical miles. Consequently, the results in the spreadsheets at the end of this appendix have conservative capacities for AVOSS configurations.

VAS criteria and separations are described in Reference [A13]. VAS data show that when the wind exceeds that of an ellipse with a 12.0-knot headwind semi-major axis and a 5.5-knot crosswind semi-minor axis, the vortices were transported out of the flight path or dissipated within 80 seconds (or 3 nautical miles for a 135-knot airspeed). We calculate the VAS criteria in the capacity/delay models and apply them as a condition for using the AVOSS matrices.

The 2.3-nautical mile minimum separation in the LaRC 2.3 matrix is due to both the reduced wake vortex hazard and to ATM improvements in air traffic control. The matrix only applies to ATM/AFAST scenarios.

ROTs The background and justification for our method of estimating ROT is described in Appendix B of Reference [A14]. In brief, ROTs are determined using algorithms derived from the tables contained in Reference [A2], the user's guide to the FAA Airfield Capacity Model, so long as the results are within one standard deviation of existing data. The same base ROTs are used for all runways, wet or dry, except in IMC-2 (low visibility) conditions when they are increased 20 percent. If DROM and ROTO are both available, the base ROTs are used, even in IMC-2.

Inputs for the TAP Technologies

This section lists the proposed inputs for the TAP technologies and the results obtained from the spreadsheet model for a single arrival-only runway. The aircraft mix and common path inputs are representative of DFW.

The discussion above addressed the input parameters in some detail. Without being repetitive, it is useful to summarize how the specific technologies are modeled.

PFAST Baseline The PFAST baseline is modeled by reducing the inefficiency buffer, $1/\lambda$, from 0.25 nautical miles to 0.1 nautical miles.

AFAST Baseline The AFAST baseline includes the PFAST reduction in $1/\lambda$, plus reductions in speed and position uncertainties. The speed and position uncertainties are reduced because speed and position data transmitted from the aircraft by the Automated Dependent Surveillance-Broadcast (ADS-B) system will enable AFAST to make more accurate predictions. The standard deviation of the position uncertainty is reduced from 0.25 nautical miles to 100 feet (≈0.2 nautical miles). The standard deviation of the speed uncertainty is reduced from 5 nautical miles to 2 nautical miles. The wind uncertainty is not reduced because no integration with the aircraft flight management system (FMS) is assumed in the AFAST baseline.

Dynamic Runway Occupancy Measurement System (DROM) DROM provides real-time measurements of runway occupancy times. We expect that DROM will confirm ROTs under 50 seconds and enable the use of 2.5-nautical-mile minimum separations for IMC-1 wet runways.

ROTO ROTO technology enables shorter ROTs in poor visibility. We model ROTO by removing the 20 percent ROT penalty and allowing 2.5 nautical mile minimum separations in IMC-2 conditions.

Aircraft Vortex Spacing System (AVOSS) We model AVOSS with reduced separation matrices. Earlier in the study, we modeled two versions of AVOSS, Builds 1 and 2, with different wake vortex separations that corresponded to transport and transport plus demise. The DFW AVOSS results indicate that the transport plus demise separations are appropriate for all cases. The distinction between AVOSS Builds has, therefore, been eliminated. Three different AVOSS matrices are used because the minimum separations in the AVOSS matrices are determined by the ATC limits. The minimums allowed depend on the meteorological condition and the presence of DROM, ROTO, and ATM technologies.

ATM 1 (AFAST/3DFMS): ATM-1 includes AFAST with a direct data link between CTAS and the aircraft's 3-D (position only) flight management system (FMS). We model ATM-1 by reducing the wind uncertainty. The standard

deviation of the wind uncertainty is reduced from 7.5 knots to 5 knots. This reduction assumes that FMS wind reports from arriving aircraft will allow AFAST to better predict winds along the flight path.

Air Traffic Management 2 (AFAST/4DFMS) ATM-2 includes integration of CTAS with the aircraft's 4-D (position and time) FMS. This integration enables Required Time of Arrival (RTN) operations. We model ATM-2 by further reducing wind and velocity uncertainties. We also reduce the inefficiency buffer, $1/\lambda$, to zero. The standard deviations of the wind and velocity are reduced to 2.0 and 1.2 knots, respectively. These are the values used by Seagull, Inc. in Reference [A7].

A summary of the input parameters for each technology and meteorological condition is in Table A-16 located at the end of this appendix.

Single Runway Results

We used the spreadsheet model to examine the results for all 19 technology cases in each of the 4 meteorological conditions. The results are displayed in Tables A-17 to A-20 located at the end of this appendix.

Comparisons With Other Work

The spreadsheet results are encouraging. The σ_{IAT} values compare well with those from other sources. Table A-14 compares model results with the simulation results from Reference [A5] and the recommended values from FAA EM-78-8A.

Table A-14. Comparison of Interarrival Time Uncertainty Standard Deviations, σ_{IAT}'s, (in Seconds)

TAP technology	Spreadsheet model σ_{IAT}	Reference A5 simulation σ_{IAT}	Reference A6 data-based σ_{IAT}	FAA EM-78-8A σ_{IAT}
Current Technology	19.9	19.49	19.6	18
PFAST baseline	19.0	–	–	–
AFAST baseline	14.3	14.53	–	11
ATM 1: AFAST – 3DFMS	10.0	–	–	8
ATM 2: AFAST – 4DFMS	4.3	–	–	–

The 4.3 second value for the ATM 2 case is very low, but not unreasonable, given the concept of closed-loop ATC / 4DFMS integration.

DFW PFAST Test Results In Reference [A15], Davis et al. describe the results of PFAST testing at DFW. They report an arrival capacity increase due to PFAST of 9.3 percent in IFR and 13.3 percent in VFR. The increases were

ascribed to excess separation reductions and runway balancing. As noted in the model development section, our capacity model implicitly assumes balanced runways for all technologies. The spreadsheet model results indicate an increase of about 1 arrival per hour over the Current Reference for all meteorological conditions. This is only a 3 percent to 4 percent improvement. While excess buffer sizes of 1.3 to 1.6 nautical miles compare reasonably well with the DFW data, the spreadsheet model runway arrival capacities are about 5 aircraft per hour lower than those reported for in Reference [A15] for PFAST. Some of the difference, 1-2 aircraft per hour, can be made up by mix optimization, but major increases in the model capacity require changes to the inputs that we cannot support.

Seagull, Inc. AFAST Performance Estimates Seagull, Inc. has investigated the benefits of various AFAST configurations using algorithms significantly different from ours. The algorithms are developed in Reference [A8]. Their approach postulates a three-step speed profile for final approach. They develop two equations for the interarrival range, one for a faster follower and the other for a faster leader. The equations are functions of 11 independent variables covering time, speed, wind and acceleration for the three stages of the flight. Interarrival time uncertainty is estimated by small perturbation analysis. The separation buffer is defined in References [A7] and [A10] as

$$B_{TH} = \mu_{TH} + 0.9x\sigma_{TH}$$

where:

B_{TH} = the threshold buffer,

μ_{TH} = the threshold mean, and

σ_{TH} = the threshold standard deviation.

The means and standard deviations in the equation include error contributions from the Center and TRACON airspace plus those from final approach. In References [A7] and [A10], excess spacing results are reported for baseline CTAS (assumed PFAST), AFAST with 3DFMS integration, and AFAST with 4DFMS integration. We compared the spreadsheet model results with those in the references by using average speeds derived from the reported values and the reported common path and uncertainty parameters. The average speeds are Small: 129 knots, Large: 133 knots, and Heavy: 141 knots. The inputs and results are given in Table A-15.

Table A-15. Comparison of LMI and Seagull Excess Spacing Buffer Results

	Excess spacing buffer in seconds		
Technology	LMI follower > leader	LMI leader > follower	Seagull both
Baseline CTAS	34–37	28–30	27–29
AFAST ATN (3DFMS)	10 –11	7–9	7–9
AFAST RTA (4DFMS)	6.5	3.5–4.5	4–5

Our excess spacing buffers were higher for the baseline CTAS and in reasonable agreement for the AFAST technologies. The degree of agreement is encouraging considering the differences in algorithms.

Summary and Conclusions

In the preceding discussions we have identified the TAP cases analyzed and developed the input parameters used in the analysis. The capacity model algorithms have been modified to better account for maneuvering inefficiencies. A spreadsheet capacity model was written to test the parameters and examine intermediate outputs of interest, particularly excess spacing buffers and the standard deviation of interarrival times.

The results indicate substantive agreement with other analyses and data. Further study of the differences between the estimated PFAST capacity and the capacity reported in Reference [A15] is recommended.

Table A-16. Spreadsheet Arrival Capacity Model Input/Output Summary

INPUTS

Common Path (nmi.)	D	7.00
SD speed (knots	SDV	5.00
SD position (nmi.)	SDX	0.25
SD wind (knots)	SDW	7.5

Aircraft Data

Class	Speeds	Mix	ROT	SDROT
Small	135	0.14	42	8
Large	140	0.71	47	8
B-757	140	0.075	47	8
Heavy	145	0.075	53	8
		seconds	nmi.	feet
Mean of inefficiency buffer (1 / lambda)		2.58	0.10	608

Target separation matrix (input matrix)

	Leader			
Follower	Small	Large	757	Heavy
Small	2.5	4	5	6
Large	2.5	2.5	4	5
757	2.5	2.5	4	5
Heavy	2.5	2.5	4	4

Non-Weighted Interarrival Time (output matrix)

	Leader			
Follower	Small	Large	757	Heavy
Small	104	132	160	187
Large	101	99	140	154
757	101	99	140	154
Heavy	101	100	135	134

RESULTS

Expected A-A Capacity	32.6	per hour
Perfect A-A Capacity	46.75	per hour
IAT and Buffer	seconds	nmi.
Mean IAT	110	4.29
Perfect IAT	77	3.0
Excess Spacing Buffer (MeanIAT - Perfect IAT)	33.5	1.3
SDiat at TH for normal distribution	19.0	0.74
SDtaa at TH for actual distribution	27.33	1.06
SDind for individuals at head of CP	18.9	0.73
FAA Model Capacity using SDiat TH	33.2	
FAA Model Mean IAT	108	4.2
Average Speed =	140	knots
Percent ROT Constrained Cases	6%	

Non-weighted excess spacing buffer (output matrix)

	Leader			
Follower	Small	Large	757	Heavy
Small	37.4	22.5	24.5	25.4
Large	36.9	35.2	36.8	23.3
757	36.9	35.2	36.8	23.3
Heavy	38.9	37.5	36.2	34.6

MIT / ROT constraint matrix (output matrix)

	Leader			
Follower	Small	Large	757	Heavy
Small	MIT	MIT	MIT	MIT
Large	MIT	MIT	MIT	MIT
757	MIT	MIT	MIT	MIT
Heavy	ROT	ROT	MIT	MIT

Table A-17. DFW Single Runway Spreadsheet Model Input Parameters

TAP technology case	Common Path nmi.	σ_v knots	σ_x nmi.	σ_w knots	1/λ seconds	IMC-2		IMC-1		VMC-2		VMC-1	
						ROT vector	Separation matrix	ROT vector	Separation matrix	ROT vector	Separation matrix	ROT vector	Separation matrix
Current Technology	7	5	0.25	7.5	0.25	120%	FAA 3.0	100%	FAA 3.0	100%	FAA 2.5	100%	VMC
2005 PFAST baseline	7	5	0.25	7.5	0.1	120%	FAA 3.0	100%	FAA 3.0	100%	FAA 2.5	100%	VMC
PFAST DROM	7	5	0.25	7.5	0.1	120%	FAA 3.0	100%	FAA 2.5	100%	FAA 2.5	100%	VMC
PFAST ROTO DROM	7	5	0.25	7.5	0.1	100%	FAA 2.5	100%	FAA 2.5	100%	FAA 2.5	100%	VMC
PFAST AVOSS	7	5	0.25	7.5	0.1	120%	LaRC 3.0	100%	LaRC 3.0	100%	LaRC 2.5	100%	VMC
PFAST DROM AVOSS	7	5	0.25	7.5	0.1	120%	LaRC 3.0	100%	LaRC 2.5	100%	LsRC 2.5	100%	VMC
PFAST ROTO DROM AVOSS	7	5	0.25	7.5	0.1	100%	LaRC 2.5	100%	LaRC 2.5	100%	LaRC 2.5	100%	VMC
2005 AFAST + data link baseline	7	2	0.02	7.5	0.05	120%	FAA 3.0	100%	FAA 3.0	100%	FAA 2.5	100%	VMC
AFAST DROM	7	2	0.02	7.5	0.05	120%	FAA 3.0	100%	FAA 2.5	100%	FAA 2.5	100%	VMC
AFAST ROTO DROM	7	2	0.02	7.5	0.05	100%	FAA 2.5	100%	FAA 2.5	100%	FAA 2.5	100%	VMC
AFAST AVOSS	7	2	0.02	7.5	0.05	120%	LaRC 3.0	100%	LaRC 3.0	100%	LaRC 2.5	100%	VMC
AFAST DROM AVOSS	7	2	0.02	7.5	0.05	120%	LaRC 3.0	100%	LaRC 2.5	100%	LaRC 2.5	100%	VMC
AFAST ROTO DROM AVOSS	7	2	0.02	7.5	0.05	100%	LaRC 2.5	100%	LaRC 2.5	100%	LaRC 2.5	100%	VMC
ATM-1 AFAST 3DFMS data link	7	2	0.02	5	0.05	120%	FAA 3.0	100%	FAA 3.0	100%	FAA 2.5	100%	VMC
ATM-1 ROTO DROM	7	2	0.02	5	0.05	100%	FAA 2.5	100%	FAA 2.5	100%	FAA 2.5	100%	VMC
ATM-1 DROM AVOSS	7	2	0.02	5	0.05	120%	LaRC 3.0	100%	LaRC 2.3	100%	LaRC 2.3	100%	VMC
ATM-1 ROTO DROM AVOSS	7	2	0.02	5	0.05	100%	LaRC 2.3	100%	LaRC 2.3	100%	LaRC 2.3	100%	VMC
ATM -2: AFAST 4DFMS data link	7	1.2	0.02	2	0	120%	FAA 3.0	100%	FAA 3.0	100%	FAA 2.5	100%	VMC
Ultimate TAP: ATM-2 ROTO DROM AVOSS	7	1.2	0.02	2	0	100%	LaRC 2.3	100%	LaRC 2.3	100%	LaRC 2.3	100%	VMC

Table A-18. DFW IMC-2 Single Runway Spreadsheet Model Results

TAP technology case	Common Path nmi.	σ_v knots	σ_x nmi.	σ_w knots	1/λ seconds	ROT vector	Separation matrix	Capacity AC/hour	Buffer sec.	Buffer nmi.	SDiat sec.	ROT %
Current technology	7	5	0.25	7.5	0.25	120%	FAA 3.0	29	38	1.5	19.9	6%
2005 PFAST baseline	7	5	0.25	7.5	0.1	120%	FAA 3.0	29.9	34	1.3	19.0	6%
PFAST DROM	7	5	0.25	7.5	0.1	120%	FAA 3.0	29.9	34	1.3	19.0	6%
PFAST ROTO DROM	7	5	0.25	7.5	0.1	100%	FAA 2.5	32.6	33	1.3	19.0	6%
PFAST AVOSS	7	5	0.25	7.5	0.1	120%	LaRC 3.0	30.8	33	1.3	19.0	6%
PFAST DROM AVOSS	7	5	0.25	7.5	0.1	120%	LaRC 3.0	30.8	33	1.3	19.0	6%
PFAST ROTO DROM AVOSS	7	5	0.25	7.5	0.1	100%	LaRC 2.5	33.6	33	1.3	19.0	6%
2005 AFAST + data link baseline	7	2	0.02	7.5	0.05	120%	FAA 3.0	32.5	24	0.9	14.3	0%
AFAST DROM	7	2	0.02	7.5	0.05	120%	FAA 3.0	32.5	24	0.9	14.3	0%
AFAST ROTO DROM	7	2	0.02	7.5	0.05	100%	FAA 2.5	35.6	24	0.9	14.3	6%
AFAST AVOSS	7	2	0.02	7.5	0.05	120%	LaRC 3.0	33.5	24	0.9	14.3	0%
AFAST DROM AVOSS	7	2	0.02	7.5	0.05	120%	LaRC 3.0	33.5	24	0.9	14.3	0%
AFAST ROTO DROM AVOSS	7	2	0.02	7.5	0.05	100%	LaRC 2.5	36.9	24	0.9	14.3	6%
ATM: AFAST 3DFMS data link	7	2	0.02	5	0.05	120%	FAA 3.0	34.7	17	0.7	10.0	0%
ATM ROTO DROM	7	2	0.02	5	0.05	100%	FAA 2.5	38.3	17	0.7	10.0	6%
ATM-1 DROM AVOSS	7	2	0.02	5	0.05	120%	LaRC 3.0	35.9	17	0.7	10.0	6%
ATM ROTO DROM AVOSS	7	2	0.02	5	0.05	100%	LaRC 2.3	43.1	17	0.7	10.0	6%
ATM 2: AFAST 4DFMS data link	7	1.2	0.02	2	0	120%	FAA 3.0	38.5	7	0.3	4.3	6%
Ultimate TAP: ATM 2 ROTO DROM AVOSS	7	1.2	0.02	2	0	100%	LaRC 2.3	48.5	8	0.3	4.3	73%

Table A-19. DFW IMC-1 Single Runway Spreadsheet Model Results

TAP technology case	Common Path nmi.	σ_v knots	σ_x nmi.	σ_w knots	1/λ seconds	ROT vector	Separation matrix	Capacity AC/hour	Buffer sec.	Buffer nmi.	SDiat sec.	ROT %
Current Technology	7	5	0.25	7.5	0.25	100%	FAA 3.0	29	38	1.5	19.9	0%
2005 PFAST baseline	7	5	0.25	7.5	0.1	100%	FAA 3.0	29.9	34	13	19.0	0%
PFAST DROM	7	5	0.25	7.5	0.1	100%	FAA 2.5	32.6	33	1.3	19.0	6%
PFAST ROTO DROM	7	5	0.25	7.5	0.1	100%	FAA 2.5	32.6	33	1.3	19.0	6%
PFAST AVOSS	7	5	0.25	7.5	0.1	100%	LaRC 3.0	30.8	33	1.3	19.0	0%
PFAST DROM AVOSS	7	5	0.25	7.5	0.1	100%	LaRC 2.5	33.6	33	1.3	19.0	6%
PFAST ROTO DROM AVOSS	7	5	0.25	7.5	0.1	100%	LaRC 2.5	33.6	33	1.3	19.0	6%
2005 AFAST + data link baseline	7	2	0.02	7.5	0.05	100%	FAA 3.0	32.5	24	0.9	14.3	0%
AFAST DROM	7	2	0.02	7.5	0.05	100%	FAA 2.5	35.6	24	0.9	14.3	6%
AFAST ROTO DROM	7	2	0.02	7.5	0.05	100%	FAA 2.5	35.6	24	0.9	14.3	6%
AFAST AVOSS	7	2	0.02	7.5	0.05	100%	LaRC 3.0	33.5	24	0.9	14.3	0%
AFAST DROM AVOSS	7	2	0.02	7.5	0.05	100%	LaRC 2.5	36.9	24	0.9	14.3	6%
AFAST ROTO DROM AVOSS	7	2	0.02	7.5	0.05	100%	LaRC 2.5	36.9	24	0.9	14.3	6%
ATM: AFAST 3DFMS data link	7	2	0.02	5	0.05	100%	FAA 3.0	34.7	17	0.7	10.0	0%
ATM ROTO DROM	7	2	0.02	5	0.05	100%	FAA 2.5	38.3	17	0.7	10.0	6%
ATM-1 DROM AVOSS	7	2	0.02	5	0.05	100%	LaRC 2.3	41.4	17	0.7	10.0	6%
ATM ROTO DROM AVOSS	7	2	0.02	5	0.05	100%	LaRC 2.3	43.1	17	0.7	10.0	6%
ATM 2: AFAST 4DFMS data link	7	1.2	0.02	2	0	100%	FAA 3.0	38.5	7	0.3	4.3	0%
Ultimate TAP: ATM 2 ROTO DROM AVOSS	7	1.2	0.02	2	0	100%	LaRC 2.3	48.5	8	0.3	4.3	73%

Table A-20 . DFW VMC-2 Single Runway Spreadsheet Model Results

TAP technology case	Common Path nmi.	σ_v knots	σ_x nmi.	σ_w knots	1/λ seconds	ROT vector	Separation matrix	Capacity AC/hour	Buffer sec.	Buffer nmi.	SDiat sec.	ROT %
Current Technology	7	5	0.25	7.5	0.25	100%	FAA 2.5	31.5	37	1.4	19.9	6%
2005 PFAST baseline	7	5	0.25	7.5	0.1	100%	FAA 2.5	32.6	33	1.3	19.0	6%
PFAST DROM	7	5	0.25	7.5	0.1	100%	FAA 2.5	32.6	33	1.3	19.0	6%
PFAST ROTO DROM	7	5	0.25	7.5	0.1	100%	FAA 2.5	32.6	33	1.3	19.0	6%
PFAST AVOSS	7	5	0.25	7.5	0.1	100%	LaRC 2.5	33.6	33	1.3	19.0	6%
PFAST DROM AVOSS	7	5	0.25	7.5	0.1	100%	LaRC 2.5	33.6	33	1.3	19.0	6%
PFAST ROTO DROM AVOSS	7	5	0.25	7.5	0.1	100%	LaRC 2.5	33.6	33	1.3	19.0	6%
2005 AFAST + data link baseline	7	2	0.02	7.5	0.05	100%	FAA 2.5	35.6	24	0.9	14.3	6%
AFAST DROM	7	2	0.02	7.5	0.05	100%	FAA 2.5	35.6	24	0.9	14.3	6%
AFAST ROTO DROM	7	2	0.02	7.5	0.05	100%	FAA 2.5	35.6	24	0.9	14.3	6%
AFAST AVOSS	7	2	0.02	7.5	0.05	100%	LaRC 2.5	36.9	24	0.9	14.3	6%
AFAST DROM AVOSS	7	2	0.02	7.5	0.05	100%	LaRC 2.5	36.9	24	0.9	14.3	6%
AFAST ROTO DROM AVOSS	7	2	0.02	7.5	0.05	100%	LaRC 2.5	36.9	24	0.9	14.3	6%
ATM: AFAST 3DFMS data link	7	2	0.02	5	0.05	100%	FAA 2.5	38.3	17	0.7	10.0	6%
ATM ROTO DROM	7	2	0.02	5	0.05	100%	FAA 2.5	38.3	17	0.7	10.0	6%
ATM-1 DROM AVOSS	7	2	0.02	5	0.05	100%	LaRC 2.3	41.4	17	0.7	10.0	6%
ATM ROTO DROM AVOSS	7	2	0.02	5	0.05	100%	LaRC 2.3	43.1	17	0.7	10.0	6%
ATM 2: AFAST 4DFMS data link	7	1.2	0.02	2	0	100%	FAA 2.5	42.9	7	0.3	4.3	6%
Ultimate TAP: ATM 2 ROTO DROM AVOSS	7	1.2	0.02	2	0	100%	LaRC 2.3	53.9	8	0.3	4.3	73%

Table A-21. DFW VMC-1 Single Runway Spreadsheet Model Results

TAP technology case	Common Path nmi.	σ_v knots	σ_x nmi.	σ_w knots	1/λ seconds	ROT vector	Separation matrix	Capacity AC/hour	Buffer sec.	Buffer nmi.	SDiat sec.	ROT %
Current Technology	7	5	0.25	7.5	0.25	100%	VMC	35.2	45	1.7	19.1	75%
2005 PFAST baseline	7	5	0.25	7.5	0.1	100%	VMC	36.5	41	1.6	19.0	75%
PFAST DROM	7	5	0.25	7.5	0.1	100%	VMC	36.5	41	1.6	19.0	75%
PFAST ROTO DROM	7	5	0.25	7.5	0.1	100%	VMC	36.5	41	1.6	19.0	75%
PFAST AVOSS	7	5	0.25	7.5	0.1	100%	VMC	36.5	41	1.6	19.0	75%
PFAST DROM AVOSS	7	5	0.25	7.5	0.1	100%	VMC	36.5	41	1.6	19.0	75%
PFAST ROTO DROM AVOSS	7	5	0.25	7.5	0.1	100%	VMC	36.5	41	1.6	19.0	75%
2005 AFAST + data link baseline	7	2	0.02	7.5	0.05	100%	VMC	40.9	3.1	1.2	14.8	75%
AFAST DROM	7	2	0.02	7.5	0.05	100%	VMC	40.9	3.1	1.2	14.8	75%
AFAST ROTO DROM	7	2	0.02	7.5	0.05	100%	VMC	40.9	3.1	1.2	14.8	75%
AFAST AVOSS	7	2	0.02	7.5	0.05	100%	VMC	40.9	3.1	1.2	14.8	75%
AFAST DROM AVOSS	7	2	0.02	7.5	0.05	100%	VMC	40.9	3.1	1.2	14.8	75%
AFAST ROTO DROM AVOSS	7	2	0.02	7.5	0.05	100%	VMC	40.9	3.1	1.2	14.8	75%
ATM: AFAST 3DFMS data link	7	2	0.02	5	0.05	100%	VMC	44.5	24	0.9	10.0	75%
ATM ROTO DROM	7	2	0.02	5	0.05	100%	VMC	44.5	24	0.9	10.0	75%
ATM-1 DROM AVOSS	7	2	0.02	5	0.05	100%	VMC	44.5	24	0.9	10.0	75%
ATM ROTO DROM AVOSS	7	2	0.02	5	0.05	100%	VMC	44.5	24	0.9	10.0	75%
ATM 2: AFAST 4DFMS data link	7	1.2	0.02	2	0	100%	VMC	49.7	15	0.6	8.0	75%
Ultimate TAP: ATM 2 ROTO DROM AVOSS	7	1.2	0.02	2	0	100%	VMC	49.7	15	0.6	8.0	75%

REFERENCES

[A1] *Estimating the Effects of the Terminal Area Productivity Program*, Lee et al, NASA Contractor Report 201682, Apr 1997 (reference for LMI capacity and delay models).

[A2] *Upgraded FAA Airfield Capacity Model (User's Guide),* FAA-DF-81-001A, May 1981.

[A3] *Parameters of Future ATC Systems Relating to Airport Capacity/Delay*, A. L. Haines, FAA-EM-78-8A, June 1978.

[A4] *Simulation Evaluation of TIMER, a Time-Based Terminal Air Traffic, Flow Management Concept,* Credeur and Capron, NASA Technical Paper 2870, Feb 1989.

[A5] *Final Approach Spacing Aids (FASA) Evaluation for Terminal Area, Time-Based Air Traffic Control,* Credeur et al, NASA Technical Paper 3399, Dec 1993.

[A6] *An Analysis of Landing Rates and Separations at the Dallas-Ft Worth Airport (Draft),* Ballin and Erzberger, NASA TM 110397, undated. (data taken over six months of winter 1994-95.

[A7] *Final Approach Enhancement and Descent Trajectory Negotiation Potential Benefits Analysis,* Couluris et al, Seagull Technology Inc. Report 97142-02, July 1997.

[A8] *Analysis of Final Approach Spacing Requirements, Part I*, Sorensen, Shen, and Hunter, Seagull Technology, Inc. Report 91112-01, Jan 91.

[A9] *Analysis of Final Approach Spacing Requirements, Part II*, Sorensen, Shen, and Hunter, Seagull Technology, Inc. Report 91112-02, Jan 91.

[A10]*Initial Air Traffic Management (ATM) Enhancement Potential Benefits Analysis*, Couluris, Weidner, and Sorensen, Seagull Technology, Inc. Report 96151-01, Sept. 96.

[A11]*Models for Runway Capacity Analysis*, Richard Harris, FAA-EM-73-5, Dec. 1972.

[A12]*A Proposed Methodology for Determining Wake-Vortex Imposed Aircraft Separation Constraints*, C.R. Tatnall, Master's Thesis, The Pennsylvania State University, August 1995.

[A13]*Aircraft Wake Vortices: An Assessment of the Current Situation*, J.N. Hallock, FAA-90-29, January 1991.

[A14]*Cost Benefit Estimates of Terminal Area Productivity Technologies*, Hemm, Shapiro, Nelson, & Lee, NS604S1, September 1997.

[A15]*Operational Test Results of the Passive Final Approach Spacing Tool*, Davis et al, IFAC 8th Symposium on Transportation Systems 97, Chania, Greece, June 1997.

Appendix B
Staggered Departure and Arrival Models

In this appendix we describe the ASAC Airport Capacity Model algorithm used to estimate the capacity of a parallel runway pair when there are spacing requirements between both aircraft using the same runway and between aircraft using one runway and aircraft using a parallel runway. This can occur when both runways are used for departures or when both runways are used for arrivals.

Unlike separation requirements for single runways, separation requirements in this situation between aircraft approaching the same runway cannot be derived by examining aircraft class pairs in isolation; the interdependence of traffic on the two runways requires, in general, knowledge of the entire sequence of operations to determine the separation required between any two aircraft approaching the same runway.

Since exact separations cannot be determined, except for a specific sequence of operations, the algorithm constructs upper and lower bounds on the separation time required between successive operations on one runway of the pair. The bounds are computed for each combination of following aircraft class and leader aircraft class (as in the single runway model). The bounds take into account the interaction with traffic on the other runway.

A user-controllable parameter determines how many historical operations are considered, and thus how much refinement is put into determining the separation bounds, so that capacity can be estimated to any desired degree of precision (at the expense of additional computation time). The capacity bounds of the runway are computed on the basis of the weighted average time between operations; the weighting factors account for the traffic mix on the targeted runway. Since we assume that operations alternate between runways, the capacities of both the targeted runway and the "other" runway will be the same. We can exploit this symmetry by computing the capacity bounds twice, once using each runway as the target. The computed bounds will generally differ, leading us to identify a best lower bound and a best upper bound on estimated capacity.

Here we discuss the capacity bounding algorithm from the perspective of departures. The staggered-operations capacity algorithm for arrivals is completely analogous.

MODELING DEPARTURE CAPACITY OF A PARALLEL RUNWAY PAIR

In modeling the interdeparture times on the target runway, we assume that a departure has just occurred on the other runway. To capture the separation times required between two aircraft on the target runway (aircraft of type i, following an aircraft of type j, which is next to depart), we need to consider also the aircraft of type l, which has just departed on the other runway, and the aircraft of type k, which is due to depart the other runway after the aircraft of type j departs the runway under consideration. The departure sequence is l, j, k, i. For conciseness we will refer to an aircraft of type x as simply aircraft x.

We define $\mu(i,j,k,l)$ to be the average time separation (in minutes) that the controller will apply to aircraft i following aircraft j on the same runway, when aircraft l has just departed the other runway and aircraft k is next to depart the other runway. We compute both upper and lower bounds on this separation.

The separation (in minutes) between i and j that we use to compute the runway's capacity is the weighted average

$$\mu_P(i,j) = \sum_{k,l} \mu\ (i,j,k,l)\, p_{xk}\, p_{xl},$$

where p_{xk} (p_{xl}) is the probability of aircraft $k(l)$ on the other runway. Upper (lower) bounds on $\mu_p(i,j)$ are computed using the upper (lower) bounds on $\mu(i,j,k,l)$.

The hourly runway capacities are estimated by

$$capacity = \frac{60}{\sum_{i,j} \mu_P(i,j)\, p_i\, p_j},$$

where p_i and p_j are the probability of i and j on the targeted runway. Lower (upper) bounds on capacity are derived from the upper (lower) bounds on separation.

To develop the definition of $\mu(i,j,k,l)$, let us define two other separations. $\mu_S(i,j)$ is the single runway separation required for aircraft i following aircraft j. These are the same separations used in the single runway model. $\mu_X(i,k)$ is the separation required between aircraft i following a departure of aircraft k on the other runway. As in the single runway model, these separations are determined

from the controller's point of view, including time to account for uncertainties in wind, speed, and position. Let us define t_i as the time of departure of aircraft i.

Given that aircraft i departs after j on the target runway and k on the other runway, then by definition

$$t_i = \max[t_j + \mu_S(i,j),\ t_k + \mu_X(i,k)].$$

In general, the relative values of t_j and t_k (and hence t_i) depend on the unspecified history before flight l's departure; however, under certain conditions, the separation $t_i - t_j$—i.e., $\mu(i,j,k,l)$—can be computed without knowledge of the prior history.

- *Markov Property*. For any sequence of departures l, j, k such that

  $$\mu_S(k,l) \le \mu_X(k,j) + \mu_X(j,l),$$

  all prior history is irrelevant in determining

  $$t_k = \mu_X(k,j) + t_j$$

  and

  $$t_i - t_j = \max[\mu_S(i,j), \mu_X(i,k) + \mu_X(k,j)].$$

- *Proof*. By definition $t_j \ge t_l + \mu_X(j,l)$, thus

  $$t_j + \mu_X(k,j) \ge t_l + \mu_X(j,l) + \mu_X(k,j).$$

  By hypothesis the right-hand side is greater than $\mu_S(k,l) + t_l$, leading to

  $$t_j + \mu_X(k,j) \ge \mu_S(k,l) + t_l.$$

The two terms above are those whose maximum defines t_k, thus the value of t_k is known in terms of t_j. Substituting $t_j + \mu_X(k,j)$ for t_k in the maximum formula for t_i, and subtracting t_j from all terms leads to the final result. QED.

Another useful relationship is the following:

- *Parallelogram Property*. For any departure sequence l, j, k for which the Markov Property does *not* hold, if

  $$\mu_S(i,j) + \mu_X(j,l) \ge \mu_S(k,l) + \mu_X(i,k)$$

then

$$t_i - t_j = \mu_S(i,j)\,.$$

◆ *Proof.* From the defining maximum formula we note that

$$t_k - t_j = \max[\mu_S(k,l) - (t_j - t_l),\ \ \mu_X(k,j)]\,.$$

Since $t_j - t_l \geq \mu_X(j,l)$, we have

$$t_k - t_j \leq \max[\mu_S(k,l) - \mu_X(j,l),\quad \mu_X(k,j)];$$

and the assumption that the Markov Property is *not* true leads to

$$t_k - t_j \leq \mu_S(k,l) - \mu_X(j,l)\,.$$

With this result in hand, let us examine the defining relation

$$t_i - t_j = \max[\mu_S(i,j),\quad t_k - t_j + \mu_X(i,k)]\,.$$

The second term in the maximum is less than

$$\mu_S(k,l) - \mu_X(j,l) + \mu_X(i,k)\,,$$

by the inequality just obtained, and by hypothesis, this bound in turn is less than $\mu_S(i,j)$, leading to the final result.

BOUNDING SEPARATIONS

The two properties discussed in the previous section allow direct determination of the separation between i and j for some classes k and l. In these cases, we set both the upper and lower bound on separation to the known value. For those cases where neither property is of assistance, we now describe how to establish bounds on the separations.

The maximum separation between i and j occurs if the prior departure on the target runway does not delay flight j by any more than the cross-runway separation from flight l. In this case j is leaving as early as possible, considering that flight l preceded it on the other runway. If we set t_j to the lower bound, $t_l + \mu_X(j,l)$, and choose any arbitrary value for t_l, then the remaining departure times, including t_i, can be computed from the defining maximum formulae, and the upper bound on the separation between i and j can be computed.

The minimum separation between i and j occurs when j is forced to lag l by the maximum amount, because of prior history. If

$$\max\_sep(j,l) = \max_m[\mu_S(j,m) - \mu_X(l,m)],$$

the largest value that t_j could take on is $t_l + \max\_sep(j,l)$. Assuming an arbitrary value for t_l and this maximum value t_j allows computation of the remaining departure times and the lower bound on the separation between i and j.

Both the lower and the upper bounds computed above depend on l and k. The bounds independent of l and k are computed by weighted sums of these l,k-dependent terms.

CONSIDERING MORE HISTORY

The bounds of the previous section are based on the extreme case for prior history. These bounds can be refined by explicitly considering prior departure sequences. Let us denote the additional flights considered by $f_1, f_2, f_3, \ldots, f_n$, each departing earlier than the previous one in the sequence. We will use F to denote the entire sequence. The flights with an odd index depart from the target runway; those with an even index depart from the other runway. The bounds on $\mu_P(i,j)$ are calculated as

$$\text{bound on } \mu_P(i,j) = \sum_{l,k,F} (\text{bound due to } l,k,F)\, p_{xl} p_{xk} \prod_{z=0}^{\left\lfloor \frac{n-1}{2} \right\rfloor} p_{f_{2z+1}} \prod_{z=1}^{\left\lceil \frac{n-1}{2} \right\rceil} p_{xf_{2z}} .$$

In practice, we may not need to consider the entire sequence F to bound t_i–t_j. If there is any subsequence f_{z+2}, f_{z+1}, f_z that satisfies the Markov Property, then we can determine f_z in terms of f_{z+1}. Given f_z and f_{z+1} we can determine all subsequent departure times, including the times of interest, t_i and t_j. Any arbitrary value of f_{z+1} will do. The capacity algorithm uses recursive code to add history if the Markov Property is not true for the last three flights in the current history F. If the Markov Property is true, the lower and upper bounds are set to the same (computable) value.

The model user can specify the maximum number of aircraft to add to the history F. The larger this maximum, the more accurate the bounds will be, but the longer the computations will take. If a particular history sequence has reached its maximum size without the Markov Property being true for some subsequence, then lower and upper bounds due to the sequence are computed.

Before explaining how the bounds are computed, we make the following observation:

- *Theorem.* If the Markov Property does not hold for any subsequence of k,j,l,F, then when f_{n-1} is at its earliest time, either all departure times within k,j,l,F are based only on same runway separations, or t_i–t_j is independent of any further history.

- *Proof.* Since the Markov Property is not true for any subsequence, the cross-runway constraints are not binding on any subsequent flights in k,j,l,F when the last two flights in any subsequence occur at their earliest times. If additional history requires that some flight f_x depart later than its unconstrained earliest time, even when f_{n-1} is at its unconstrained earliest time—and at this history-constrained earliest possible time for f_x, $t_{f_x} + \mu_X(f_{x-1}, f_x) > t_{f_{x+1}} + \mu_S(f_{x-1}, f_{x+1})$, then all departure times after f_x (including t_i, and t_j) can be determined in terms of t_{f_x}. Furthermore, in this situation, adding additional history will not change the relative times of departures after f_x. If additional history would cause f_{n-1} to be later than its earlier time, this would cause f_x to be deferred by an equal increment, as by the assumption it is the accumulated same runway constraints from f_{n-1} back to f_x that have determined t_{f_x}. A later time for f_{n-1} may also activate some other cross-runway constraint, causing f_{x+1} to occur later, but by no more than the additional delay to f_x; thus, f_x would continue to be a point from which later departure times can be computed. If there is no such f_x for the current history, k,j,l,F, this is equivalent to stating that all separations in k,j,l,F are determined by the same runway separations, μ_S, Q.E.D.

Now assume that the last flight added is not on the target runway. Then f_{n-1} is on the target runway. When f_{n-1} is at its earliest time, j is also at its earliest time. As the departure time of f_{n-1} is delayed, it may begin to delay flight j via the accumulated same runway separations. Thus, the upper bound on separation between i and j occurs when $t_{f_{n-1}} = t_{f_n} + \mu_X(f_{n-1}, f_n)$ the lower bound on $t_{f_{n-1}}$; the lower bound on separation occurs when $t_{f_{n-1}} = t_{f_n} + \max\_sep(f_{n-1}, f_n)$ and the upper bound on $t_{f_{n-1}}$.

On the other hand, if the last flight added is on the target runway, then f_{n-1} is on the other runway. As the departure of f_{n-1} increases from its earliest time, it may cause flight k to depart later. The cross-runway constraint between i and k may force i to depart later, increasing the time between the departure of i and j. (By the theorem, delaying a flight on the other runway either will not change the departure time j or will increase the departure time of i and j equally.) Thus the upper bound on separation occurs when $t_{f_{n-1}}$ is at its upper bound, and the lower bound on separation occurs when $t_{f_{n-1}}$ is at its lower bound.

MODELING CURRENT FAA PROCEDURES

Modeling current procedures requires selecting appropriate values for μ_S and μ_X. Setting $\mu_S(i,j)$ is described in the single runway model description. We examine here appropriate values for μ_X.

Departures

One rule in existing procedures requires a 2-minute departure hold on either runway of a parallel pair separated by 2,500 feet or less after the departure of a heavy jet. We initially used this 2-minute rule to establish spacing behind heavies. During reviews of preliminary results we were informed that standard practice is to use an alternate procedure that requires standard wake vortex separation distances in lieu of 2 minutes. We now use the separation distance criteria.

A further restriction when both runways of a pair are used for departures occurs when visual separation cannot be applied when a departure is 1 mile from the threshold. In this case departures on the parallel runways must be released so as to achieve a 1-mile separation. The same departure logic used in the single runway model to ensure separation along a single departure path can be used to determine the time separation that the controller will apply in this situation. That logic only needs to be modified to reflect a 1-mile departure path and 1-mile separation criterion.

When ceiling or visibility requires the latter separation criterion to be used, the μ_X value for any pair is the maximum of that required for heavy jet separation and that required for the 1-mile separation.

Arrivals

Diagonal separation between arrivals to parallel runways may need to be applied in IMC. The diagonal separation required depends on the distance between the runway centerlines and the radar available to monitor aircraft positions.

Regardless of the particulars, the diagonal separation can be converted into an equivalent separation parallel to the runways, by elementary right-triangle trigonometry. (The diagonal separation requirement is the hypotenuse; the distance between the runway centerlines is one of the shorter sides. The equivalent lateral separation is the other shorter side, which can be solved for.) Once the equivalent lateral separation is determined, the same procedures used to determine single runway controller separations to achieve a miles-in-trail goal can be applied.

Appendix C
Capacity and Delay Models

This appendix provides details about the Capacity and Delay models. Summary flowcharts are included for illustration.

CAPACITY MODELS

Each LMI capacity model consists of an airport-unique segment and pre-compiled code segments that are common to all the airport models. The pre-compiled segments are compiled as Pascal "units." There are three such units. The Standard Input Unit contains all the common "variable type" definitions and the procedure to convert input parameters from nautical miles and knots to statute miles and statute miles per minute, respectively. The Numerical Routines Unit contains a procedure for calculating cumulative probability. The Runway Unit, which requires more detailed discussion, is a large segment that contains the capacity algorithms.

Runway Unit The Runway Unit contains several procedures and functions, some of which are used by all airports (e.g., get_arv_cap) and others that are only used for certain airports (e.g., get_2d_cap).

- *procedure get_arv_cap* This procedure returns the inter-arrival times and arrival capacity for a single runway using the algorithms discussed in Appendix A. The calculations are modified based on the runway operating mode (maximum arrival or balanced) and the runway type (single, close-spaced parallel, or crossing). The procedure cycles through each of the leader follower pairs calling the appropriate procedures and functions (discussed below) to determine the hourly capacities for the all-arrival and equal arrival-departure cases. The sum of the results, weighted by the aircraft mix, gives the capacities. The mean of the inefficiency buffer is added to the inter-arrival times during the calculation of the capacity.

  - *function bf* This function in get_arv_cap calculates the probability that a departure will not fit between an arrival pair. The calculated probability is compared with a specified probability (currently fixed at 0.9) and bf returns the difference. The argument of bf is a time, x, that is added to the mean separation. As the extra time increases, the result approaches the point where a departure will fit between arrivals with the specified probability. The function bf increases the departure hold by 2 miles in IMC-2 and removes the communications delay when using intersecting runways.

- *function aad* This function in get_arv_cap calculates the equal arrival/departure capacities of the runway when operating in the alternating arrival-departure mode. The function makes repeated calls to function bf. The initial two calls add 0 and 5 minutes to the mean of the departure separation bracketing the point where a departure will fit between arrivals. A binary search routine is used to find the exact value of added time necessary.

- *procedure gainer* Procedure gainer in get_arv_cap uses the algorithms developed in Appendix A to determine miles-in-trail (MIT) and runway occupancy time (ROT) separation times for each aircraft pair when the lead aircraft is faster than the following aircraft.

- *procedure looser* Procedure gainer in get_arv_cap uses the algorithms developed in Appendix A to determine MIT and ROT separation times for each aircraft pair when the lead aircraft is slower than the following aircraft.

- *function get_dep_cap* This function returns the single runway interdeparture times and departure capacity for all aircraft leader/follower combinations using the algorithms developed in *Estimating the Effects of the Terminal Area Productivity Program*, Lee, et al., NASA Contractor Report 210682, April 1997. As with the arrival calculation, this procedure cycles through the aircraft pairs, calling the procedures below to estimate the departure capacity. The weighted results are summed to find the departure capacity.

  - *procedure dgainer* This procedure in get_dep_cap calculates the interdeparture time when the following airport is faster than the leading aircraft. The larger of the distance to the departure turn or the wake vortex separation is applied in this procedure.

  - *procedure dlooser* This procedure in get_dep_cap calculates the interdeparture time when the following aircraft is slower than the leading aircraft.

  - *procedure dequal* This procedure in get_dep_cap is called when climbout speeds are equal. The procedure calls both dgainer and dlooser and sets the interdeparture time to the longer of the two cases.

The following procedures are for closely spaced parallel runways, and are not used by the JFK capacity model. They are located in the Runway Unit and are included here for completeness:

- *procedure xseparate* This procedure calculates the minimum interdeparture times for aircraft on closely spaced parallel runways. The mini-

mum cross-runway departure distance is 1 nautical mile or the wake vortex minimum. The result is a set of nonweighted values for each pair. The xseparate procedure is called by get_2d_cap.

- *procedure get_2d_cap* This procedure returns the nonweighted individual pair interdeparture times and the weighted upper and lower bounds on interdeparture times for aircraft on closely spaced parallel runways (i.e., dependent operation). When either the Markov Property or the Parallelogram Property described in Appendix B is true, the history of prior flights is irrelevant and the separations can be calculated explicitly. In cases where the properties are not true, the result is dependent on the history of prior departures, and it is possible to calculate upper and lower bounds to the interdeparture times. The standard value used for prior history is 4, but the capability is included for larger values of prior history. The procedure can accommodate different aircraft mixes on the two runways. For all cases, upper and lower bounds are returned. Where history is irrelevant, those bounds are equal. The "main" section of the capacity model divides the upper and lower bounds individually into 60, averages the result, and multiplies by 2 to get the dependent departure capacity for the parallel pair. The development of the closely spaced parallel runway algorithms is described in Appendix B.

  Procedure get_2d_cap uses both the minimum interdeparture times calculated in get_dep_cap and the cross-runway interdeparture times calculated in xseparate.

  - *function triangle* This is a Boolean function in get_2d_cap that evaluates the Markov property. (The *parallelogram* property is calculated in the body of get_2d_cap.)

  - *function eval_history* This procedure in get_2d_cap calculates the upper and lower bounds of the interdeparture times in closed form for a prior history of 4.

  - *procedure bound* This procedure in get_2d_cap calculates the upper and lower bounds of the interdeparture times for prior histories greater than 4 using a recursion routine.

- *function adjust_for_crossing* This procedure reduces the departure rate to allow arrival aircraft to cross the inboard departure runway. It was originally written for DFW, and is also used for other airports. Usually, the taxiways are cleared when a heavy aircraft lands and a large interdeparture gap is required. This procedure takes effect when there are not enough heavies in the mix to provide the necessary gaps.

- *function compute_free* This procedure calculates the number of departures that can be accommodated when operating at maximum arrival capacity. If the meteorological condition is IMC-2 or worse, no departures are allowed once the arrival is within 2 nautical miles of the threshold. For intersecting runways, a 2-minute departure hold is applied after a heavy or B757 arrival.

The final procedure/function discussed is contained in the body of the JFK capacity model and is unique to that model.

- *function get_rate_31L* When the parallel 31 runways are used, 31R is used exclusively for turboprop departures, while 31L is used for departures of all classes including turboprops. This procedure calculates the fraction of turboprops that will use 31L to keep the departure rates balanced for the two runways. This procedure is a good example of the airport-unique procedures that have been developed to deal with airport idiosyncrasies.

A semidetailed flowchart for the JFK model illustrates the basic model operation. Separate flowcharts are included for the principal runway unit procedures and functions. Procedure get_2d_cap is included for information even though is not used for JFK capacity. Note: The capacity models execute in 1 to 3 seconds on a 166 MHz Pentium PC.

Figure C-1. JFK Capacity Model (Page 1 of 3)

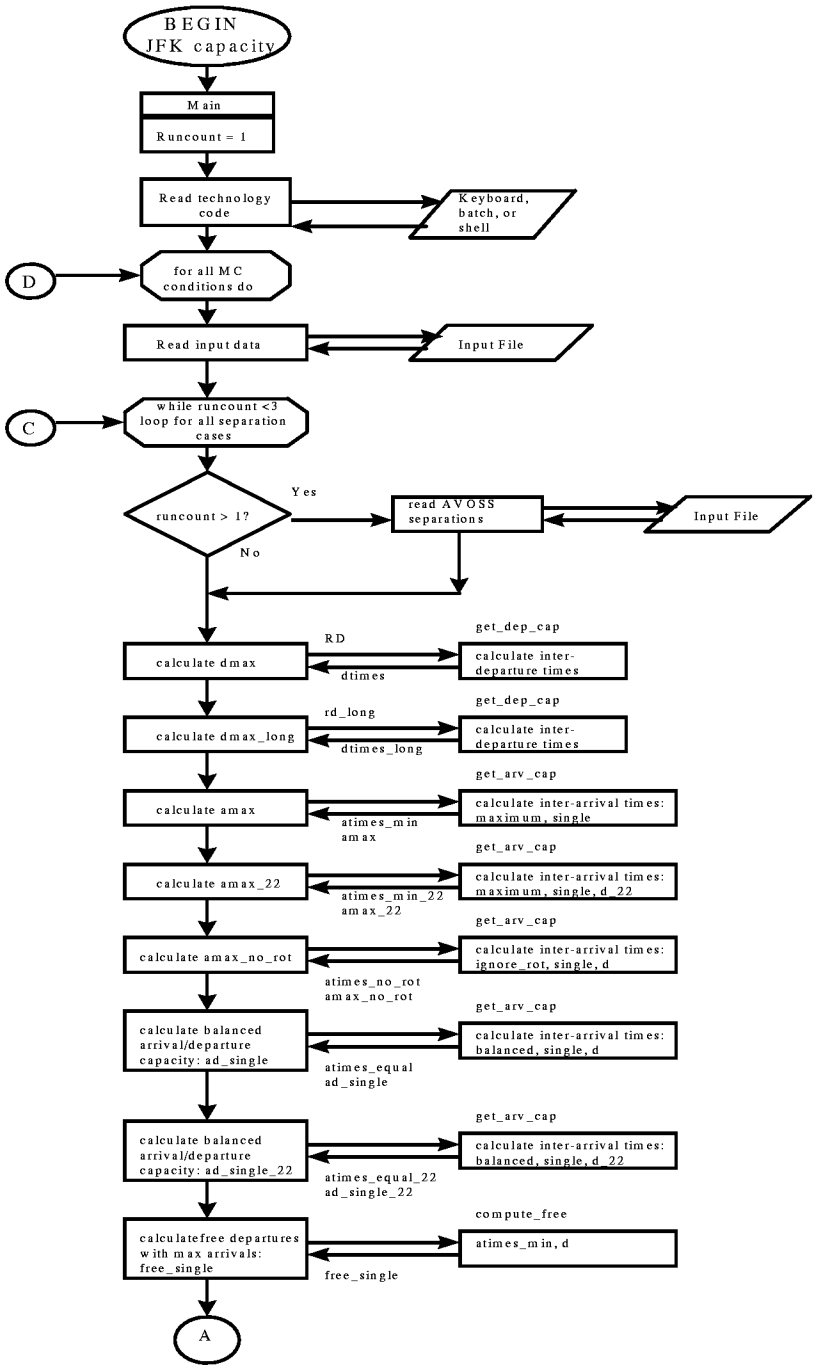

Figure C-1. JFK Capacity Model (Page 2 of 3) (Continued)

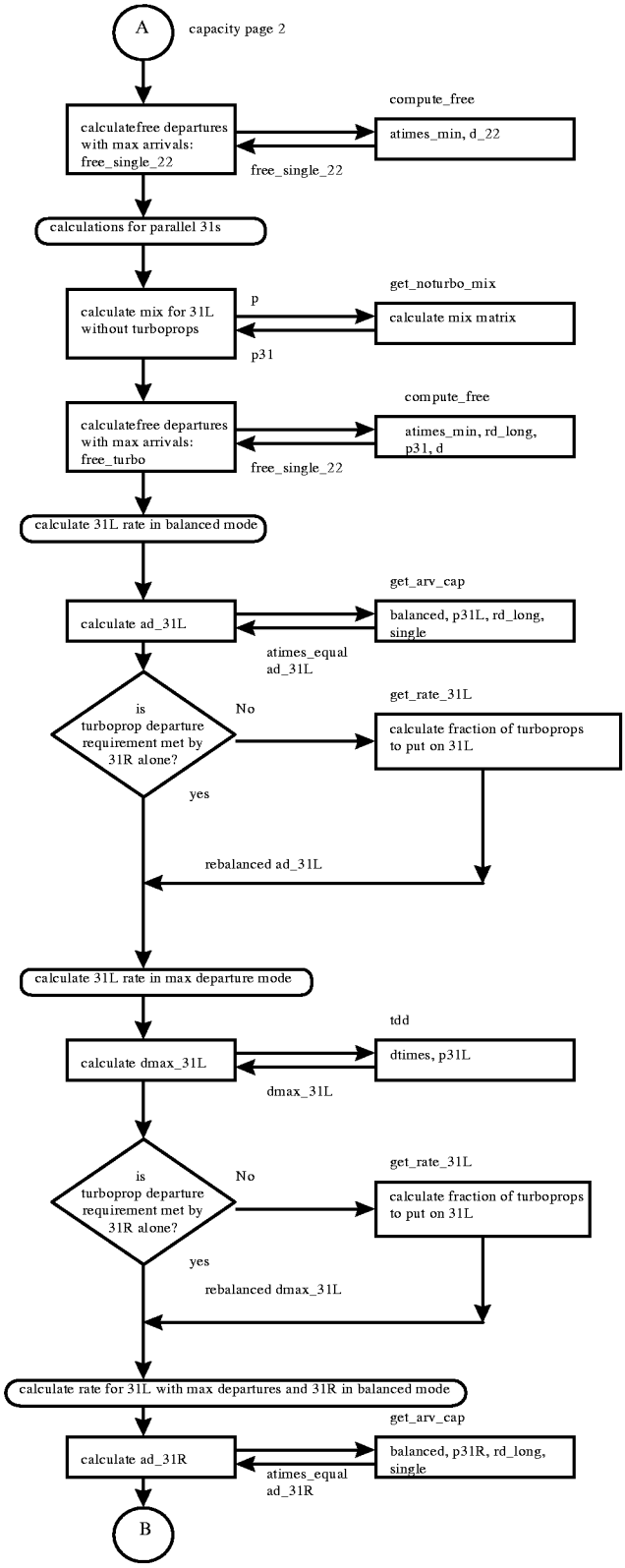

Figure C-1. JFK Capacity Model (Page 3 of 3) (Continued)

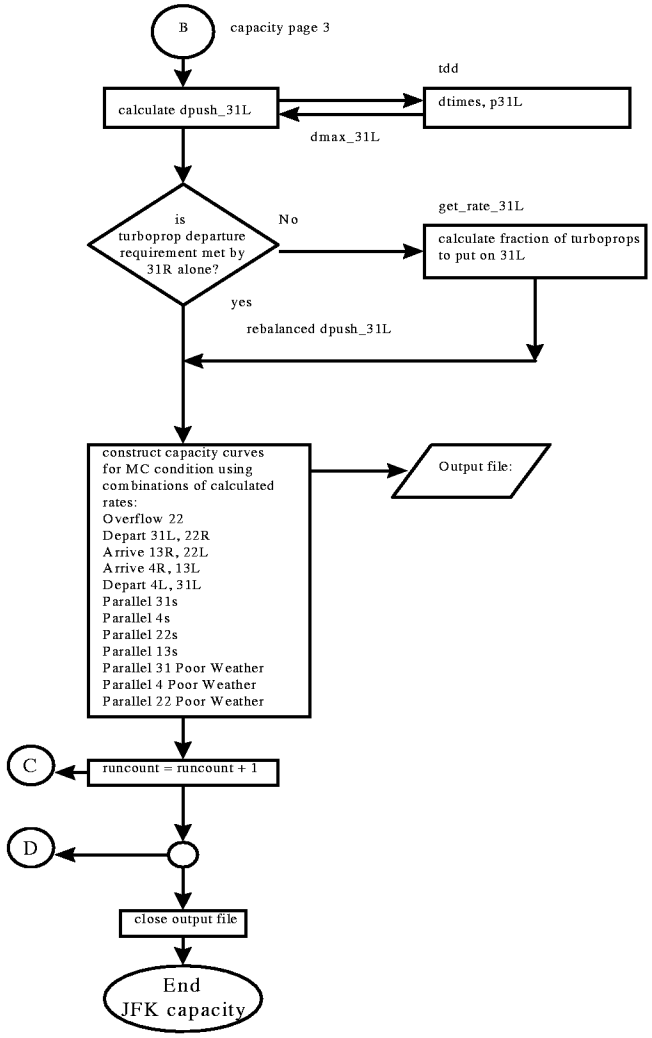

Figure C-2. Procedure get_rate_31L from JFK Capacity Model

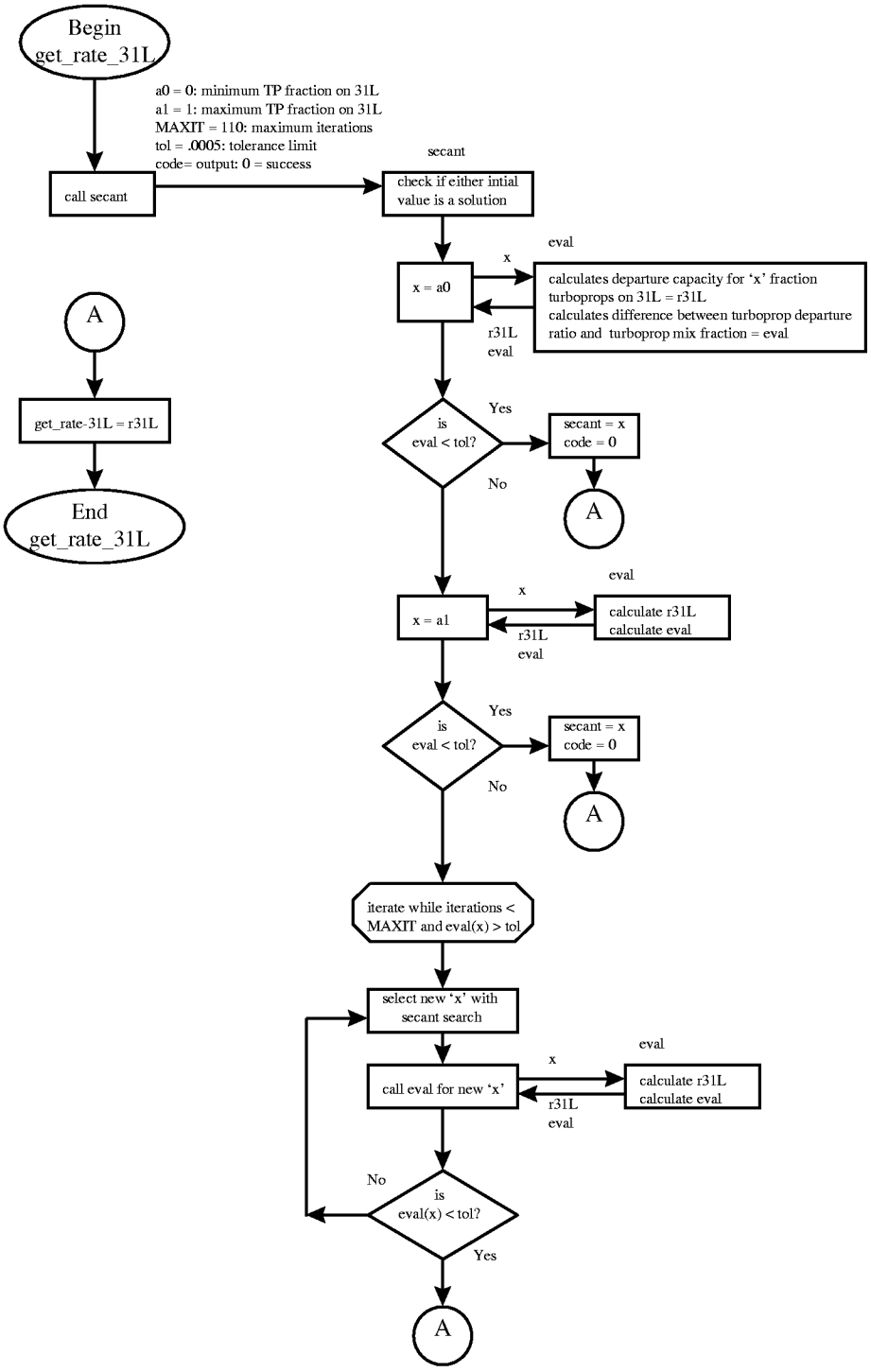

Figure C-3. Procedure get_dep_cap from Runway Unit

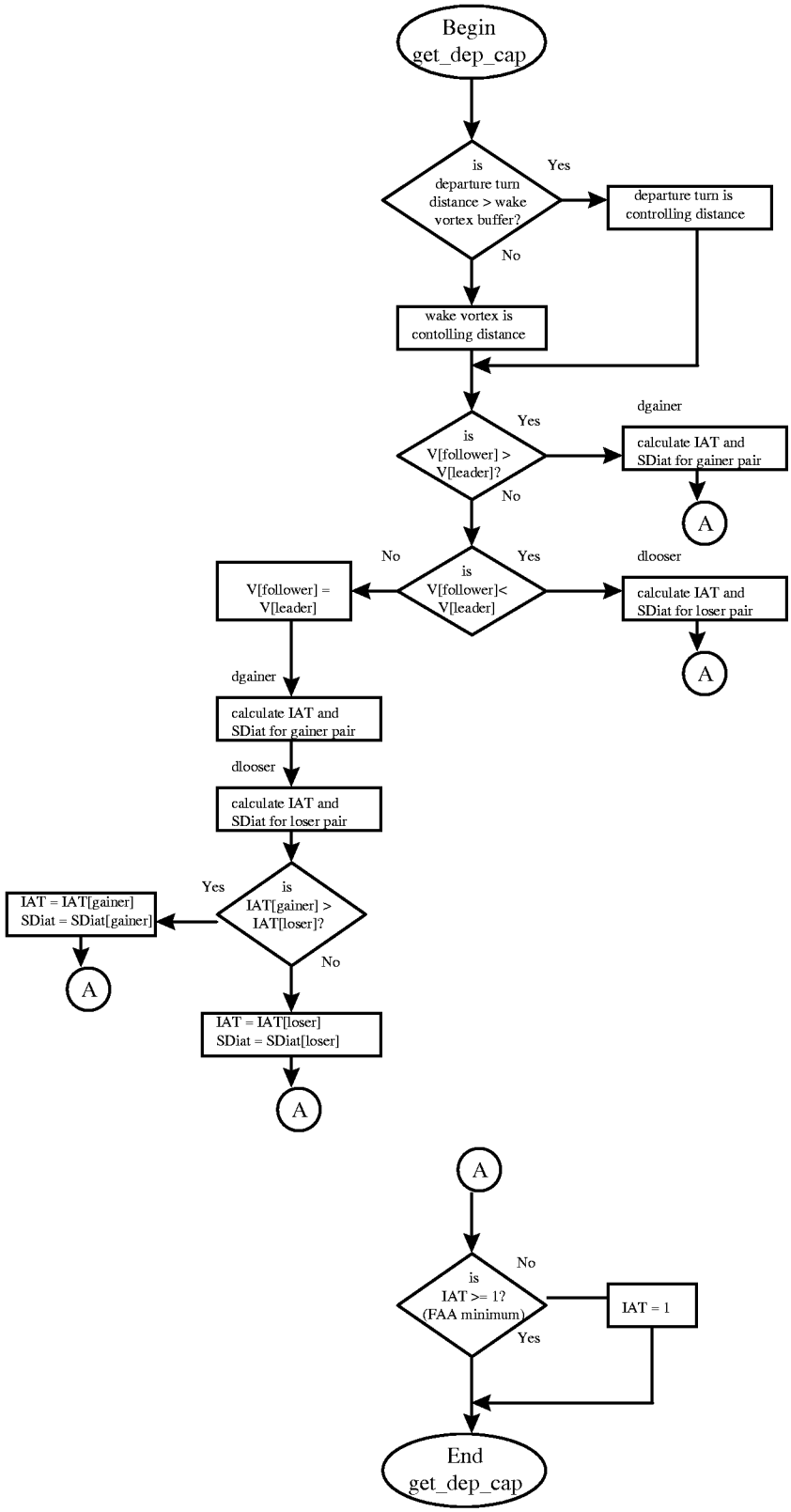

Figure C-4. Procedure get_arv_cap from Runway Unit

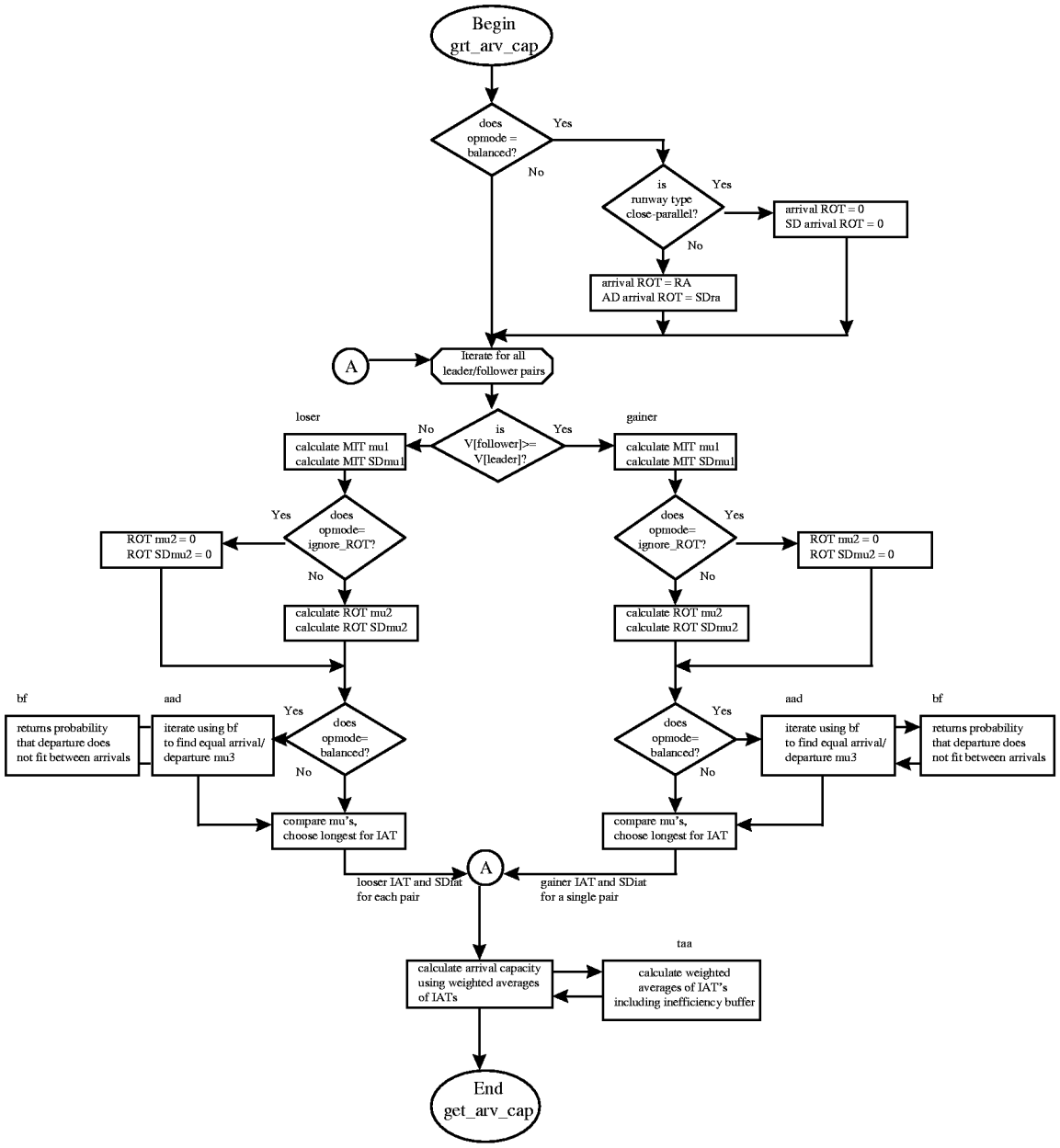

Figure 3-5 Procedure get_2d_cap for Runway Unit (not used for JFK)

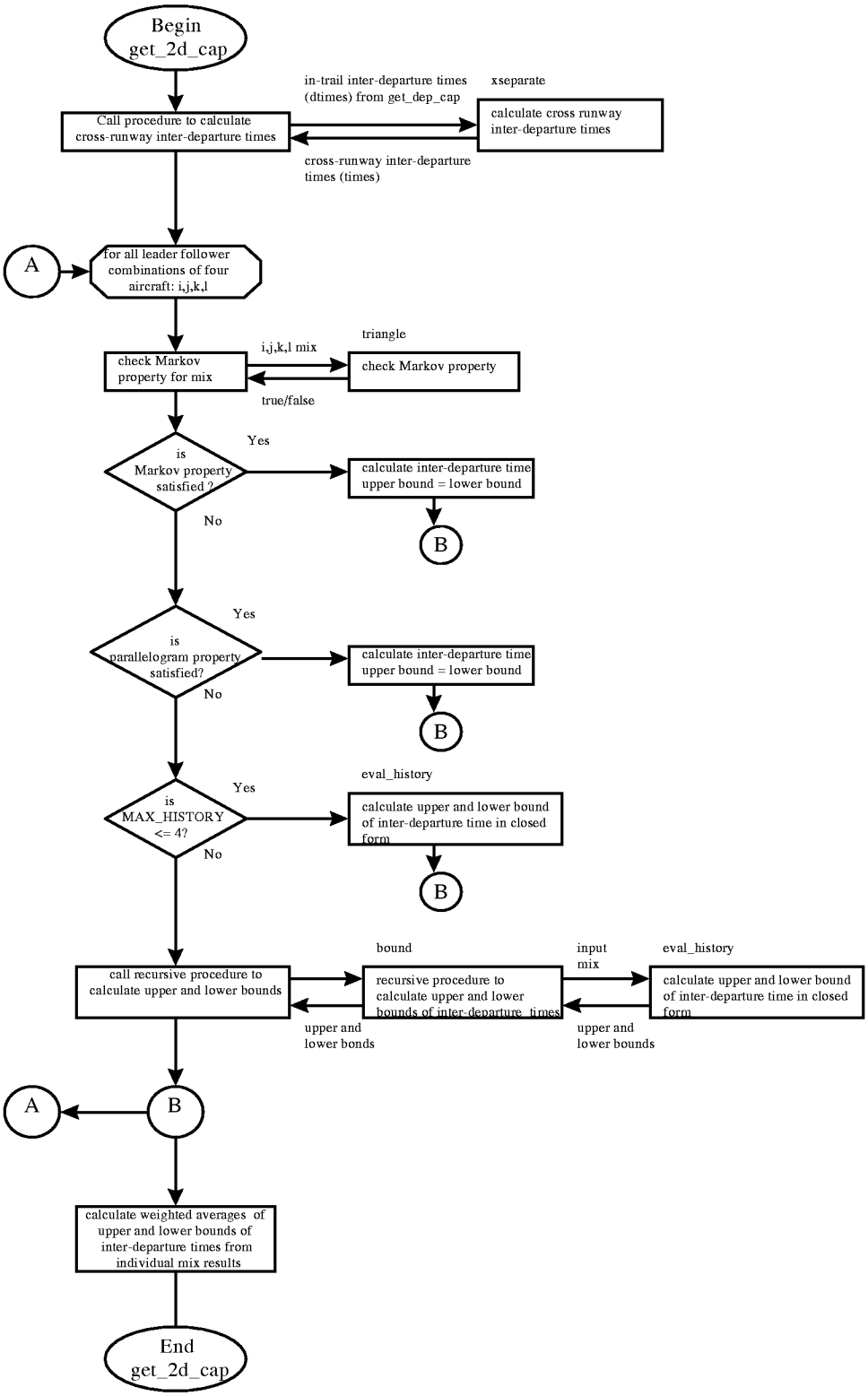

DELAY MODELS

The delay models have airport-unique algorithms and structures that have been developed during the course of their development. The models do have several procedures in common. In the future, the common procedures could be extracted, standardized, and compiled as Pascal units.

The typical delay model steps through the operating hours of the airport hour-by-hour, day-by-day so long as there are weather data available. For each hour the arrival and departure demands, plus any residual demands from the previous hour, are compared to decide whether to optimize the current hour for departures or arrivals. The airport runway configurations are tested to find the configuration having the maximum arrival (or departure) capacity while also meeting minimum ceiling, visibility, and wind criteria. The capacity and demand data are used by the queuing procedure to calculate each hour's delay and any residual demand. Both annual and total delay results are calculated and output.

The following are the procedures and functions used in the JFK delay model. They are typical of those found in the latest airports to be modeled.

- *procedure RO* This procedure contains the queuing engine and is common to all the models. The input includes the hour's demand, the hour's capacity, and the existing queue. The procedure returns the hour's delay, the variance of the delay, and the size of the residual queue. The procedure is called separately for arrivals and departures. Several queuing engines have been used over the past two years. The queuing engine in all the current models solves the differential equations for a nonstationary M/M/1 queue using the closure hypothesis reported in *A Closure Approximation for the Nonstationary M/M/s Queue*, M. H. Rothkopf and S. S. Oren, *Management Science*, Vol. 25, No. 6, June 1979.[1]

  - *function PO* This procedure calculates the closure condition for the solution of the differential equations.

  - *procedure Step* This procedure numerically integrates the differential equations using the closure condition.

- *function get_max* This procedure returns either maximum departure or maximum arrival capacity for an input capacity curve.

- *procedure get_capacity_curves* This procedure opens the input capacity file, reads the capacity curve (.cap) file, and closes the input file.

[1] M/M/1 defines a queue with a Poisson distributed arrival rate, a Poisson distributed service rate, and a single server.

- ➤ *function read_curve* Using pointer variables, this procedure dynamically adjusts to read the number of points specified in the input file.

- ◆ *procedure get_cap* This procedure returns the arrival and departure capacity from the selected curve based on the departure-to-arrival demand ratio.

- ◆ *procedure compute_rwy_winds* This procedure calculates cross- and tailwinds for usable runway identification.

- ◆ *procedure get_wx* This procedure reads an hour's data from the weather file and determines the airport meteorological operating condition (IMC-1, etc.) from the ceiling and visibility.

- ◆ *procedure do_a_day* This procedure controls the analysis of single day of operation. For each hour of the day, the procedure reads the current hour's demand, finds legal (usable) configurations, chooses the highest capacity usable configuration (subject to practical constraints), calls the VAS check, and finally, calls the queuing engine.

  - ➤ *function find_legal* This function determines whether a configuration is legal based on ceiling and visibility minimums.

  - ➤ *function GoodVAS* This function determines if the winds for all the arrival runways in the input configuration meet the VAS wind ellipse criteria.

  - ➤ *function ok_winds* This function checks that the cross- and tailwinds of all the runways in the input configuration are within legal limits.

  - ➤ *function find_usable* This function cycles through the runway configurations and counts up the number of usable configurations based on ceiling, visibility, and wind results.

  - ➤ *function minmax_cw* This function cycles through the configurations and finds the usable runway with the "least bad" crosswind.

  - ➤ *function max_cap_usable* This function returns the highest capacity configuration with crosswind no worse than "worst usable" configuration.

Main The main section of the model performs the following tasks:

- ◆ Initializes variables

- ◆ Opens the input and output files

- Reads technology scenario and demand-year command line inputs
- Calculates the appropriate hourly demand using the demand factor corresponding to the demand year to scale the input demand profile
- Calls get_capacity_curves to read in the capacity data
- Calls do_a_day for each day in the weather data file to calculate arrival and departure delays
- Calculates annual delays whenever the weather data changes to a new year
- Calculates totals and averages when the weather data are exhausted.
- Sends results to output files
- Closes the input and output files.

The following utility output routines are called by main only in the batch version of the model:

- *procedure print_curves* This procedure writes the input capacity curves to the individual case output file.
- *procedure print_demand* This procedure writes the input demand data to the individual case output file.
- *procedure WXstat* This procedure calculates weather statistics and writes them to the individual case output file.
- *procedure summary_output* This procedure writes (appends) average delays to an output file that stores the accumulated summary results of all the cases being run.

A semidetailed flowchart of the JFK Delay Model is included below to illustrate the basic flow of the analysis.

The delay models typically are run using 35 years of weather data to develop meaningful average results. All the models except Boston complete one technology/demand year case (e.g., PFAST with AVOSS in 2015) in about two minutes on a 166 MHz Pentium PC. Boston takes twice as long. A full set of 19 technologies for 1 demand year takes somewhat less than 1 hour per airport, and a complete analysis of the 10 airports, including Boston, for 2 demand years and 19 technologies takes about 16 hours.

The ability to identify weather and demand by time and date allows unprecedented in-depth analysis of airport operations (e.g., seasonal issues, effects of operating hours, and demand leveling). The capacity and delay models can also accommo-

date additions of new runway capacity or analysis of operation modes such as AILS independent runway operation. These capabilities have barely been tapped in the current effort.

Figure C-5. JFK Delay Model (Page 1 of 2)

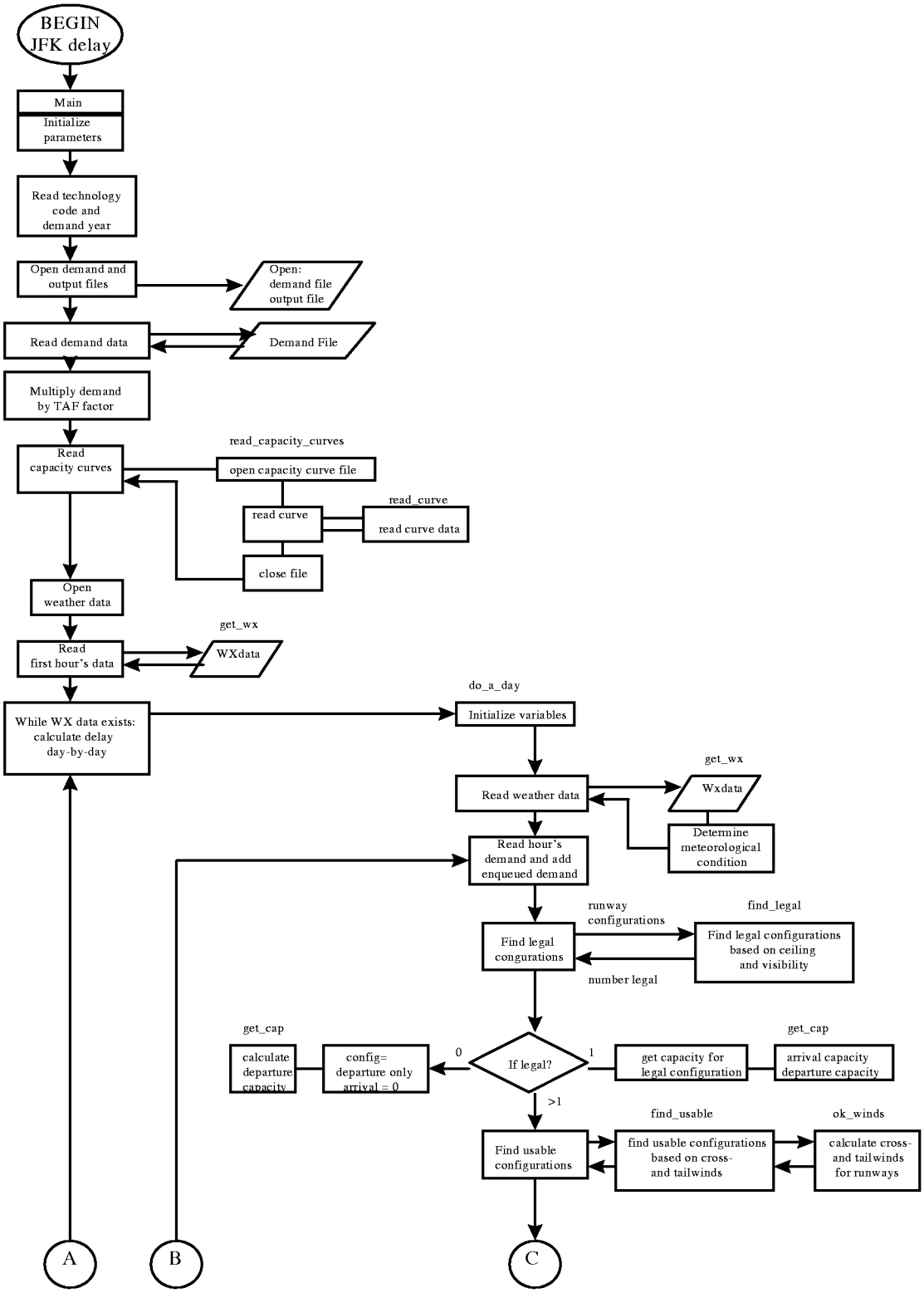

Figure C-6. JFK Delay Model (Page 2 of 2) (Continued)

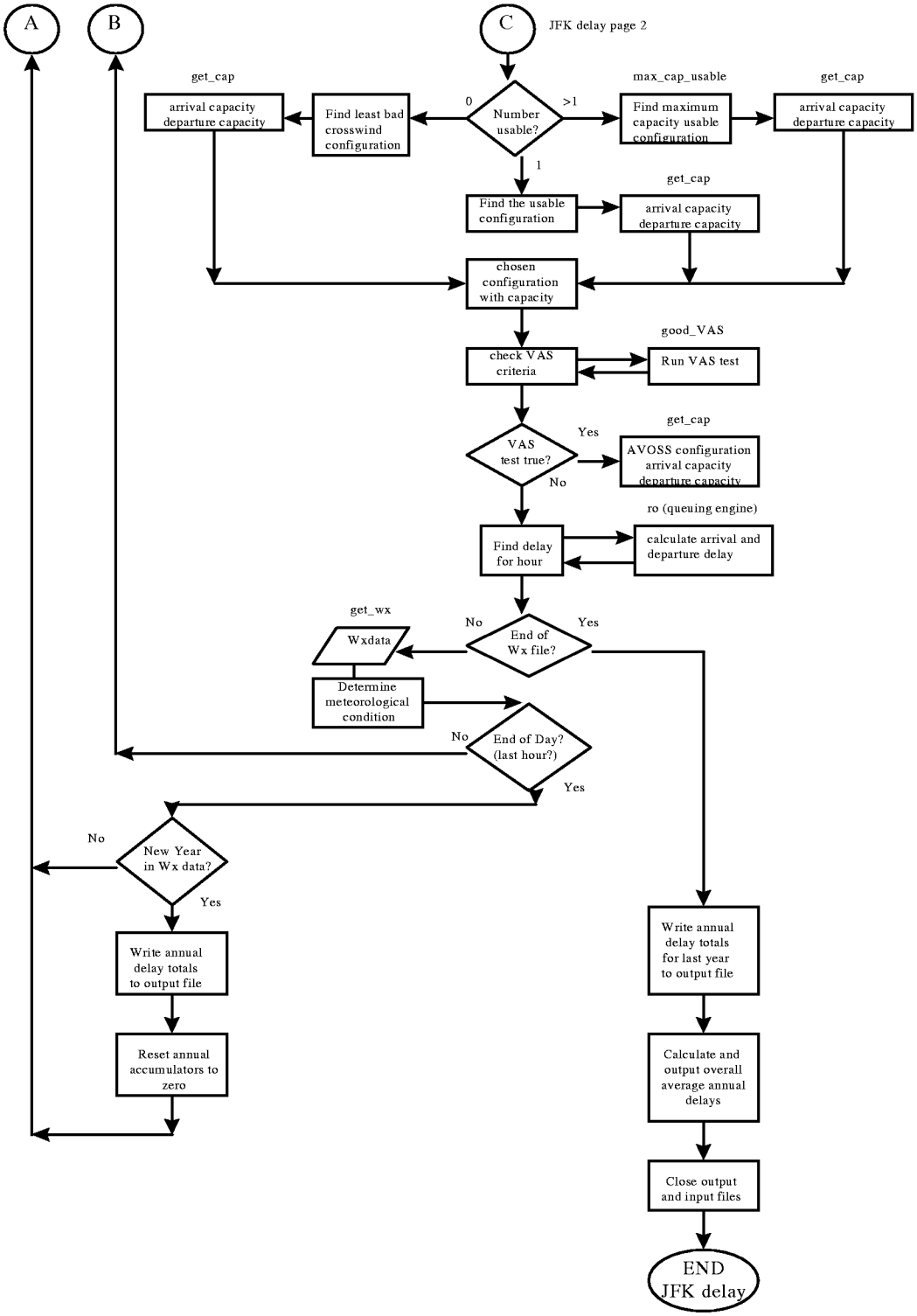

Appendix D
TAP Run-Time Shell User's Guide

MINIMUM SYSTEM REQUIREMENTS

The following minimum system requirements are necessary for using the TAP Run-Time Shell:

- IBM-compatible personal computer with a CD-ROM drive
- Windows 95
- Microsoft Access 7.0 32-bit Open Database Connectivity (ODBC) drivers
- ODBC32 User Data Source Name for "MS Access 7.0 Database" (see the *ODBC Driver* section at the end of this guide for more discussion of ODBC driver installation).

CONTENTS OF DISTRIBUTION CD

The distribution CD includes the following folder and file organization:

Table D-1. Contents of Distribution CD

File	Description
Lmishell directory	
Lmishell\tapshell.exe	TAP Run-Time Shell (executable)
Lmishell\tapshell.ini	TAP Run-Time Shell initialization file
Lmishell\tapshell.mdb	TAP Run-Time Shell Access database
Lmishell\Atlcaps.exe	ATL Airport Capacity Model (executable)
Lmishell\Atldlys.exe	ATL Airport Delay Model (executable)
Lmishell\Boscaps.exe	BOS Airport Capacity Model (executable)
Lmishell\Bosdlys.exe	BOS Airport Delay Model (executable)
Lmishell\Dfwcaps.exe	DFW Airport Capacity Model (executable)
Lmishell\Dfwdlys.exe	DFW Airport Delay Model (executable)
Lmishell\Dtwcaps.exe	DTW Airport Capacity Model (executable)
Lmishell\Dtwdlys.exe	DTW Airport Delay Model (executable)
Lmishell\Ewrcaps.exe	EWR Airport Capacity Model (executable)
Lmishell\Ewrdlys.exe	EWR Airport Delay Model (executable)
Lmishell\Jfkcaps.exe	JFK Airport Capacity Model (executable)
Lmishell\Jfkdlys.exe	JFK Airport Delay Model (executable)

Table D-1. Contents of Distribution CD (continued)

File	Description
Lmishell\Laxcaps.exe	LAX Airport Capacity Model (executable)
Lmishell\Laxdlys.exe	LAX Airport Delay Model (executable)
Lmishell\Lgacaps.exe	LGA Airport Capacity Model (executable)
Lmishell\Lgadlys.exe	LGA Airport Delay Model (executable)
Lmishell\Ordcaps.exe	ORD Airport Capacity Model (executable)
Lmishell\Orddlys.exe	ORD Airport Delay Model (executable)
Lmishell\Sfocaps.exe	SFO Airport Capacity Model (executable)
Lmishell\Sfodlys.exe	SFO Airport Delay Model (executable)
Imitap directory	
Imitap\atl\inputs*.in	ATL Airport Capacity Model input files
Imitap\atl\models\1993dmd.txt	ATL Airport Delay Model demand data input file
Imitap\atl\models\Atlcaps.pif	Shortcut to ATL Airport Capacity Model
Imitap\atl\models\Atldlys.pif	Shortcut to ATL Airport Delay Model
Imitap\bos\inputs*.in	BOS Airport Capacity Model input files
Imitap\bos\models\1993dmd.txt	BOS Airport Delay Model demand data input file
Imitap\bos\models\Boscaps.pif	Shortcut to BOS Airport Capacity Model
Imitap\bos\models\Bosdlys.pif	Shortcut to BOS Airport Delay Model
Imitap\dfw\inputs*.in	DFW Airport Capacity Model input files
Imitap\dfw\models\1993dmd.txt	DFW Airport Delay Model demand data input file
Imitap\dfw\models\Dfwcaps.pif	Shortcut to DFW Airport Capacity Model
Imitap\dfw\models\Dfwdlys.pif	Shortcut to DFW Airport Delay Model
Imitap\dtw\inputs*.in	DTW Airport Capacity Model input files
Imitap\dtw\models\1993dmd.txt	DTW Airport Delay Model demand data input file
Imitap\dtw\models\Dtwcaps.pif	Shortcut to DTW Airport Capacity Model
Imitap\dtw\models\Dtwdlys.pif	Shortcut to DTW Airport Delay Model
Imitap\ewr\inputs*.in	EWR Airport Capacity Model input files
Imitap\ewr\models\1993dmd.txt	EWR Airport Delay Model demand data input file
Imitap\ewr\models\Ewrcaps.pif	Shortcut to EWR Airport Capacity Model
Imitap\ewr\models\Ewrdlys.pif	Shortcut to EWR Airport Delay Model
Imitap\jfk\inputs*.in	JFK Airport Capacity Model input files
Imitap\jfk\models\1993dmd.txt	JFK Airport Delay Model demand data input file
Imitap\jfk\models\Jfkcaps.pif	Shortcut to JFK Airport Capacity Model
Imitap\jfk\models\Jfkdlys.pif	Shortcut to JFK Airport Delay Model
Imitap\lax\inputs*.in	LAX Airport Capacity Model input files
Imitap\lax\models\1993dmd.txt	LAX Airport Delay Model demand data input file
Imitap\lax\models\Laxcaps.pif	Shortcut to LAX Airport Capacity Model
Imitap\lax\models\Laxdlys.pif	Shortcut to LAX Airport Delay Model
Imitap\lga\inputs*.in	LGA Airport Capacity Model input files
Imitap\lga\models\1993dmd.txt	LGA Airport Delay Model demand data input file
Imitap\lga\models\Lgacaps.pif	Shortcut to LGA Airport Capacity Model
Imitap\lga\models\Lgadlys.pif	Shortcut to LGA Airport Delay Model
Imitap\ord\inputs*.in	ORD Airport Capacity Model input files

Table D-1. Contents of Distribution CD (continued)

File	Description
lmitap\ord\models\1993dmd.txt	ORD Airport Delay Model demand data input file
lmitap\ord\models\Ordcaps.pif	Shortcut to ORD Airport Capacity Model
lmitap\ord\models\Orddlys.pif	Shortcut to ORD Airport Delay Model
lmitap\sfo\inputs*.in	SFO Airport Capacity Model input files
lmitap\sfo\models\1993dmd.txt	SFO Airport Delay Model demand data input file
lmitap\sfo\models\Sfocaps.pif	Shortcut to SFO Airport Capacity Model
lmitap\sfo\models\Sfodlys.pif	Shortcut to SFO Airport Delay Model
Lmitapwx directory	
Lmitapwx*.dat	Airport Delay Model 35 year weather data input files

INSTALLATION

Two steps are necessary to install the Run-Time Shell, one step is optional.

STEP 1: COPY THE LMISHELL\TAPSHELL.INI FILE FROM THE DISTRIBUTION CD TO THE WINDOWS 95 DIRECTORY ON THE C: DRIVE (NORMALLY WINDOWS 95 IS LOCATED IN C:\WINDOWS)

The file lmishell\tapshell.ini is the Run-Time Shell initialization file. The initialization file is the only file on the distribution CD that *must* be copied to the computer's hard drive. That file, shown in Figure D-1, tells Windows where to find the Access database file used by the Run-Time Shell (i.e., lmishell\tapshell.mdb).

STEP 2: (OPTIONAL): COPY SOME OR ALL OF THE FILES FROM THE DISTRIBUTION CD TO THE HARD DRIVE.

Any or all of the files on the distribution CD can be copied to a hard drive.

IMPORTANT: *The folder structure on hard drive must be identical to that on the CD. Also, if the Run-Time Shell Executable file (tapshell.exe) is copied to a hard drive, then all of the Airport Capacity Model executable files and all of the Airport Delay Model executable files must also be copied to the same hard drive.*

STEP 3: EDIT THE LMISHELL\TAPSHELL.INI FILE TO IDENTIFY THE LOCATION OF THE ACCESS DATABASE FILE (\LMISHELL\TAPSHELL.MDB).

The Run-Time Shell files, including the Access database file, can be left on the CD and executed, or they can be copied and executed from the hard drive (see Step 2). In either case, the initialization file located in the Windows directory (see Step 1 and Figure D-1) needs to point to the correct drive location of the Run-Time Shell Access database file, \LMISHELL\tapshell.mdb. For example, if you are using the Run-Time Shell Access database located on the distribution CD and the CD-ROM on your computer is drive d:, then the text "DBQ=c:\LMISHELL\tapshell.mdb" in the initialization file must be changed to "DBQ=d:\LMISHELL\tapshell.mdb".

Figure D-1. Run-Time Shell Initialization File

```
[Default]
Database=DSN=MS Access 7.0 Database;DBQ=c:\LMISHELL\tapshell.mdb
```

RUN-TIME SHELL MAIN WINDOW OVERVIEW

This section provides an overview of model operation. Following sections discuss model operation in detail. The model can be started from Windows Explorer, My Computer, or the Run command. In all cases, locate the LMISHELL\tapshell.exe file (the file with the LMI logo icon) on the appropriate drive and double click the icon. When the Run-Time Shell is executed, the main window displays as shown in Figure D-2.

Note: To exit the Run-Time Shell, either click the **[Exit]** button or choose the **File / Exit** menu item.

Figure D-2. Run-Time Shell Main Window

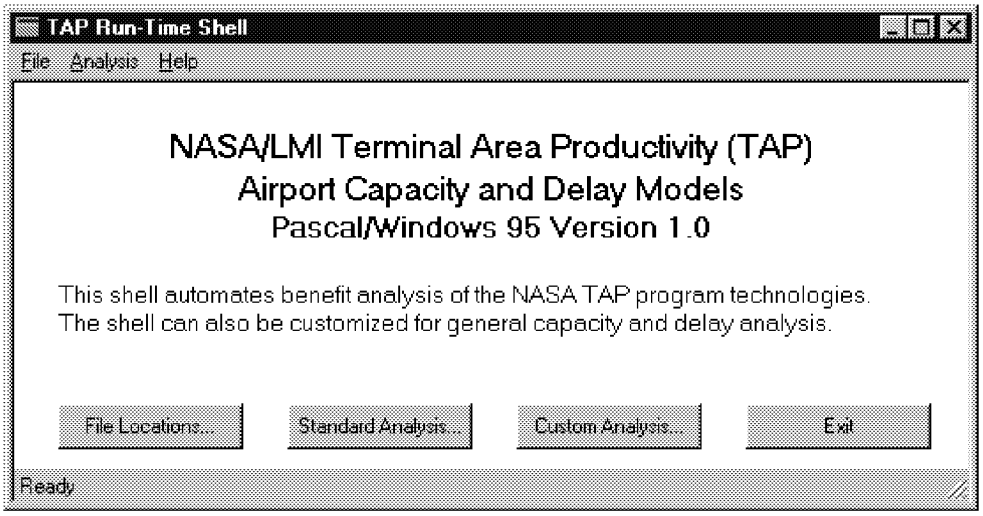

Note: To display the version number and copyright information about the Run-Time Shell, choose the **Help / About TAP Shell** from the menu bar. The **TAP Run-Time Shell** dialog displays as shown in Figure D-3.

Figure D-3. About TAP Run-Time Shell Dialog

SPECIFYING FILE LOCATIONS

Selecting the Drives

When the Run-Time Shell is executed for the first time, the file location drives must be specified for the four file categories. This step is required for two reasons. CD-ROM devices have various drive designations (e.g., d: or f:). File location selections enable the shell files to be located on other drives (e.g., c:).

To specify the file location drives, either click on the **[File Locations]** button, choose **File / File Locations** on the menu bar, or press the **F2** key.

The **"File Locations"** dialog displays as shown in Figure D-4.

Figure D-4. File Locations Dialog

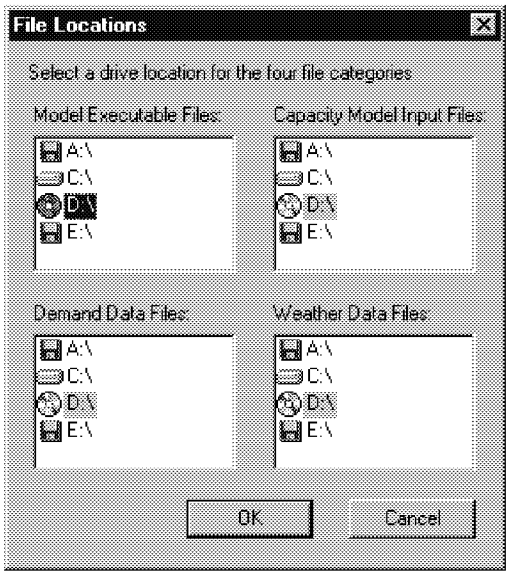

The first time the Run-Time Shell is executed on a computer, the drive location for each of the four file categories defaults to the computer's CD-ROM drive. If you have copied the files of a particular category from the CD to a different drive, such as a hard drive or a network drive, you must specify the new drive location for the file category. To select the different drive location for a particular category, simply click on the desired drive in the category's list box. To save the changes, click the **[OK]** button. If there are no changes or you do not wish to save the changes, click the **[Cancel]** button.

IMPORTANT: The *first* time the **"File Locations"** dialog is used, you *must* click the **[OK]** button to save the selections, even if no changes are made to the default selections.

The file location drive settings are saved between executions of the Run-Time Shell. New settings only need to be specified if the input data files are moved to a different drive.

Additional Information about the Files

The Airport Capacity and Delay model executable files are DOS based programs. They are accessed by the Run-Time Shell through "Shortcuts" to the Airport Capacity Model files and "Shortcuts" to the Airport Delay Model files. These files all have the extension .pif. As shown in Table D-1, these files reside in the folders lmitap\atl\models, lmitap\bos\models, lmitap\dfw\models, lmitap\dtw\models, lmitap\ewr\models, lmitap\jfk\models, lmitap\lax\models, lmitap\lga\models, lmitap\ord\models, and lmitap\sfo\models.

The capacity model input files all have the extension .in. They reside in the folders lmitap\atl\inputs, lmitap\bos\inputs, lmitap\dfw\inputs, lmitap\dtw\inputs, lmitap\ewr\inputs, lmitap\jfk\inputs, lmitap\lax\inputs, lmitap\lga\inputs, lmitap\ord\inputs, and lmitap\sfo\inputs.

The demand data files are input data files for the Airport Delay Models. The demand data files for the airports all have the same name, 1993dmd.txt. These files are located in the folders lmitap\atl\models, lmitap\bos\models, lmitap\dfw\models, lmitap\dtw\models, lmitap\ewr\models, lmitap\jfk\models, lmitap\lax\models, lmitap\lga\models, lmitap\ord\models, and lmitap\sfo\models.

The weather data files also are input data files for the Airport Delay Models. These files all have the extension .dat and are located in the folder Lmitapwx.

PERFORMING STANDARD ANALYSIS

To perform a standard technology analysis, either click the **[Standard Analysis]** button, choose the **Analysis / Standard** menu item, or press the **F3** key. The **"Standard Technology Analysis"** dialog is displayed. See Figures D-5 and D-6.

Figure D-5. Standard Technology Analysis Dialog—Capacity Only Option Selected

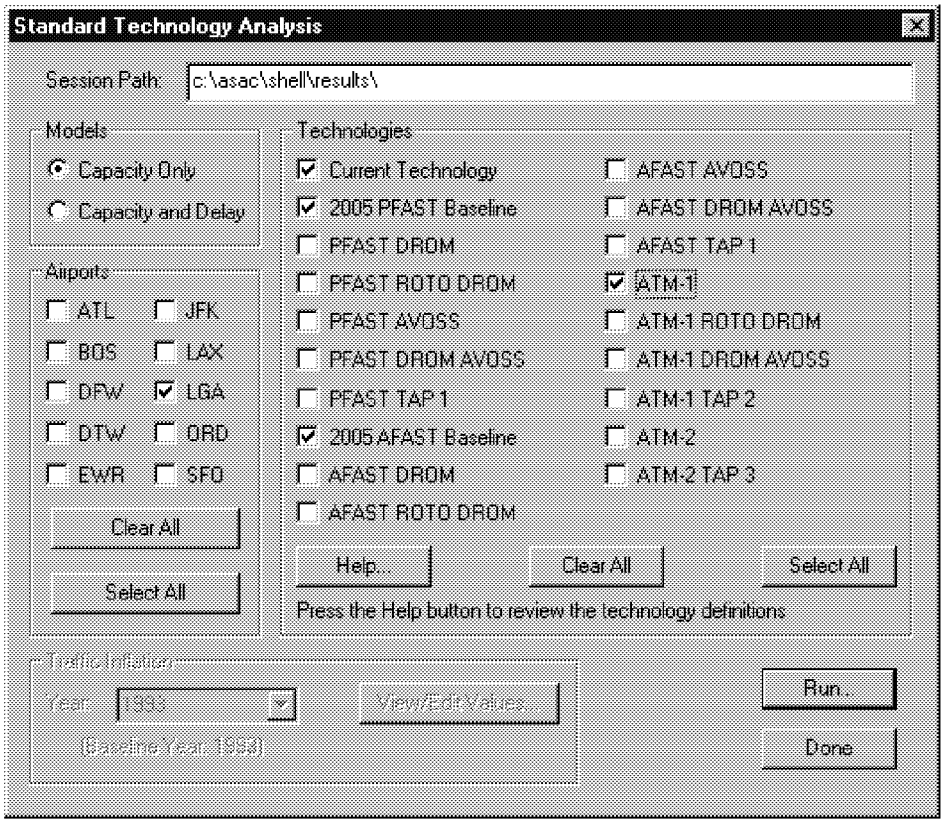

Figure D-6. Standard Technology Analysis Dialog—Capacity and Delay Option Selected

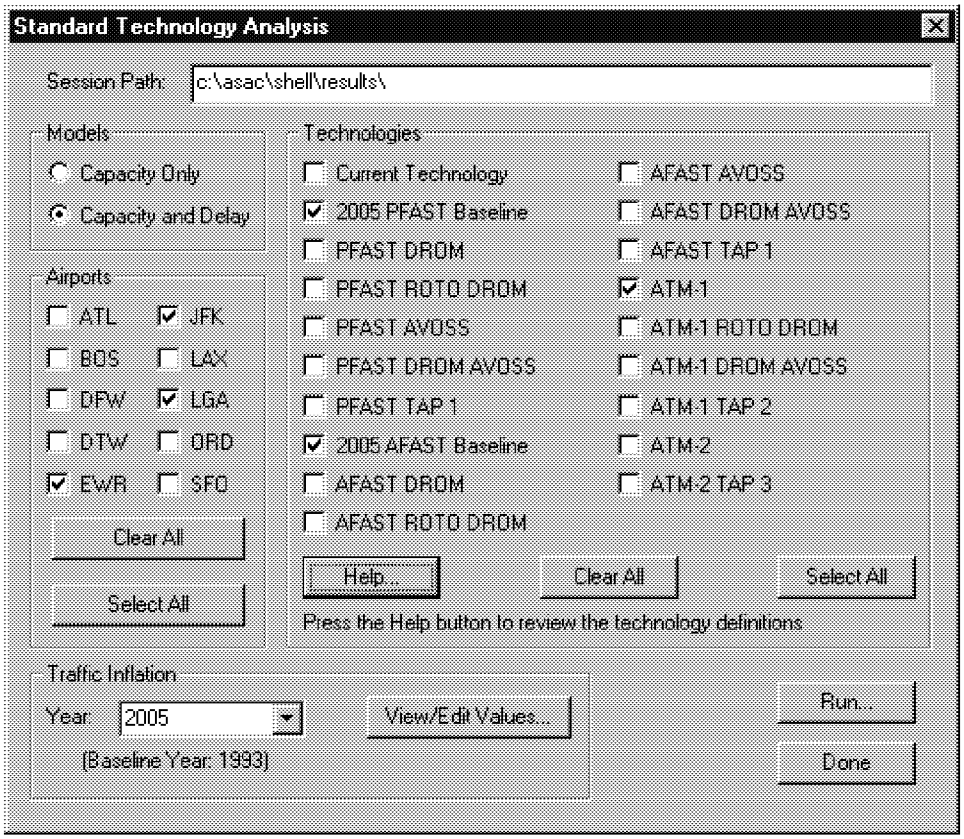

To run a standard technology analysis, complete the following steps:

- Type the full path name of a folder that exists on your computer in the **Session Path** edit field (e.g., c:\TAP_runs\set1\)

  Note: The Session Path specifies the location where the output files generated by the Airport Capacity and Airport Delay Models are placed. Since the Airport Capacity and Airport Delay Models are DOS-based applications, *the name of each subfolder in the session path can be a maximum of eight characters long.*.

- Under **Models,** select the [**Capacity Only**] option button if the analysis is to run only the Airport Capacity Models and not the Airport Delay Models. To run both the Airport Capacity and Airport Delay Models, select the [**Capacity and Delay**] option button.

- Under **Airports**, select one or more airports by clicking the appropriate checkboxes. To select all the airports, click the [**Select All**] button within the **Airports** group. To deselect all of the airports, click the [**Clear All**] button within the **Airports** group.

- Under **Technologies**, select one or more technologies by clicking the appropriate checkboxes. To select all of the technologies, click the [**Select All**] button within

the **Technologies** group. To deselect all of the technologies, click the [**Clear All**] button within the **Technologies** group.

Note: To review the technology definitions, click the [**Help**] button. The **"Technology Help"** dialog is displayed as shown in Figure D-7.

Figure D-7. Technology Help Dialog

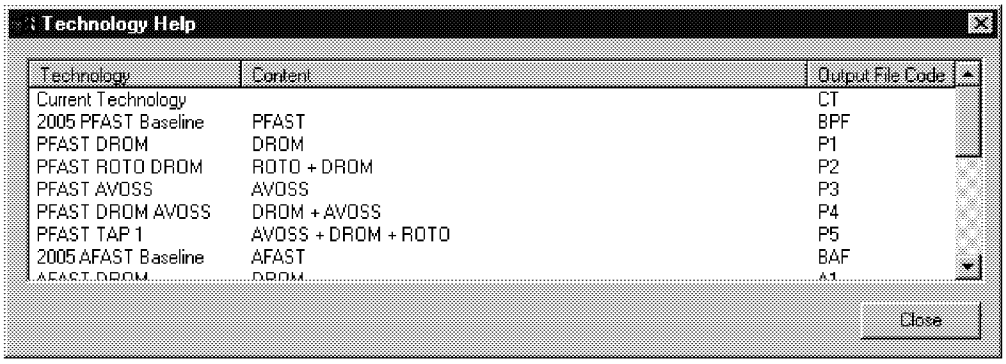

- If the **Capacity and Delay** option is selected, the **Traffic Inflation** group is enabled (and not grayed out) as shown in Figure D-6. In this case, use the **Traffic Inflation Year** drop-down list box to specify a year for traffic increase projections. To view and/or edit the traffic inflation values, click the [**View/Edit Values**] button. (See Figure D-24 in the section *Viewing and Editing Traffic Inflation Values*.)

  Note: Traffic inflation information is only required for the Airport Delay Models. Therefore, if the **Capacity Only** option is selected, the **Traffic Inflation** group is disabled and grayed out as shown in Figure D-5.

- Click the [**Run**] button to perform the standard technology analysis.

When the standard technology analysis is performed, the **"Standard Analysis in Progress"** dialog displays as shown in Figure D-8. To terminate the analysis before completion, click the [**Cancel**] button.

For each airport and technology selected, the Airport Capacity Model is executed once for each of the airport's meteorological conditions. Newark (EWR) and Los Angeles (LAX) have five meteorological conditions. For EWR, they are VMC1, VMC2, IMC_CM, IMC1, and IMC2. For LAX, they are VMC1, VMC2, IMC1-DRY, IMC1-WET, and IMC2. The remaining eight airports all have the four meteorological conditions: VMC1, VMC2, IMC1, and IMC2. When an Airport Capacity Model is executing, the **"Standard Analysis in Progress"** dialog displays the name of the model, the technology, and the meteorological condition.

Figure D-8. Standard Analysis in Progress Dialog

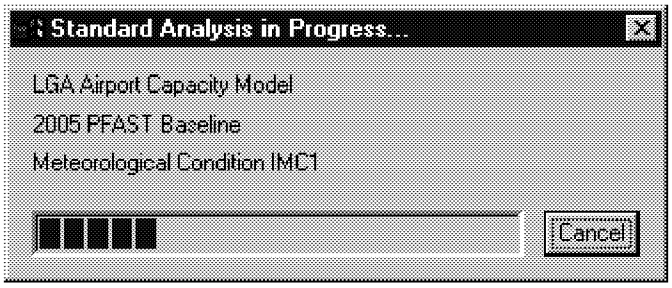

If the [**Capacity and Delay**] option button is selected, both the Airport Capacity and the Airport Delay Models are executed once for each airport and technology selected. When an Airport Capacity Model is executing, the **"Standard Analysis in Progress"** dialog (Figure D-8) displays the name of the model and the technology. When the Airport Delay Model is executing, a DOS window displays the output from the Delay Model as it is executing (Figure D-9).

Figure D-9. Delay Model DOS Window

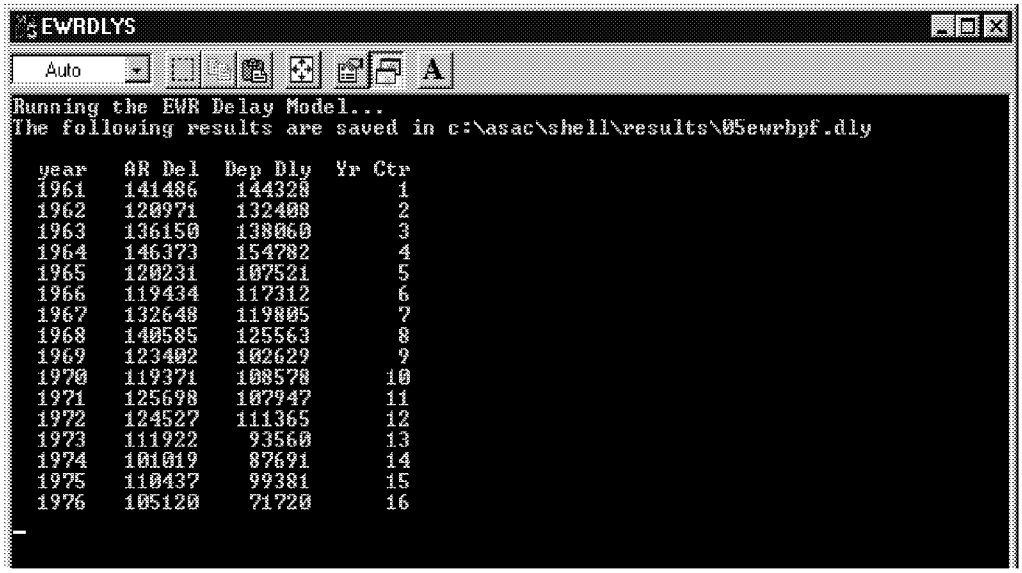

Tip! Canceling a Run

Each execution of the Capacity Model only takes a few seconds. Capacity Model runs *can* be canceled at any time by clicking the [**Cancel**] button.

Each execution of the Delay Model takes 2.5 to 5.0 minutes. Delay Model runs *cannot be* canceled while the model is executing and the DOS window is displayed. The Capacity Model always is executed between Delay Model executions when a series of technologies and/or airports are being run. The series can be canceled whenever a Capacity Model is being executed.

Using the **Ctrl+C** command to cancel the Delay Model will cause unpredictable behavior by the Run-Time Shell and *should not be used*!

Input and Output Data Files

An Airport Capacity Model input data file is provided for each airport, technology, and meteorological condition triple. The following convention is used to name these input data files: The first three characters of the file name specify the airport; the next two or three characters specify the technology; and the last two characters specify the meteorological condition. The extension for the input files is .in. See Table D-2 for the technology codes and Table D-3 for the meteorological condition codes. For example, the file dfwbpfi1.in is the Capacity Model input data file for the DFW airport, the 2005 PFAST baseline technology, and the IMC1 meteorological condition.

Table D-2. Technology Codes

Technology	Content	File Code
Current Technology	Current Technology	CT
2005 PFAST Baseline	PFAST	BPF
PFAST DROM	DROM	P1
PFAST ROTO DROM	ROTO + DROM	P2
PFAST AVOSS	AVOSS	P3
PFAST DROM AVOSS	DROM + AVOSS	P4
PFAST TAP 1	AVOSS + DROM + ROTO	P5
2005 AFAST Baseline	AFAST	BAF
AFAST DROM	DROM	A1
AFAST ROTO DROM	ROTO + DROM	A2
AFAST AVOSS	AVOSS	A3
AFAST DROM AVOSS	DROM + AVOSS	A4
AFAST TAP 1	AVOSS + DROM + ROTO	A5
ATM-1	AFAST + 3DFMS + Data Link	BAT
ATM-1 ROTO DROM	ATM-1 + ROTO + DROM	C1
ATM-1 DROM AVOSS	ATM-1 + DROM + AVOSS	C2
ATM-1 TAP2	ATM-1 + ROTO + DROM + AVOSS	C3
ATM-2	AFAST + 4DFMS + Data Link	C4
ATM-2 TAP 3	AFAST + 4DFMS + Data Link + ROTO + DROM + AVOSS	C5

Table D-3. Meteorological Condition Codes

Meteorological Condition	Input File Code
VMC1	V1
VMC2	V2
IMC_CM (EWR)	IC
IMC1-DRY (LAX)	ID
IMC1-WET (LAX)	IW
IMC1	I1
IMC2	I2

A single Airport Capacity Model output file, containing the capacity curves for all of the airport's meteorological conditions, is produced for each airport and technology pair. The convention for naming the Capacity Model output files is as follows: The first three characters of the file name specify the airport code, and the next two or three characters specify the technology code. The extension for the output files is .cap. For example, the file "atla1.cap" is the Capacity Model output file for the ATL airport and the AFAST DROM technology.

An individual Airport Delay Model output file is produced for each airport and technology pair. The convention for naming the Delay Model output files is as follows: The first two characters of the file name are the last two characters of the selected traffic demand year; the next three characters of the file name specify the airport code; and the last two or three characters specify the technology code. The extension for the output files is .dly. For example, the file "05atla1.dly" is the Delay Model output file for the traffic inflation year of 2005, the ATL airport, and the AFAST DROM technology.

The file naming conventions are summarized in Table D-4.

Table D-4. File Naming Convention Summary

File Type	Name Parameters	Example
Input Files	Airport Code + Technology Code + Meteorological Code + .in Extension	DFWCTI2.in (4 for each technology) (5 for EWR and LAX)
Capacity Model Output	Airport Code + Technology Code + .cap Extension	DFWCT.cap (1 per technology)
Delay Model Individual Technology Output	Demand Year Number + Airport Code + Technology Code + .dly Extension	05DFWCT.dly (1 per technology)

Capacity Model Results

If the **Capacity Only** option is selected, the **"Capacity Model Results"** dialog displays when the analysis is completed. If the analysis completed successfully without any errors, then the [**Errors**] button is disabled and grayed out as shown in Figure D-10.

Figure D-10. Capacity Model Results Dialog—Without Errors

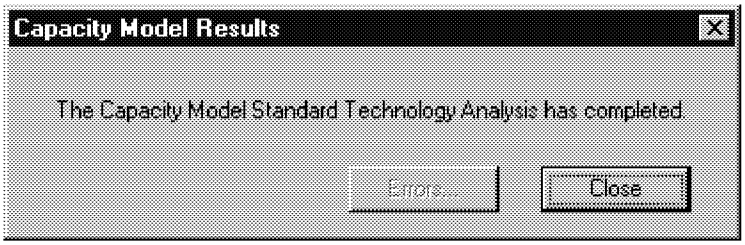

If errors occurred during the analysis, the [**Errors**] button is enabled and not grayed out as shown in Figure D-11.

Figure D-11. Capacity Model Results Dialog—With Errors

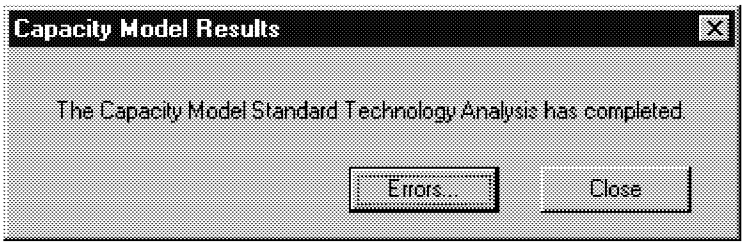

- Click the [**Errors**] button to display the **"Capacity Model Errors"** dialog with the location of the error message file. See Figure D-12.

Figure D-12. Capacity Model Errors Dialog

- Use your favorite text editor to view the error message file.
- Click the [**OK**] button to close the **"Capacity Model Errors**" dialog.
- Click the [**Close**] button to close the **"Capacity Model Results**" dialog.

Capacity and Delay Model Results

If the **Capacity and Delay** option is selected and the run is error-free, the **"Delay Model Summary Results"** dialog displays when the analysis is completed (see Figure D-13).

Figure D-13. Delay Model Summary Results Dialog - Without Errors

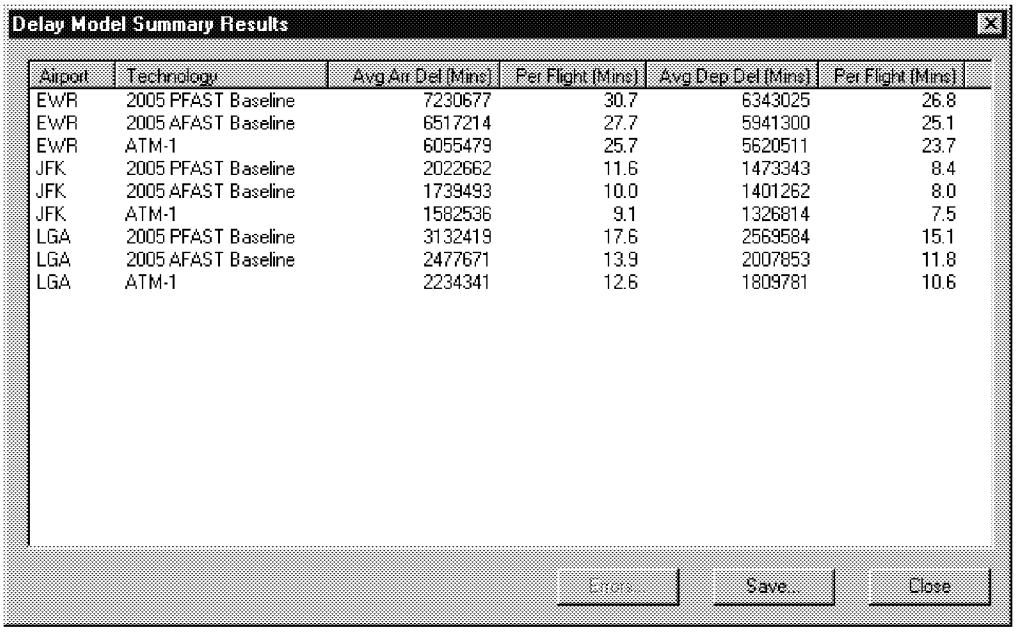

- To save the Delay Model summary results to a file, click the **[Save]** button. The **"Save As"** dialog displays. See Figure D-14.

Figure D-14. Save As Dialog

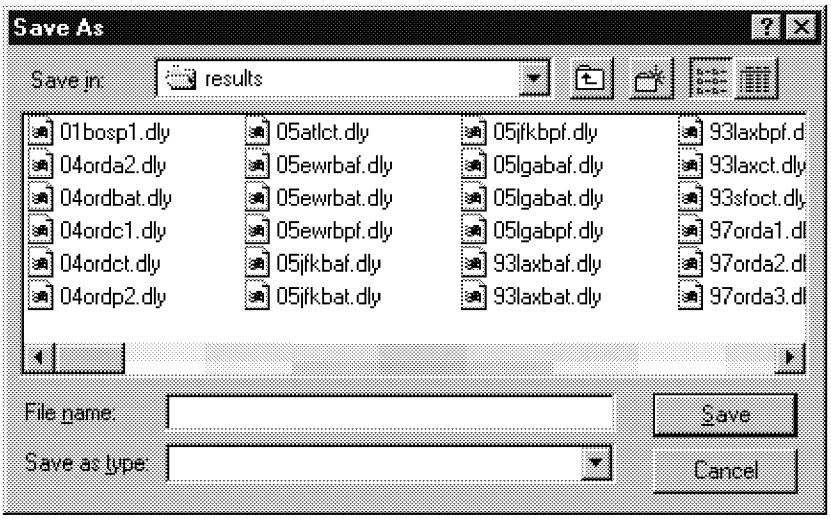

- Enter a file name in the **File name** edit field.
- Use the **Save in** drop-down list box to specify where the file should be located.
- Click the **[Save]** button to complete the save operation or click the **[Cancel]** button to abort the save operation.
- Click the **[Close]** button to close the **"Delay Model Summary Results"** dialog.

If errors occurred during the analysis, the [**Errors**] button is enabled and not grayed out as shown in Figure D-15.

Figure D-15. Delay Model Summary Results Dialog—With Errors

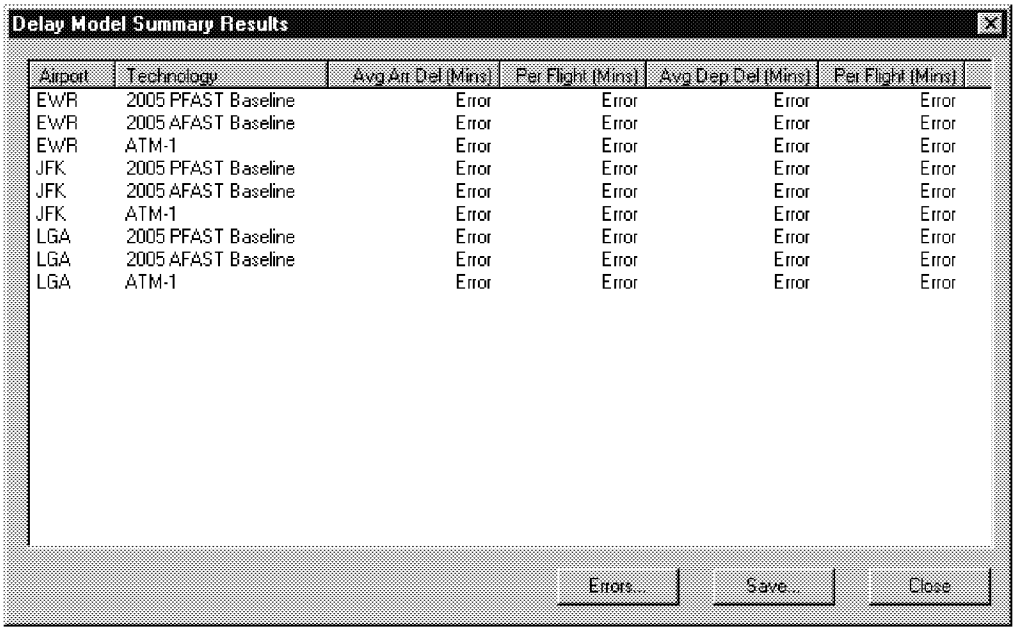

- Click the [**Errors**] button to display the **"Delay Model Errors"** dialog and the location of the error message file. (see Figure D-16).

Figure D-16. Delay Model Errors Dialog

- Use your favorite text editor to view the error message file.
- Click the [**OK**] button to close the **"Delay Model Errors"** dialog.
- To run another standard technology analysis, select new options and click the [**Run**] button.

  Note: *Remember to enter a new session path if you do not want the Capacity and Delay Model output files from the previous analysis to be overwritten.*

- Click the [**Done**] button to close the **"Standard Technology Analysis"** dialog.

PERFORMING CUSTOM ANALYSIS

To perform a custom technology analysis, either click the **[Custom Analysis]** button, choose the **Analysis / Custom** menu item, or press the **F4** key. The **"Custom Technology Analysis"** dialog displays. See Figures D-17 and D-18.

Figure D-17. Custom Technology Analysis Dialog—Capacity Only Option Selected

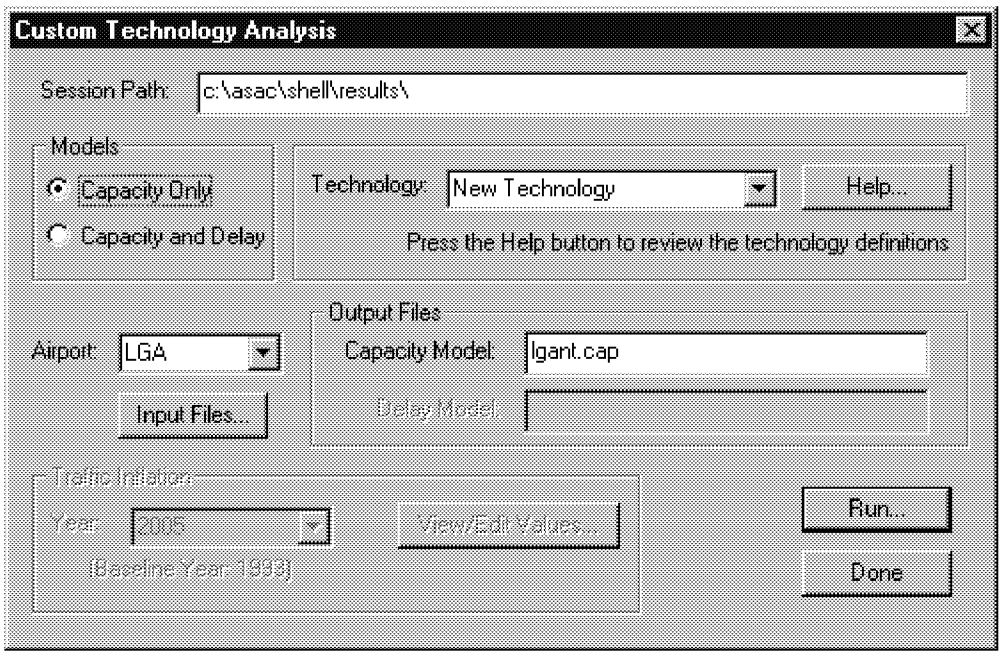

Figure D-18. Custom Technology Analysis Dialog—Capacity and Delay Option Selected

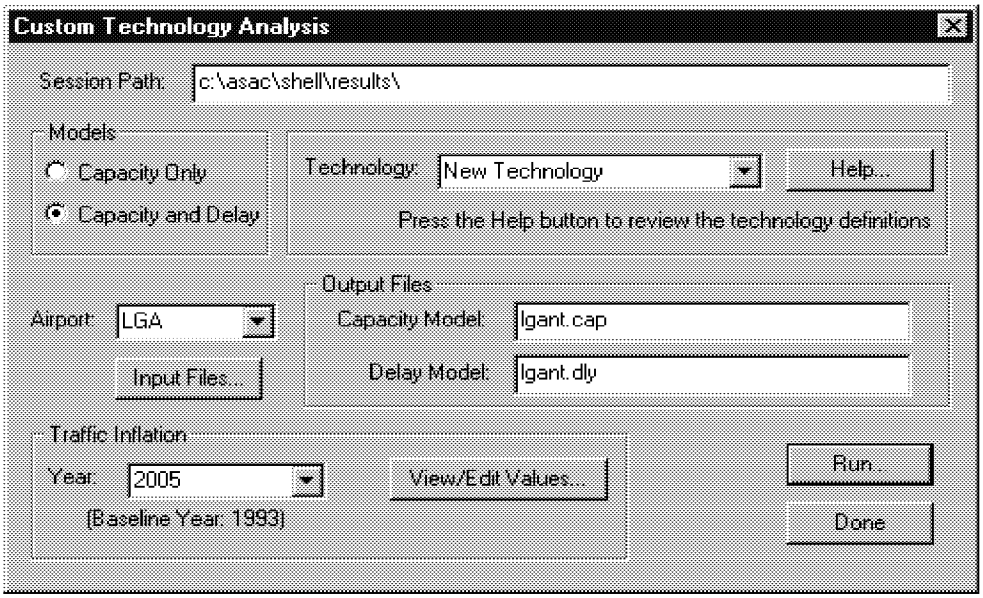

To run a custom technology analysis, complete the following steps:

- Enter the full path name of a folder that exists on your computer in the **Session Path** edit field. The session path specifies the location where the output files generated by the Airport Capacity and Airport Delay Models are placed. *Since the Airport Capacity and Airport Delay Models are DOS-based applications, the name of each subfolder in the session path can be a maximum of eight characters long plus a 3 character extension.*

- Select the [**Capacity Only**] option button if the analysis is to run only the Airport Capacity Model and not the Airport Delay Model. To run both the Airport Capacity and Airport Delay Models, select the [**Capacity and Delay**] option button.

- Use the **Airport** drop-down list box to select an airport.

- To select the Airport Capacity Model input files, click the [**Input Files**] button. See the section below on *Custom Technology Analysis Input Files.*

- Use the **Technology** drop-down list box to select a technology.

  Note: *This selection is for Shell information presentation only and does not select input parameters or designate an output file name.*

  Note: To review the technology definitions, click the [**Help**] button. The "**Technology Help**" dialog displays as shown in Figure D-7.

- the **Traffic Inflation** group is disabled and grayed out as shown in Figure D-17 when the **Capacity Only** option is selected inflation because traffic information

only is required for the Airport Delay Model. When the **Capacity and Delay** option is selected, the **Traffic Inflation** group is enabled (and not grayed out) as shown in Figure D-18. In this latter case, use the **Traffic Inflation Year** drop-down list box to specify a year for traffic increase projections.

Note: To view and/or edit the traffic inflation values, click the **View/Edit Values** button. See the section below on *Viewing and Editing Traffic Inflation Values.*

- Type a name for the Airport Capacity Model output file in the **Capacity Model** edit field in the **Output Files** group.

  Note: *The maximum allowable length for this name is twelve (12) characters including the "dot" and extension.*

- If the **Capacity Only** option is selected, an Airport Delay Model output file is *not* required; therefore, the **Delay Model** edit field in the **Output Files** group is disabled and grayed out as shown in Figure D-17. Alternatively, if the **Capacity and Delay** option is selected, the **Delay Model** edit field in the **Output Files** group is enabled and not grayed out as shown in Figure D-18. In this latter case type a name for the Airport Delay Model output file. The last two characters of the selected traffic inflation year are prepended to this file name; therefore, *the maximum allowable length for this name is ten (10) characters including the "dot" and extension.*

- Click the **[Run]** button to perform the custom technology analysis.

When the custom technology analysis is performed, the **"Custom Analysis in Progress"** dialog displays as shown in Figure D-19.

- To terminate the analysis, click the **[Cancel]** button.

  Note: The Airport Capacity Model is executed multiple times, once for each of the airport's meteorological conditions. See the Performing a Standard Analysis Section for a discussion of the meteorological conditions. When the Airport Capacity Model is executing, the **"Custom Analysis in Progress"** dialog displays the name of the model, the technology, and the meteorological condition.

Figure D-19. Custom Analysis in Progress Dialog

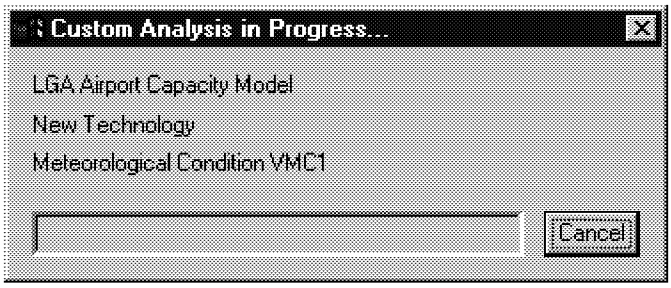

If the [**Capacity and Delay**] option button is selected, the Airport Delay Model is executed. When the Airport Delay Model is executing, a DOS window displays the output from the Airport Delay Model as it is executing, as shown in Figure D-9 in the *Performing a Standard Analysis* Section.

If the **Capacity Only** option is selected, the **"Capacity Model Results"** dialog displays when the analysis is completed. If the **Capacity and Delay** option is selected, the **"Delay Model Summary Results"** dialog displays when the analysis is completed. The results dialogs are explained in detail in the *Performing a Standard Analysis* Section.

- To run another custom technology analysis, select new options and click the [**Run**] button.

  Note: *Remember to enter a new session path if you do not want the Capacity and Delay Model output files from the previous analysis to be overwritten.*

- To close the **"Custom Technology Analysis"** dialog, click the [**Done**] button.

Custom Technology Analysis Input Files

Airport Capacity Model input files must be selected for each of the airport's meteorological conditions. Eight of the airports have four meteorological conditions, and two of the airports (EWR and LAX) have five. A sample input file for JFK is shown in Figure D-20. While most of the input categories are common to all the airports, certain airports have additional inputs such as the departure mix and the second common path that appear in Figure D-20 for JFK.

Note: The airport input files included on the distribution CD can be copied to other file locations to serve as templates for custom technology analysis. Input files for the basic TAP analysis are contained on the distribution CD in the directories identified in Table D-1. The input files use the naming conventions identified in Tables D-3 and D-4. *It is recommended that custom input files use the same naming conventions with substitution of new two- or three-character technology codes.*

- Use the **Airport** drop-down list to select an airport.

- Click the [**Input Files**] button to display a dialog with input boxes appropriate for the selected airport. See Figures D-21, D-22, and D-23.

- To select an input file, either type the entire file name, including the drive and folder, in the appropriate edit field, or click the [**Browse**] button to use the **Select Data File** dialog shown in Figure D-24.

- Either type a file name in the **File name** edit field or click a file name that displays in the list box.

- Use the **Look in** drop-down list box to specify where the file is located.

- Click the [**Select**] button to complete the select operation or click the [**Cancel**] button to abort the select operation.

Figure D-20. Input File: JFK PFAST Baseline with AVOSS in IMC-2

```
     Output file name: c:\airports\jfk\jfkP3I2.in
Mean of the efficiency buffer distribution
     0.1
Meteorological condition: 1=VMC1, 2=VMC2, 3=IMC1, 4=IMC2
  4
Number of aircraft classes in separation matrix
  4
First (basic) arrival separation matrix in nautical miles
   3.0   4.0   5.0   6.0
   3.0   3.0   4.0   5.0
   3.0   3.0   4.0   5.0
   3.0   3.0   4.0   4.0
Flag indicating heavy class aircraft for departure calculations
     0     0     1     1
Aircraft mix: small, large, B757, heavy
 0.120 0.410 0.050 0.420
Average approach speed over common path in knots
 135.0 140.0 140.0 145.0
Standard Deviation of approach speed in knots
   5.0   5.0   5.0   5.0
Standard deviation of position uncertainty in nautical miles
  0.25  0.25  0.25  0.25
Common path length in nautical miles
 8.0
Standard deviation of wind speed in knots
 7.5
Arrival runway occupancy times in minutes
   0.900   1.080   1.080   1.180
Standard deviation of arrival runway occupancy time in minutes
   0.130   0.130   0.130   0.130
Departure runway occupancy time in minutes
   0.500   0.667   0.667   0.667
Standard deviation of departure runway occupancy time in minutes
   0.100   0.100   0.100   0.100
Departure speed in knots
   130.0   180.0   180.0   180.0
Standard deviation of departure speed in knots
     5.0     5.0     5.0     5.0
Distance to departure turn in nautical miles
     5.0
Communications delay in minutes
   0.100
Standard deviation of communications delay in minutes
  0.0100
Second mix for departures - JFK only
 0.120 0.410 0.050 0.420
Second common path length
  12.0
Second (AVOSS) arrival separation matrix in nautical miles:
   3.0   3.0   3.5   3.5
   3.0   3.0   3.0   3.0
   3.0   3.0   3.0   3.0
   3.0   3.0   3.0   3.0
```

Figure D-21. Custom Technology Analysis Input Files Dialog

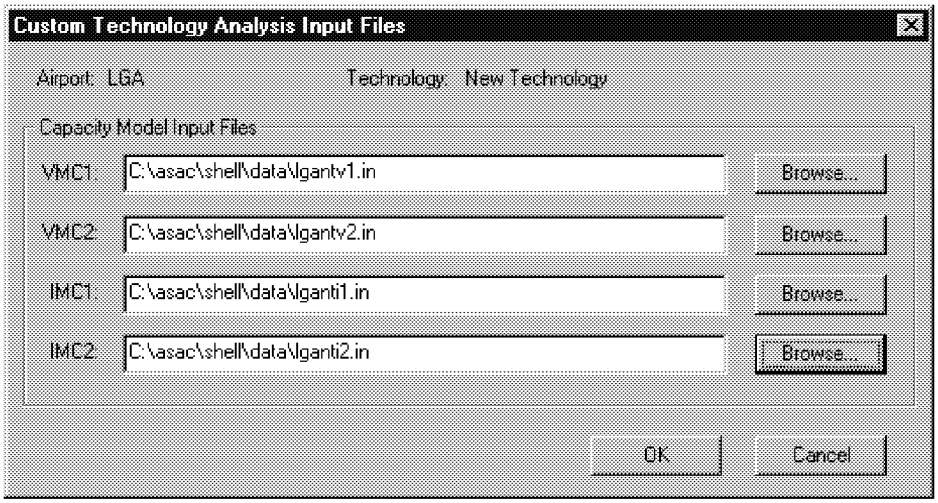

Figure D-22. Custom Technology Analysis Input Files Dialog—EWR

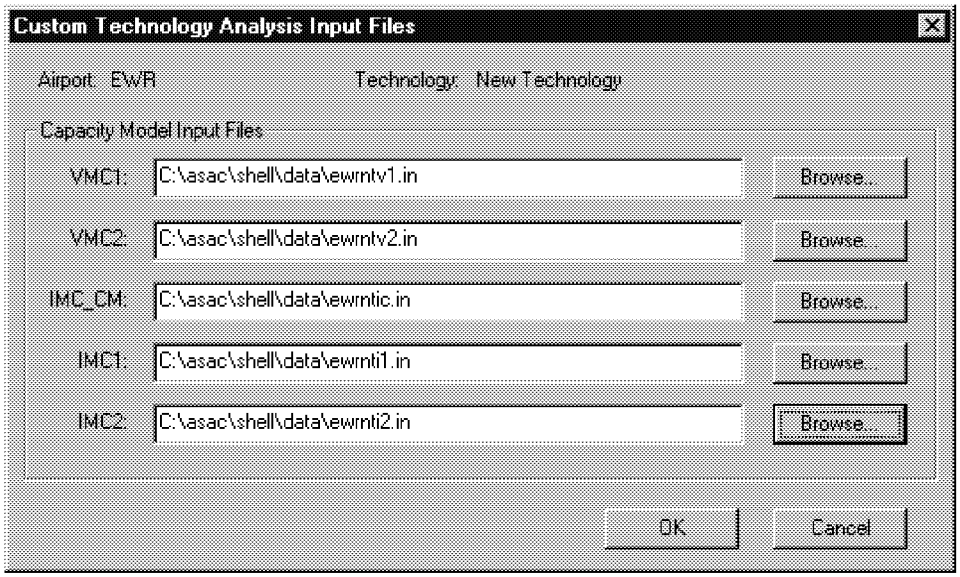

Figure D-23. Custom Technology Analysis Input Files Dialog—LAX

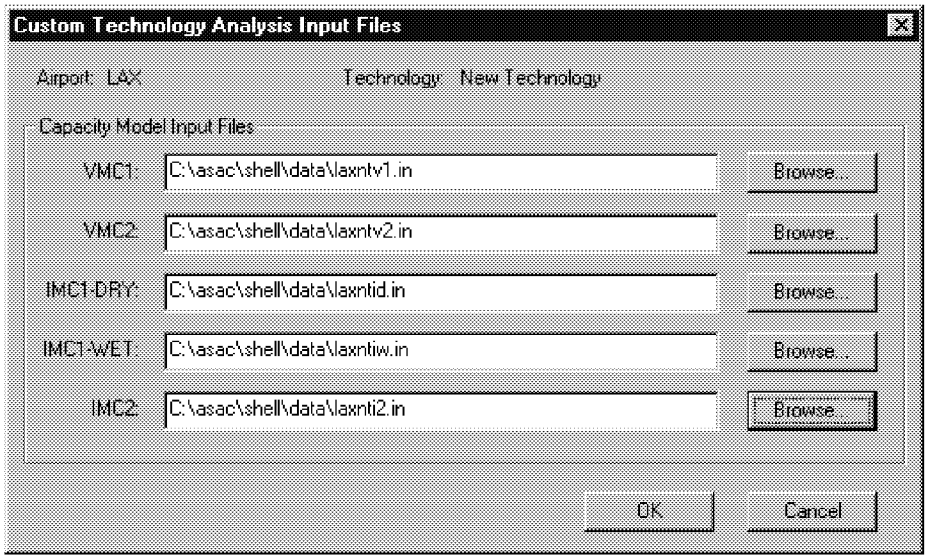

Figure D-24. Select Data File Dialog

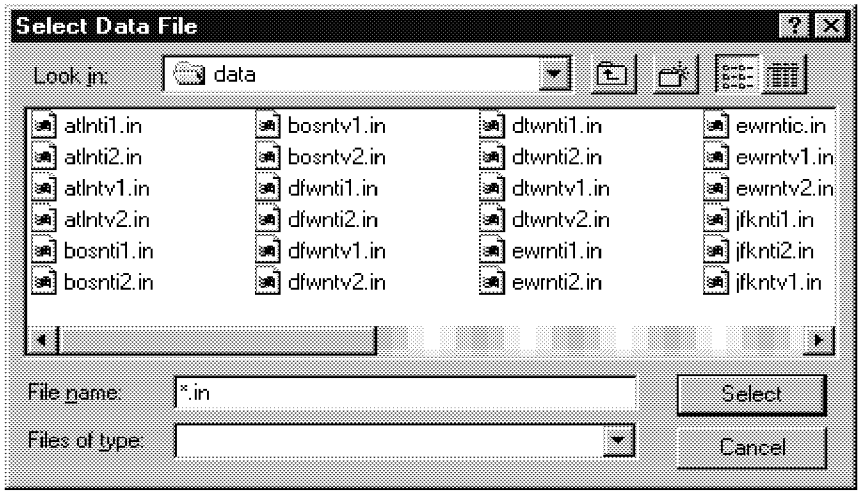

VIEWING AND EDITING TRAFFIC INFLATION VALUES

Figure D-25. Traffic Inflation Values Dialog

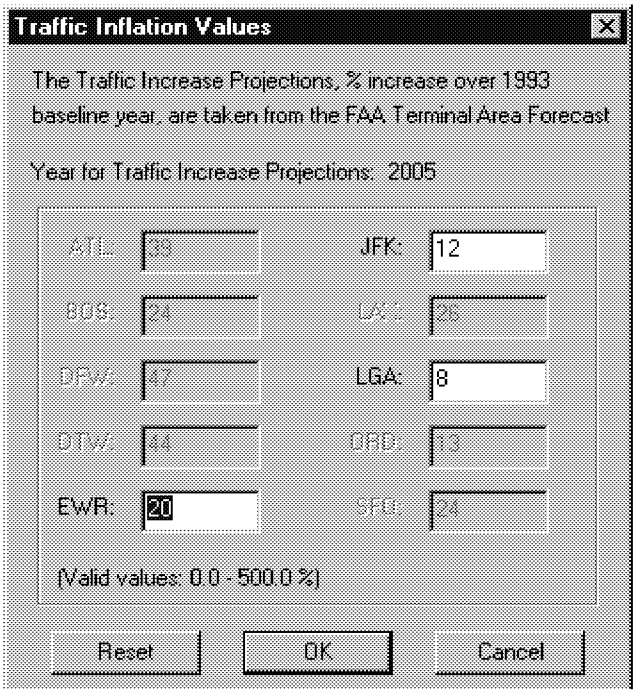

The traffic inflation value edit fields are enabled for airports that are selected for the technology analysis. If an airport is not included in the analysis, then its traffic inflation value edit field is disabled and grayed out.

- To change a traffic inflation value, simply type a new value in the appropriate edit field.
- Click the [**Reset**] button to restore the original values.
- To save any changes, click the [**OK**] button.
- If there are no changes or you do not wish to save the changes, click the [**Cancel**] button.

ODBC DRIVER

The presence of the required ODBC driver can be checked by the following procedure:

- Double click the **My Computer** icon,
- Double click the **Control Panel** icon,
- Double click the **32bit ODBC** icon.

Figure D-26 shows a typical Windows configuration with the required ODBC driver and DSN designation highlighted.

Figure D-26. ODBC Window

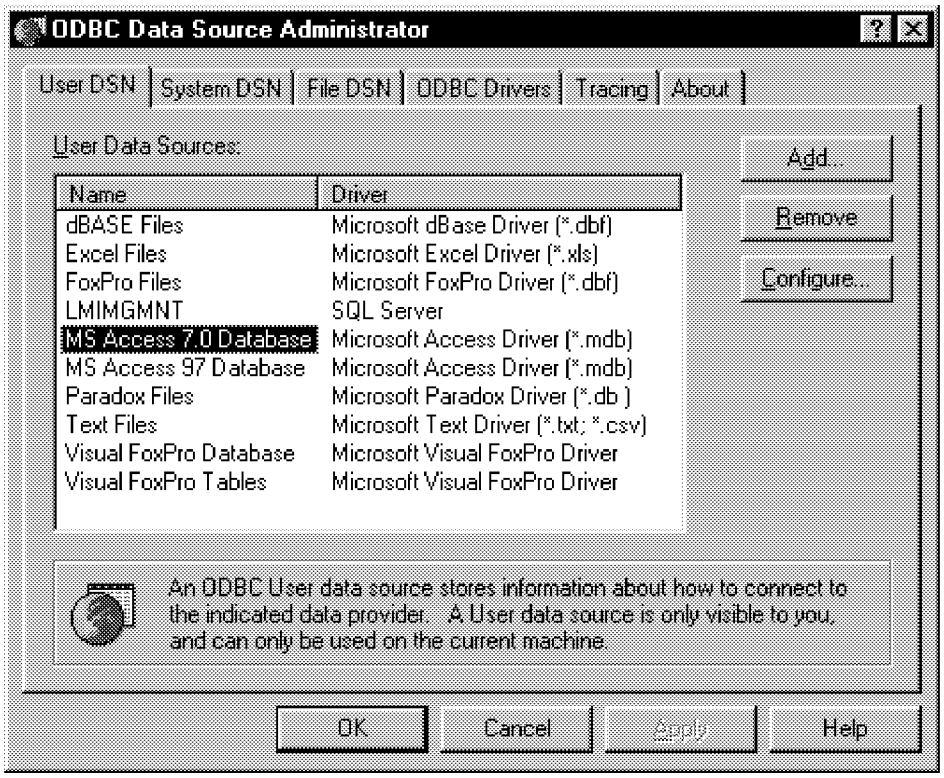

If the window does not include the **MS Access 7.0 Database** DSN, then it must be installed using the following procedure:

- Click [**Add...**] to open the **"Create New Data Source"** window (see Figure D-27).
- Highlight **Microsoft Access Driver (*mdb)**, as shown, and click [**Finish**] to open the **"ODBC Microsoft Access 97 Setup"** window (see Figure D-28).

- Type **MS Access 7.0 Database** in the **Data Source Name** field and click **[OK]**.

If errors persist after the correct DSN displays, then a new ODBC driver may need to be installed. (In one case during test, we encountered a defective version of the 32bit ODBC driver and had to install an update.)

Figure D-27. Create New Data Source Window

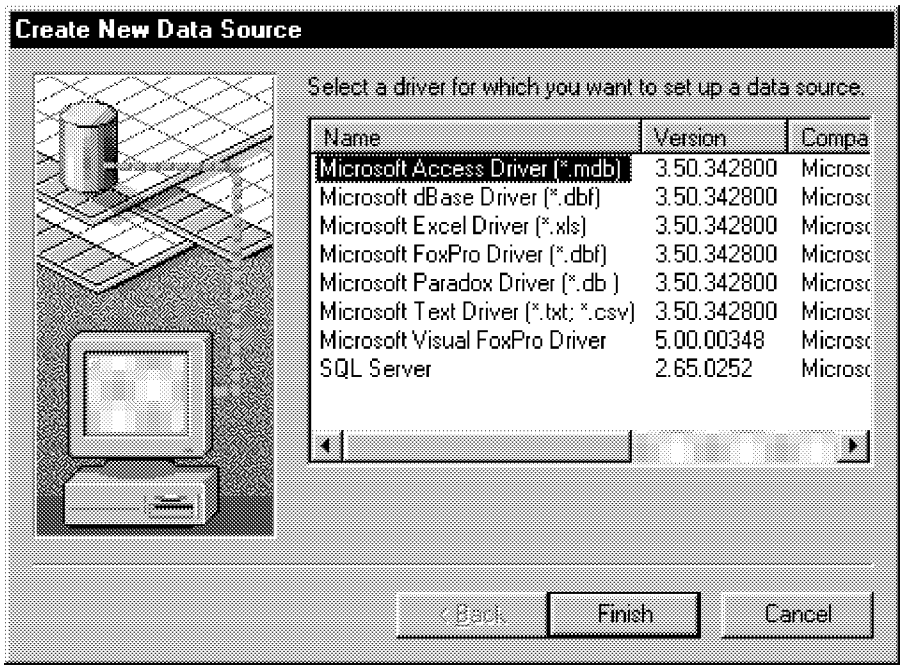

Figure D-28. ODBC Microsoft Access 97 Set-up Window

Appendix E
Abbreviations

AFAST	Active Final Approach Spacing Tool
AILS	Airborne Information for Lateral Spacing
ASAC	Aviation Systems Analysis Capability
AT	Airspace Tool
ATC	Air Traffic Control
ATL	The William B. Hartsfield Atlanta International Airport, Atlanta, Georgia
ATM	Air Traffic Management (a TAP program)
AVOSS	Aircraft Vortex Spacing System (a TAP technology)
BOS	General Edward Lawrence Logan International Airport, Boston, Massachusetts
CTAS	Center-TRACON Automation System
DFW	Dallas-Fort Worth International Airport, Dallas/Fort Worth, Texas
DOC	Direct Operating Cost
DOT	Department of Transportation
DROM	Dynamic Runway Occupancy Measurement System (a TAP technology)
DTW	Detroit Metropolitan Wayne County Airport, Detroit, Michigan
EWR	Newark International Airport, Newark, Ohio
FAA	Federal Aviation Administration
FMS	flight management system
IFR	Instrument Flight Rules
IMC	Instrument Meterological Conditions
JFK	John F. Kennedy International Airport
LAX	Los Angeles International Airport, Los Angeles, California
LGA	La Guardia Airport, New York, New York

LVLASO	Low Visibility Landing and Surface Operations (a TAP program)
MIT	Miles-in-Trail
NASA	National Aeronautics and Space Administration
OAG	Official Airline Guide
ORD	Chicago O Hare International Airport
PFAST	Passive Final Approach Spacing Tool
ROT	runway occupancy times
ROTO	Roll-Out and Turn-Off (a TAP technology)
RSO	Reduced Spacing Operations (a TAP program)
SDIAT	the standard deviation of the interarrival time, also SD_{IAT}
SFO	San Francisco International Airport, San Francisco, California
TAF	Terminal Area Forecast
TAP	Terminal Area Productivity
TRACON	Terminal Radar Approach Control
VFR	Visual Flight Rules
VMC	Visual Meteorological Conditions

REPORT DOCUMENTATION PAGE

Form Approved
OMB No. 0704-0188

1. AGENCY USE ONLY *(Leave blank)*	2. REPORT DATE	3. REPORT TYPE AND DATES COVERED
	January 1999	Contractor Report

4. TITLE AND SUBTITLE
Benefit Estimates of Terminal Area Productivity Program Technologies

5. FUNDING NUMBERS
C NAS2-14361

WU 538-16-11-01

6. AUTHOR(S)
Robert Hemm, Gerald Shapiro, David Lee, Joana Gribko ,
and Bonnie Glaser

7. PERFORMING ORGANIZATION NAME(S) AND ADDRESS(ES)
Logistics Management Institute
2000 Corporate Ridge
McLean, VA 22102-7805

8. PERFORMING ORGANIZATION REPORT NUMBER
NS809S1

9. SPONSORING / MONITORING AGENCY NAME(S) AND ADDRESS(ES)
National Aeronautics and Space Administration
Langley Research Center
Hampton, VA 23681-0001

10. SPONSORING / MONITORING AGENCY REPORT NUMBER
NASA/CR-1999-208989

11. SUPPLEMENTARY NOTES
Langley Technical Monitor: Robert E. Yackovetsky
Final Report

12a. DISTRIBUTION / AVAILABILITY STATEMENT
Unclassified - Unlimited

Subject Category 01
Availability: NASA CASI (301) 621-0390
Distribution: Nonstandard

12b. DISTRIBUTION CODE

13. ABSTRACT *(Maximum 200 words)*

This report documents benefit analyses for the NASA Terminal Area Technology (TAP) technology programs. Benefits are based on reductions in arrival delays at ten major airports over the 10 years from 2006 through 2015. Detailed analytic airport capacity and delay models were constructed to produce the estimates. The goal of TAP is enable good weather operations tempos in all weather conditions. The TAP program includes technologies to measure and predict runway occupancy times, reduce runway occupancy times in bad weather, accurately predict wake vortex hazards, and couple controller automation with aircraft flight management systems. The report presents and discusses the estimate results and describes the models. Three appendixes document the model algorithms and discuss the input parameters selected for the TAP technologies. The fourth appendix is the user's guide for the models.

The results indicate that the combined benefits for all TAP technologies at all 10 airports range from $550 to $650 million per year (in constant 1997 dollars). Additional benefits will accrue from reductions in departure delays. Departure delay benefits are calculated by the current models.

14. SUBJECT TERMS
terminal area productivity, area capacity, airport delay, cost benefit analysis, airport models, air transport

15. NUMBER OF PAGES
144

16. PRICE CODE
A07

17. SECURITY CLASSIFICATION OF REPORT	18. SECURITY CLASSIFICATION OF THIS PAGE	19. SECURITY CLASSIFICATION OF ABSTRACT	20. LIMITATION OF ABSTRACT
Unclassified	Unclassified	Unclassified	Unlimited